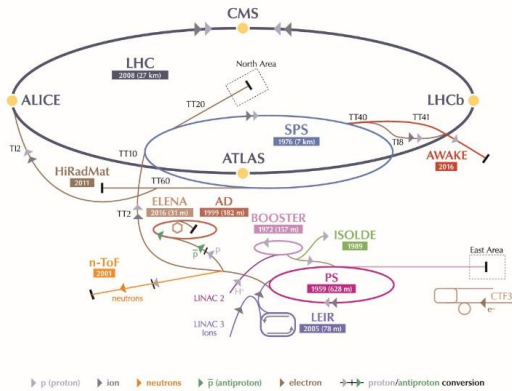


# Computations for Vacuum Systems of Accelerators

R. Kersevan, CERN-TE-VSC-VSM



**MAX IV**  
LABORATORY

LHC Large Hadron Collider SPS Super Proton Synchrotron PS Proton Synchrotron  
 AD Antiproton Decelerator CTF3 Clic Test Facility AWAKE Advanced WAKEfield Experiment ISOLDE Isotope Separator Online Device  
 LEIR Low Energy Ion Ring LINAC LINear ACcelerator n-ToF Neutrons Time Of Flight HiRadMat High-Radiation to Materials

## Agenda:

- Why do we need to make sophisticated vacuum calculations for particle accelerators?
- How many ways are there to do it?
- How is it done in practice? Theory and examples;
- Synchrotron radiation, e-cloud, and all the rest;
- Conclusions.

# 1. Why do we need to make sophisticated vacuum calculations for particle accelerators?

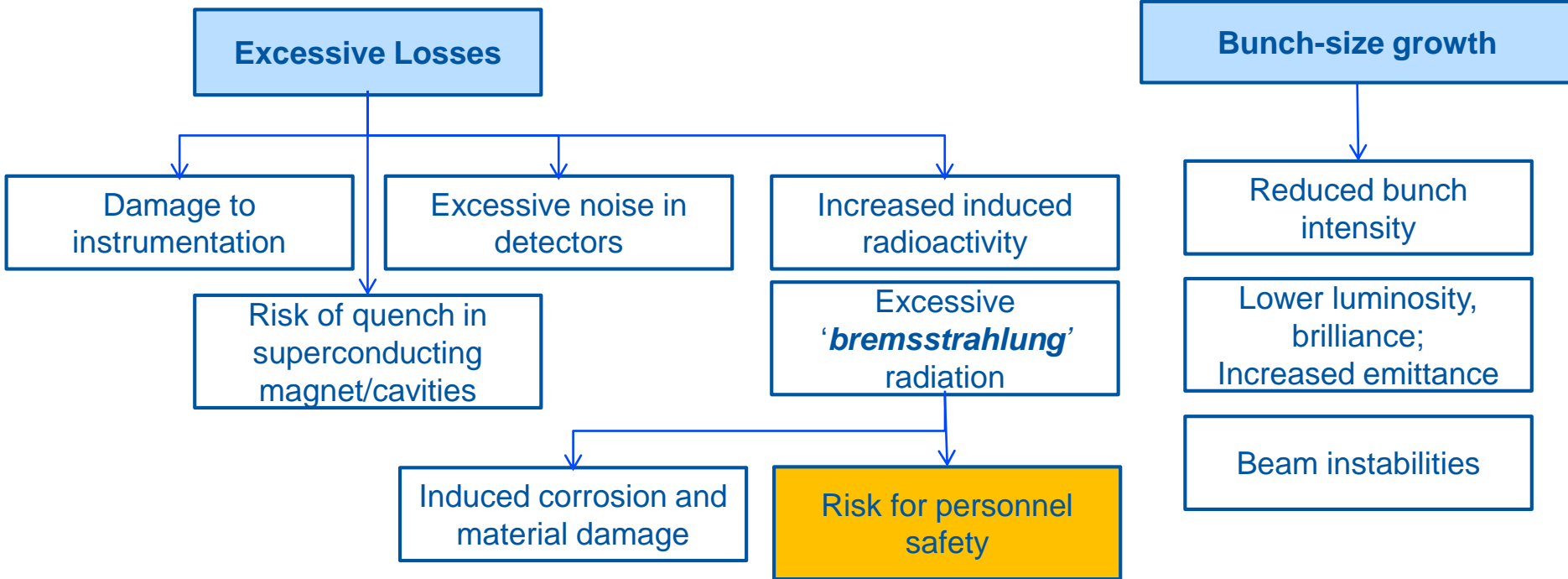
- Energetic particles, charged or neutral, interact with matter;
- In particular, inside the vacuum system of an accelerator, they interact with the residual-gas, which may be detrimental to the correct operation of the machine;
- The degree of sensitivity to the level (total pressure) and quality (gas composition) of the vacuum is a function of the accelerator type;
- Few examples, to clarify. The vacuum level and quality of...
  - Lepton colliders (e.g. B-factories, synchrotron radiation (SR) light sources) are strongly affected by the SR-induced outgassing yield of the materials making the chamber and SR absorbers. Most of the outgassed gases are  $H_2$  and light carbon-containing species ( $C_xH_y$ , CO,  $CO_2$ , plus water). Their interaction regions (IRs) are very sensitive to the radiation background (damage to the electronics inside the detectors);
  - High-energy hadron colliders (protons and ions) are strongly affected by the secondary electron emission yield (SEY) of the materials making the chamber (e-cloud effect). The outgassed species can be heavy gases and/or sputtered materials which could lead to beam losses ( $\rightarrow$  severe damage of vacuum chamber/leak, radiation damage), heating of cryogenic magnets and cavities ( $\rightarrow$  quenching), and so on;
  - SR light sources: same as lepton colliders, with the addition of the requirement that the bremsstrahlung (BS) level inside the experimental hutches be low enough to let the users in during the operation of the machine;
- As a general rule: the lower the pressure (locally and globally) the better, but gas composition is very important. The higher the atomic number of the atoms composing the residual gas the higher the scattering probability (e.g.  $\approx Z(Z+1)$  for bremsstrahlung)
- Clear mathematical relationships are known for the description of the interaction between charged beams and residual gases: elastic and inelastic scattering, on leptons and hadrons (in most cases on  $e^-$  and nucleons), and other interactions;

**The designer of a new machine is therefore interested into knowing what the pressure profile will be, in order to predict the overall performance of his/her accelerator: beam lifetime, ion trapping, emittance blow-up, bremsstrahlung level, material activation, and more.**

# Why do we need vacuum in accelerators?

Collisions between gas molecules and particles have to be minimized, otherwise the energy of the beam or its trajectory can be modified, leading to:

Source: P. Chiggiato, JUAS



A 'good vacuum' (low molecular density) is also necessary to:

- Avoid electrical discharge in high-voltage devices (tens of MV/m in RF cavities, couplers, waveguides);
- Reduce the heat transfer to cryogenic devices (e.g. insulating vacuum in cryostats)

## Beam Loss Mechanisms

- Depending on the type (collider, storage ring, cyclotron, etc...), the energy of its beam(s), the type of particle(s) being accelerated, and several machine-specific parameters (the “optics” of the machine), each accelerator is subjected to a variety of **beam loss mechanisms**, which affect its performance sometimes in dramatic ways;
- One important class of beam losses is the one related to the **interactions of the beam(s) with the residual gas (RG) inside the vacuum chamber**, along the path of the beam(s);
- These interactions can be due either to **elastic** or **inelastic scattering** off the **nuclei** of the RG molecules or their **electrons**. Examples are **Coulomb scattering**, **Bremsstrahlung scattering**, **charge-exchange**. The result of these interactions can either be a **direct loss** or the generation of **high-energy secondaries** (photons, neutrons);
- These scattering interactions are described by precise analytic formulae, and can be correlated to the beam loss rates measured along/around the accelerator;
- **A careful analysis in terms of expected pressure profile -depending explicitly on the gas composition- can be very helpful in order to design and operate efficiently and safely the accelerator itself and the experimental areas around it;**

The beam lifetime  $\tau$  is defined by the current decay rate  $1/\tau = -\dot{I}/I$ , which is the sum of the Touschek (T) rate and the gas scattering (G) rate

$$\frac{1}{\tau} = \frac{1}{\tau_T} + \frac{1}{\tau_G} = \frac{1}{\tau_T} + cn (\sigma_{\text{elast}}^N + \sigma_{\text{inel}}^N + \sigma_{\text{elast}}^e + \sigma_{\text{inel}}^e). \quad (1)$$

The Touschek decay rate can be written as (e.g. [4])

$$\frac{1}{\tau_T} = \frac{Nr_e^2 c}{8\pi\sigma_x\sigma_y\sigma_z\gamma^2(\Delta p/p)^3} \cdot D \left( \frac{(\Delta p/p)^2 \sigma_{x'}^2}{\gamma^2} \right), \quad (2)$$

where  $D \approx 0.3$  is a slowly varying function that is evaluated numerically. Relativistic effects and beam polarization modify the Touschek rate on the level of 10-20% [5].

The total cross sections for elastic and inelastic scattering on residual gas nuclei (N) and electrons (e) are [4]

$$\sigma_{\text{elast}}^N = \frac{2\pi r_e^2 Z^2}{\gamma^2} \frac{\bar{\beta}\beta_a}{a^2} \quad (3)$$

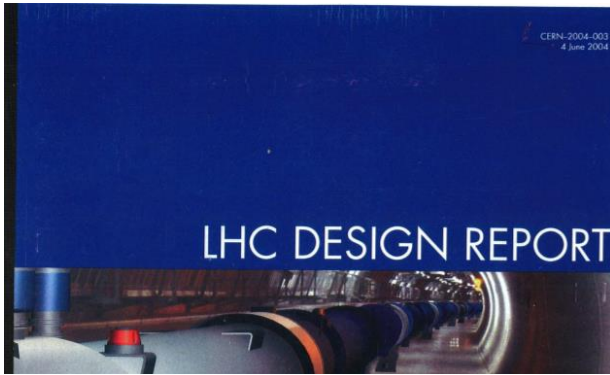
$$\sigma_{\text{inel}}^N = \frac{4r_e^2 Z^2}{137} \frac{4}{3} \left( \ln \frac{183}{Z^{1/3}} \right) \left( \ln \frac{1}{\Delta p/p} - \frac{5}{8} \right) \quad (4)$$

$$\sigma_{\text{elast}}^e = \frac{2\pi r_e^2 Z}{\gamma} \frac{1}{\Delta p/p}$$

$$\sigma_{\text{inel}}^e = \frac{4r_e^2 Z}{137} \frac{4}{3} \left( \ln \frac{2.5\gamma}{\Delta p/p} - 1.4 \right) \left( \ln \frac{1}{\Delta p/p} - \frac{5}{8} \right),$$

Valid for electron machines, such as light sources;

Ref.: S. Khan, "Study of the BESSY II beam lifetime", Proc. PAC-99, NY, p2831-2833



# How about the LHC? How's its vacuum lifetime vs gas density?

$\sim 5.1 \cdot 10^{-9}$  mbar at 20 °C

The vacuum lifetime is dominated by the nuclear scattering of protons on the residual gas. The cross sections for such an interaction at 7 TeV vary with the gas species [5, 6] and are given in Tab. 12.1, together with the gas density and pressure (at 5 K) compatible with the requested 100 hour lifetime. This number ensures that the contribution of beam-gas collisions to the decay of the beam intensity is small as compared to other loss mechanisms; it also reduces the energy lost by scattered protons in the cryomagnets to below the nominal value of 30 mW m<sup>-1</sup> per beam.

Table 12.1: The nuclear scattering cross sections at 7 TeV for different gases and the corresponding densities and equivalent pressures for a 100 h lifetime

GAS	Nuclear scattering cross section(cm <sup>2</sup> )	Gas density (m <sup>-3</sup> ) for a 100 hour lifetime	Pressure (Pa) at 5 K, for a 100 hour lifetime
H <sub>2</sub>	9.5 10 <sup>-26</sup>	9.810 <sup>14</sup>	<b>6.710<sup>-8</sup></b>
He	1.26 10 <sup>-25</sup>	7.410 <sup>14</sup>	5.110 <sup>-8</sup>
CH <sub>4</sub>	5.66 10 <sup>-25</sup>	1.610 <sup>14</sup>	1.110 <sup>-8</sup>
H <sub>2</sub> O	5.65 10 <sup>-25</sup>	1.610 <sup>14</sup>	1.110 <sup>-8</sup>
CO	8.54 10 <sup>-25</sup>	1.110 <sup>14</sup>	7.510 <sup>-9</sup>
CO <sub>2</sub>	1.32 10 <sup>-24</sup>	7 10 <sup>13</sup>	4.910 <sup>-9</sup>



12 SEP 1978

KEK-78-9  
June 1978  
A/P

SOME NOTES ON THE PHOTOELECTRON INDUCED GAS DESORPTION PROBLEMS  
IN THE PHOTON FACTORY AND TRISTAN

Alastair G. MATHEWSON, Gen'ichi HORIKOSHI  
and Hajime MIZUNO

$$\tau = \frac{X_0}{W\rho c}$$

$W$ : energy-spread  
dependence;  
 $\rho$ : density;

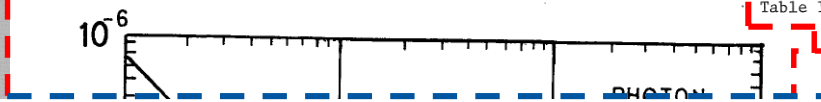
The radiation length  $X_0$  depends on the mass  $M$  and the square of the atomic number  $Z$  of the residual gas molecules. For electron energies  $\gg mc^2$ , i.e. relativistic, the radiation length  $X_0$  may be given by<sup>4)</sup>

$$X_0 = \frac{716}{Z(Z + 1.3)[\ln(183 Z^{-1/3}) + 1/8]}$$

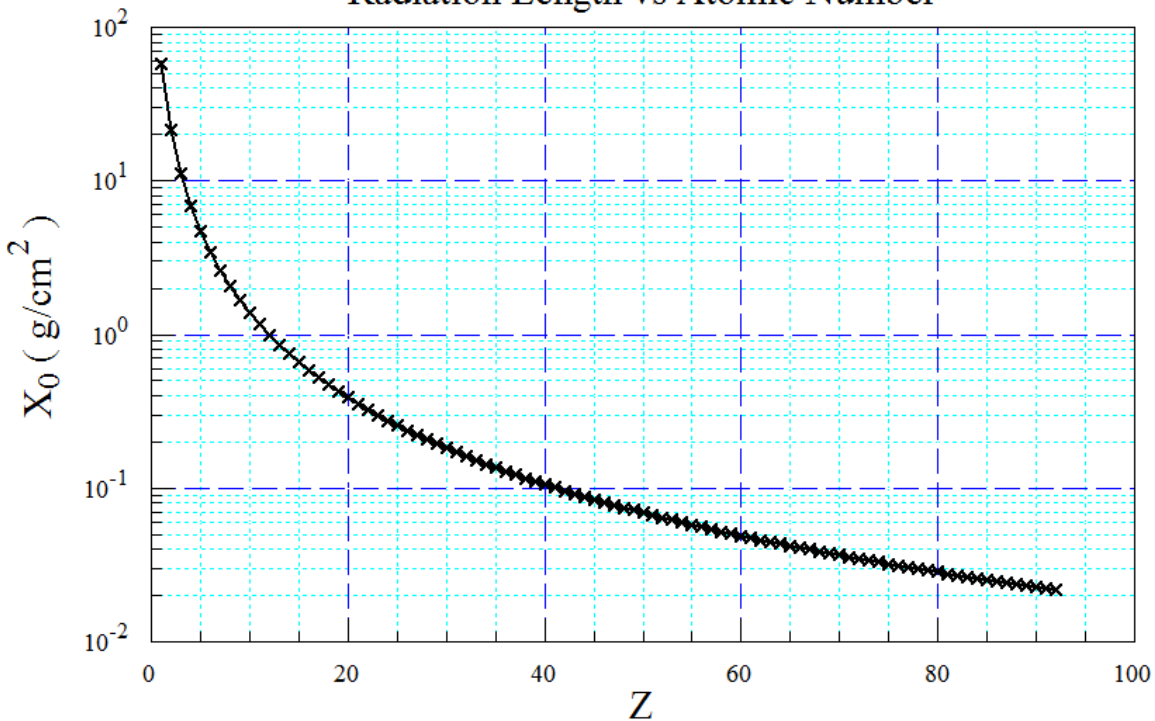
For a mixture of elements the radiation length is obtained by summing the individual values using the fraction  $f_i$  of each element ( $i$ ) by weight<sup>5)</sup>

$$\frac{1}{X_0} = \sum_i \frac{f_i}{X_i}$$

The radiation lengths for various elements and molecules are given in Table III.



Radiation Length vs Atomic Number



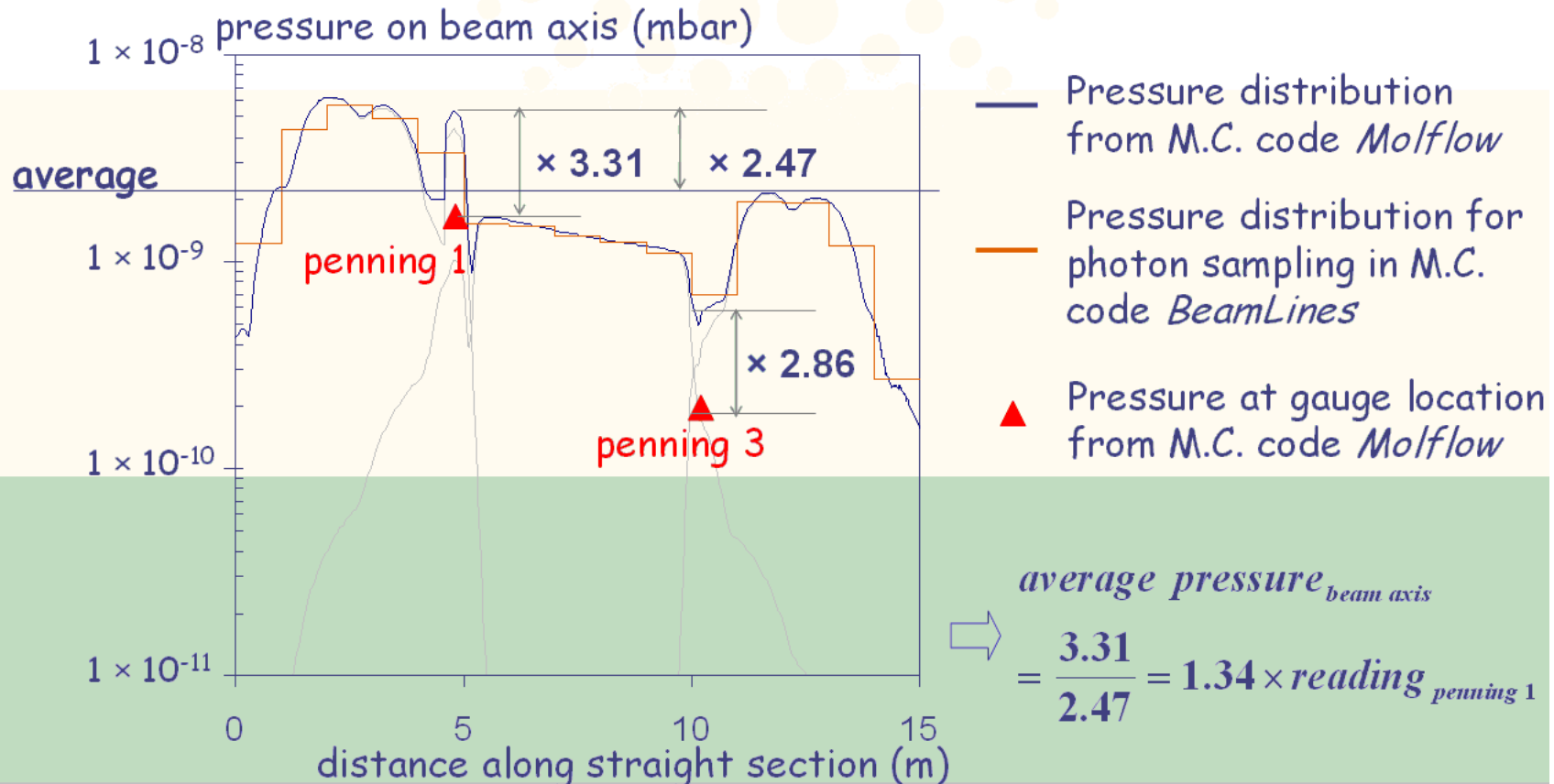
Substance	Molecular Weight	Radiation Length (g cm <sup>-2</sup> )
H	1	58
C	12	42.5
O	16	34.2
CH <sub>4</sub>	16	45.5
H <sub>2</sub> O	18	35.9
CO	28	37.3
Ar	40	19.4
CO <sub>2</sub>	44	36.1

ALASTAIR G. MATHEWSON ET AL., KEK LABORATORY  
Note KEK-78-9, 1978



Purpose: evaluate the bremsstrahlung generation along a straight section

**MOLFLOW: 3D Monte Carlo calculation of pressure distribution in storage ring vacuum chamber (developed by R. Kersevan)**



## How many methods exist to calculate vacuum quantities, like pressure profiles?

1. Analytical;
  2. Semi-Analytical;
  3. Continuity Principle of Gas Flow (CPoGF);
  4. Finite-Elements (FE);
  5. Angular Coefficients (AC);
  6. Direct Simulation Monte Carlo (DSMC), and Solutions of the BE;
  7. Test-Particle Monte Carlo (TPMC);
  8. Electric Network Analogy (ENA);
  9. Multi-physics codes (e.g. COMSOL);
- Which one to choose is a matter of choice and opportunity.
  - During the years, many accelerator laboratories have developed their own code, others have used commercial codes, others again have used some other lab's code (e.g. Molflow+);

## 1. Analytical;

- Historically, due to the lack of computing power at the dawn of vacuum science and technology (beginning to middle of 20<sup>th</sup> century) **analytical solutions** are the first ones which have been developed (e.g. Clausius, Knudsen, Smoluchowski, Clausing, Dushman, etc...). This kind of solutions have been used until computers have become available to the vacuum community, in the late 50's~early 60's, driven by nuclear and aerospace research;
- The best review and literature reference of this kind of early analytical calculations is given in:
  - “A review of the molecular flow conductance for systems of tubes and components and the measurement of pumping speed”, W. Steckelmacher, Vacuum Volume 16, Issue 11, November 1966, Pages 561-584
- In general, the equations governing the motion of diluted gases are obtained by solving the **Boltzmann equation (BE)**, i.e. a set of integro-differential equations which have applicability for fluids in general (plasma physics, for instance);
- The solution of the BE can be very demanding: in general, there is **no solution in closed form**, unless some very simple and basic geometries and boundary conditions are met;
- Historically the first solutions sought have been those for the calculation of **transmission probabilities and conductances**;
- For **tubes of constant cross-section** defined by a simple analytic formula (e.g. circle, ellipse, rectangle, equilateral triangle) a solution to the collision-less BE can be found, also called **Clausing integral equation**;
- Alas, this kind of solutions generally involves **complex integrals**, like elliptic ones or defined in terms of complex functions, not easily calculable unless **numerical methods** are employed;

• Few examples follow:



# 1. Analytical;

## Conductance of a circular tube:

### The Flow of Highly Rarefied Gases through Tubes of Arbitrary Length

P. Clausing

Natuurkundig Laboratorium, N. V. Philips' Gloeilampenfabrieken, Eindhoven, The Netherlands  
(Received 26 November 1931)

*Editor's Note: Translated from the German [Ann. Physik (5) 12, 961 (1932)]. Since this classic paper is referred to so frequently by workers in vacuum technology, it has been decided to publish an English translation. The translation was made available through the courtesy of Veeco Instruments, Inc., who also supported its publication.*

#### Contents

(I) The expressions of Knudsen, v. Smoluchowski, and Dushman for steady-state molecular flow; (II) transformation of the equations to kinetic variables, transmission probability; (III) derivation of the Dushman formula; (IV) the problem of the short, round cylindrical tube; (V) the problem of the long, round cylindrical tube; (VI) the application of the flow equation in high-vacuum engineering; summary.

#### I. The Expressions of Knudsen, v. Smoluchowski, and Dushman for Steady-State Molecular Flow

Knudsen<sup>1</sup> has given the following expression for the steady flow of a highly rarefied gas through a tube of arbitrary cross section

$$J = \frac{8}{3} \left( \frac{2}{\pi} \right)^{1/2} \frac{S^2}{sL} \frac{1}{(d)^3} (p_1 - p_2), \quad (1)$$

where  $J$  is the amount of gas flow per second, measured by the volume it would occupy at unit pressure,  $d$  is the density of the gas at unit pressure,  $S$  is the cross-sectional area of tube,  $s$  is the circumference of the cross section, and  $L$  is the length of the tube.  $p_1$  and  $p_2$  are the pressures in the two volumes connected by the tube, and we assume that the first is always to the left of the second (the indices 1 and 2 in this article refer exclusively to the two volumes).

For the derivation it is assumed that  $L$  is very large in comparison both to the transverse dimensions of the cross section of the tube as well as to the mean free path of the molecules, and further, that the molecules leave the wall of the tube diffusely in accordance with the cosine law.<sup>2</sup>

For a long circular cylindrical tube with radius  $r$ ,

Eq. (1) gives

$$J = \frac{4(2\pi)^{1/2}}{3} \frac{r^2}{L} \frac{1}{(d)^3} (p_1 - p_2). \quad (2)$$

For an orifice in a very thin wall, Knudsen<sup>6</sup> found

$$J = S / (2\pi)^{1/2} \cdot 1/d^3 (p_1 - p_2), \quad (3)$$

which gives for a circular opening

$$J = (\pi/2)^{1/2} \cdot r^2/d^3 (p_1 - p_2). \quad (4)$$

M. v. Smoluchowski<sup>7</sup> has shown that Eq. (1) is not correct and that it should be replaced with

$$J = \frac{1}{2(2\pi)^{1/2}} \frac{A}{L} \frac{1}{(d)^3} (p_1 - p_2),$$

where

$$A = \int_s \int_{-\pi/2}^{+\pi/2} \frac{1}{2} \rho^2 \cos \vartheta d\vartheta ds, \quad (5)$$

in which  $\rho$  represents a chord of the cross section, which forms an angle  $\vartheta$  with the normal at  $ds$ .<sup>8</sup> It is probably accidental that Eq. (2) is correct; for the circular cylinder the error of the Knudsen equation is removed.

As stated, Eqs. (2) and (5) apply only for relatively long tubes. When  $L=0$  the result would be that  $J=\infty$  in both cases instead of changing to Eq. (3).

Dushman<sup>10</sup> was the first to propose an expression which applies also to short tubes and which, for  $L=0$ , does not give  $J=\infty$ , but rather Eq. (3). (For practical reasons Dushman considered only circular cylindrical tubes and round orifices.)

A second expression has been derived by the author.<sup>9,11,12</sup> Although it gives the same results as the Dushman formula for  $L/r=0$  and  $L/r \rightarrow \infty$  [Knudsen's Eqs. (2) and (4)], the two equations deviate considerably from each other in the intermediate region. In

640 P. Clausing

dance with the second auxiliary theorem they leave  $S_A$  in accordance with the cosine law. Further, these are the molecules going from the surface A to the surface B+C, and in accordance with the first auxiliary theorem these molecules fall upon B+C evenly, that is, they fall upon the two surfaces B and C in proportion to the surface areas  $2\pi R h$  and  $2\pi R v$ . The fraction,

$$2\pi R h / (2\pi R h + 2\pi R v) = h / (h + v), \quad (31)$$

of the molecules proceeding upward through  $S_A$  thus passes  $S_B$ , and Eq. (31) represents the probability  $w_{ee}(v)$  being sought. A simple calculation from Fig. 1 gives

$$w_{ee}(v) = (1/2r^2) \{v^2 - v(v^2 + 4r^2)^{1/2} + 2r^2\}. \quad (32)$$

According to Eqs. (28), (30), and (27) this gives

$$w_{er}(v) dv = \frac{1}{2r^2} \left\{ (v^2 + 4r^2)^{1/2} + \frac{v^2}{(v^2 + 4r^2)^{1/2}} - 2v \right\} dv, \quad (33)$$

$$w_{rr}(v) = \frac{1}{4r} \left\{ (v^2 + 4r^2)^{1/2} + \frac{v^2}{(v^2 + 4r^2)^{1/2}} - 2v \right\} \quad (34)$$

and

$$w_{rr}(v) dv = \frac{1}{4r} \left\{ 2 + \frac{v^2}{(v^2 + 4r^2)^{1/2}} - \frac{3v}{(v^2 + 4r^2)^{1/2}} \right\} dv. \quad (35)$$

For  $v > 2r$  the following series applies<sup>13</sup>

$$w_{ee}(v) = \frac{1}{4} \left( \frac{v}{r} \right)^2 - \frac{1}{8} \left( \frac{v}{r} \right)^4 + \frac{5}{64} \left( \frac{v}{r} \right)^6 - \dots, \quad (36)$$

$w_{er}(v)$ , and therefore also  $w_{er}(v)$ ,  $w_{rr}(v)$ , and  $w_{rr}(v)$  are functions which rapidly become smaller with an increase of  $v$ .

Up to now we have only considered the case  $v > 0$ . For negative values of  $v$  the radicals of Eqs. (32)–(35) must be given a negative sign. Negative probabilities  $w_{er}$  and  $w_{rr}$  will then indeed be encountered, but it will always turn out that these are probabilities which will have to be taken into account with the minus sign [see Eqs. (58) and (60)].

We now imagine an  $x$  axis running along the tube in such a way that  $x$  increases from zero to  $L$  from left to right, and we observe a molecule that is at the point  $x$ . The probability that the molecule will enter

$$\alpha = \alpha \left( \frac{r}{L}, \frac{x}{L} \right) = \alpha \left( \frac{r}{L}, \frac{L-x}{L} \right) = \frac{\{(L-x)[(L-x)^2 + 4r^2]^{1/2} - (L-x)^2\} - \{x(x^2 + 4r^2)^{1/2} - x^2\}}{Lx^2 - \{2x-L\}\{x^2 + 4r^2\} - \frac{L(L-x)^2 - \{2(L-x)-L\}\{(L-x)^2 + 4r^2\}}{(x^2 + 4r^2)^{1/2}}}. \quad (41)$$

The remarkable thing about Eq. (41) is that, despite its dependence on  $x$ , for large values of  $r/L$  it is practically independent of  $x$ , as Table I demonstrates.

In order to obtain a definite result, an agreement should be reached on the choice of  $\alpha$ . For example,

the second volume without returning to the first we shall call the escape probability and designate it  $w(x)$ . It is then clear that the transmission probability is determined by

$$W = \int_0^L w_{er}(x) \cdot w(x) dx + w_{rr}(L), \quad (37)$$

and  $w(x)$  by the integral equation

$$w(x) = \int_0^L w_{er}(\xi - x) d\xi \cdot w(\xi) + w_{rr}(L - x), \quad (38)$$

or [using Eqs. (35) and (34)]

$$w(x) = \frac{1}{4r} \int_0^L \left\{ 2 + \frac{(\xi-x)^2}{[(\xi-x)^2 + 4r^2]^{1/2}} - \frac{3(\xi-x)}{[(\xi-x)^2 + 4r^2]^{1/2}} \right\} w(\xi) d\xi + \frac{1}{4r} \left\{ [(L-x)^2 + 4r^2]^{1/2} + \frac{(L-x)^2}{[(L-x)^2 + 4r^2]^{1/2}} - 2(L-x) \right\}. \quad (39)$$

From this integral equation two approximation solutions can be specified:

(1) For  $r \ll L$ , it is easy to show by substitution that for points of the tube at a sufficient distance from the openings,  $w(x) = x/L$  is a solution of Eq. (39). The substitution of  $w(x) = x/L$  in Eq. (37), however, does not give the correct result  $W = 8r/3L$ , but only  $W = 4r/3L$ . Due to the rapid decrease of  $w_{er}(x)$ , the integrand in Eq. (37) contributes to the value of the integral mainly for small values of  $x$  and in this case  $w(x) = x/L$  is no solution.<sup>17</sup>

(2) If  $r/L$  is large (i.e.,  $r/L \geq 1$ )

$$w(x) = \alpha + [(1 - 2\alpha)/L] \cdot x, \quad (40)$$

( $\alpha$  is a constant) is a good approximation to the solution of Eq. (39) over the entire length of the tube. If Eq. (40) were the correct solution, the substitution of Eq. (40) in Eq. (39) would produce an equation, which upon solution for  $\alpha$  would give a value independent of  $x$ . The actual substitution however gives

one might choose  $\alpha$  averaged over the entire tube, or for every  $r/L$  take  $\alpha = \alpha(r/L, 0)$ . For short tubes this selection is unimportant as is shown by Table I. If, however, it is considered important that the equation obtained by the substitution of Eqs. (33),



# 1. Analytical: From a circular tube to a simple particle accelerator, a pump connection.

## Analytic formulae:

- Simplest case: a straight tube, with uniform cross-section and outgassing from one end (be it thermal or other), pumped by one pump at the far end:

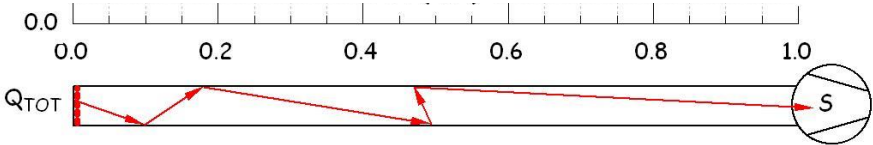
At the pump:  $P = Q_{TOT}/S$



$$P(x) = Q_{TOT} \left( \frac{1}{S} + \frac{L-x}{c} \right)$$



$$\left\{ \begin{aligned} P_{AVERAGE} &= \frac{1}{L} \int_0^L P(x) dx = Q_{TOT} \left( \frac{L}{2c} + \frac{1}{S} \right) = \frac{Q_{TOT}}{S_{EFF}} \\ P_{MAX} &= Q_{TOT} \cdot L/c \end{aligned} \right. \quad S_{EFF} = \left( \frac{L}{2c} + \frac{1}{S} \right)^{-1}$$



$c$ : specific cond. (l·m/s);  $A$ : specific linear vacuum chamber area (m<sup>2</sup>/m);  $q$ : specific outgassing rate (mbar·l/s/cm<sup>2</sup>);  $S$ : installed pumping speed (l/s);

# 1. Analytical: From a circular tube to a simple periodic particle accelerator:

- Another simple case: assume that the vacuum chamber of your circular accelerator is a straight tube, with uniform cross-section and outgassing (be it thermal or other), pumped by equally spaced lumped pumps ( $L=1\text{m}$ ):

$$\left\{ \begin{array}{l} Q(x) = -c \frac{dP(x)}{dx} \\ \frac{dQ(x)}{dx} = Aq \end{array} \right.$$

$$\downarrow$$

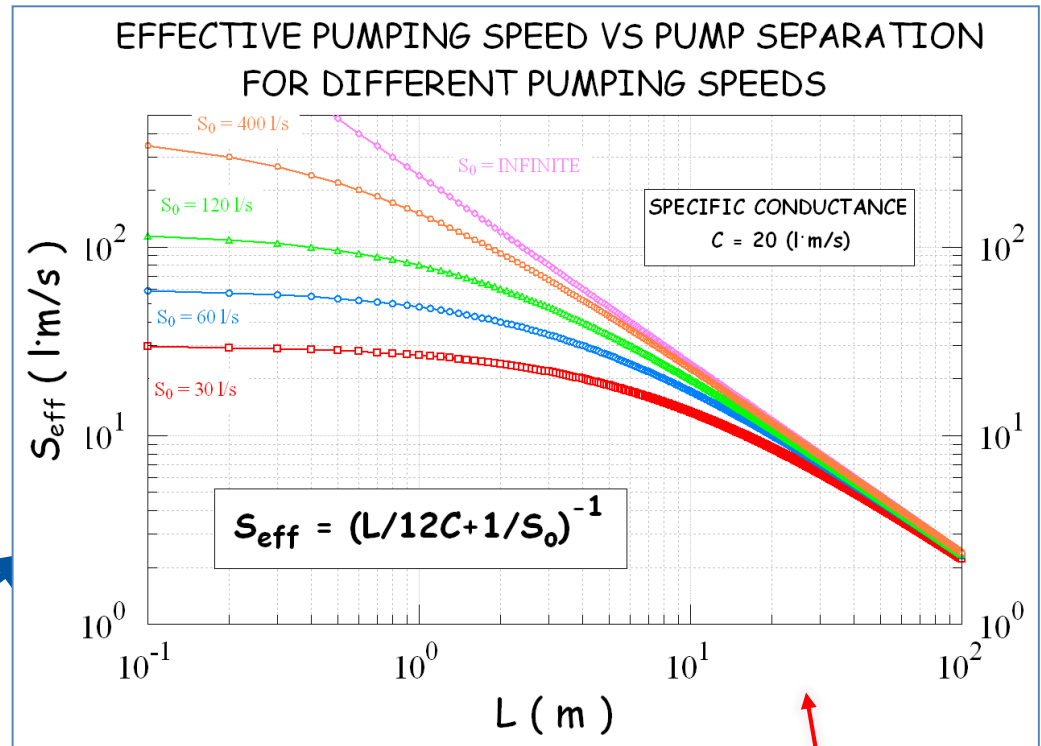
$$c \frac{d^2 P}{dx^2} = -Aq$$

$$\downarrow$$

$$\left\{ \begin{array}{l} \frac{dP}{dx}(x=L/2) = 0 \\ P(x=0) = AqL/S \end{array} \right.$$

$$\downarrow$$

$$P(x) = \frac{AqL}{2c}(Lx - x^2) + \frac{AqL}{S}$$



$$\left\{ \begin{array}{l} P_{AVERAGE} = \frac{1}{L} \int_0^L P(x) dx = AqL \left( \frac{L}{12c} + \frac{1}{S} \right) = AqL (1/S_{EFF}) \\ P_{MAX} = AqL \left( \frac{1}{8c} + \frac{1}{S} \right) \end{array} \right.$$

$$S_{EFF} = \left( \frac{L}{12c} + \frac{1}{S} \right)^{-1}$$

$c$ : specific cond. (l·m/s);  $A$ : specific linear vacuum chamber area (m<sup>2</sup>/m);  $q$ : specific outgassing rate (mbar·l/s/cm<sup>2</sup>);  $S$ : installed pumping speed (l/s);

# 1. Analytical; Conductance of other vacuum components:

## Free Molecule Transmission Probabilities

A. S. Berman

Citation: *Journal of Applied Physics* **36**, 3356 (1965); doi: 10.1063/1.1702984

View online: <http://dx.doi.org/10.1063/1.1702984>

View Table of Contents: <http://aip.scitation.org/toc/jap/36/10>

Published by the American Institute of Physics

### Free Molecule Transmission Probabilities\*

A. S. BERMAN

Flow Research Department, Technical Division, Oak Ridge Gaseous Diffusion Plant, Union Carbide Corporation, Nuclear Division, Oak Ridge, Tennessee (Received 22 February 1965)

APPROXIMATIONS to the solution of the Clausius integral equation to calculate the free molecule flow in various systems are well known and can be found in standard texts on kinetic theory and vacuum techniques. The approximations usually are presented as tables or as empirical equations fitted to such tables. Less well known is the use of a variational principle for obtaining an upper bound to the transmission probability. This approach has been described in detail by DeMarcus.<sup>1</sup> DeMarcus<sup>2</sup> also compared the results obtained for short capillaries by the variational technique with those obtained by a "squeezing" method which yields both upper and lower bounds to the transmission probability. The variational results were found to agree extremely well with those obtained by the "squeezing" method.

The variational technique has also been used by DeMarcus<sup>3</sup> to compute the influence of specular reflection on the free molecule transport through capillaries.

The detailed description<sup>4</sup> of the variational method gives the expressions for transmission probability in the form of unevaluated definite integrals, and the results of computations are given only in the form of numerical tables. In view of current wide-spread interest in free molecule flows, the integrations indicated by DeMarcus have been evaluated to obtain equations for the calculation of transmission probability.

This note gives these equations for the transmission probability for capillaries, flat plates, and dilute beds of spheres. Further, series expansions for short systems, and asymptotic expressions for long systems are presented for capillaries and flat plates. An asymptotic expression is given for dilute beds of spheres.

All equations are given in terms of reduced length  $L$  defined as follows:

$$L = \begin{cases} l/r & \text{for capillaries,} \\ l/h & \text{for flat plates,} \\ l/2r_p & \text{for beds of spheres,} \end{cases}$$

where in each case  $l$  is the length of the system. The capillary radius is  $r$ , the plate spacing is  $h$ , and for the sphere bed,  $r_p$  is the hydraulic radius given by twice the ratio of void fraction to specific surface.

Transmission probability is designated by  $Q$  and steady free molecule transports can be computed from the equation

$$G = \frac{1}{4}QA\bar{v}\Delta p,$$

where  $G$  is the transport in pressure volume units per unit time,  $\Delta p$  is the pressure differences across the system,  $\bar{v}$  is the mean thermal speed of the gas being transported, and  $A$  is the cross-sectional area open to flow.

The results for the transmission probability  $Q$  are conveniently given as the difference of two terms to be called  $Q_1$  and  $Q_2$ . Thus, for each system the transmission probability is given by

$$Q = Q_1 - Q_2.$$

#### Capillaries:

$$Q_1 = 1 + (L^2/4) - (L/4)(L^2 + 4)^{1/2},$$

$$Q_2 = \frac{[(8 - L^2)(L^2 + 4)^{1/2} + L^2 - 16]^2}{72L(L^2 + 4)^{3/2} - 288 \ln[L + (L^2 + 4)^{1/2}] + 288 \ln 2}$$

For small  $L$ ,

$$Q = 1 - (L/2) + (L^2/4) - (5L^3/48) + (L^4/32) - (13L^5/2560) - (L^6/3840) + \dots$$

For large  $L$ ,

$$Q \sim \frac{8}{3L} - \frac{2 \ln L}{L^2} - \frac{91}{18L^3} + \frac{32 \ln L}{3L^4} + \frac{8}{3L^5} - \frac{8(\ln L)^2}{L^6} + 0(1/L^7).$$

The small  $L$  series, as given, is in error by about 0.04% at  $L=1$  and less than  $10^{-4}\%$  at  $L=0.5$ . The asymptotic equation is in error by about 1% at  $L=20$ .

#### Flat plates:

$$Q_1 = \frac{1}{2}[1 + (1 + L^2)^{1/2} - L],$$

$$Q_2 = \frac{\frac{3}{2}\{L - \ln[L + (L^2 + 1)^{1/2}]\}^2}{L^2 + 3L^2 - 4 - (L^2 + 4)(1 + L^2)^{1/2}}$$

For small  $L$ ,

$$Q = 1 - (L/2) + (L^2/4) - (L^3/24) - (L^4/16) + \dots$$

For large  $L$ ,

$$Q \sim \left\{ \frac{(96 - 24x^2 + 9x^4) \ln(2/x) - 48x \{ \ln(2/x) \}^2}{96 - 144x + 128x^2 - 60x^3 + 14x^4} - \frac{-48 + 28x + 20x^2 - 6x^3 - 7x^4}{96 - 144x + 128x^2 - 60x^3 + 14x^4} \right\},$$

where  $x = (1/L)$ . The series solution, as given, is in error by about 0.2% at  $L=0.5$  and less than  $10^{-4}\%$  at  $L=0.1$ . The asymptotic solution is in error by about 0.7% at  $L=1.5$  and less than  $10^{-4}\%$  at  $L=5$ .

#### Dilute bed of spheres:

$$Q_1 = \frac{1}{2}[1 + (1 - L)e^{-L} + L^2 E_1(L)],$$

$$Q_2 = \frac{\{3L - 4 + L^2 E_1(L) + e^{-L}[4 + L(1 - L)]\}^2}{18[L^2 - 2 + 2e^{-L}(1 + L)]},$$

where

$$E_1(L) = \int_L^\infty \frac{e^{-x}}{x} dx$$

is the exponential integral for which tables are readily available.

For large  $L$ ,

$$Q \sim 192L/[1 + L(204 + 144L)],$$

which is in error by about 0.6% at  $L=1$  and about 0.004% at  $L=3$ .

For some values of  $L$ , the use of the exact expressions for  $Q_1$  and  $Q_2$  may require handling a large number of significant figures in the computation of transmission probability. For these situations the series and asymptotic results will be found very useful.

\* This note is based on work performed at the Oak Ridge Gaseous Diffusion Plant operated by Union Carbide Corporation for the U. S. Atomic Energy Commission.

<sup>1</sup> W. C. DeMarcus, Union Carbide Corporation Report K-1302, Part 3 (1957).

<sup>2</sup> W. C. DeMarcus and E. H. Hopper, *J. Chem. Phys.* **23**, 1344 (1955).

<sup>3</sup> W. C. DeMarcus, *Advances in Applied Mechanics*, Supplement 1, "Rarefied Gas Dynamics" (Academic Press Inc., New York, 1961), p. 161.



## 2. Semi-analytical; Conductance of other vacuum components: Empirical equation

### Free Molecule Flow in an Annulus

Abraham S. Berman

Citation: *Journal of Applied Physics* **40**, 4991 (1969); doi: 10.1063/1.1657335

View online: <http://dx.doi.org/10.1063/1.1657335>

View Table of Contents: <http://aip.scitation.org/toc/jap/40/12>

Published by the American Institute of Physics

This note will present the results of the upper bounds obtained for various annuli by the variational technique of DeMarcus.<sup>2,3</sup>

Consider an annulus of length  $l$ , inner radius  $r_i$ , and outer radius  $r_o$ . Let  $L$  be the length to spacing ratio  $[l/(r_o-r_i)]$  and  $\sigma$  be the radius ratio  $(r_i/r_o)$ . The transmission probability of the annulus is designated by  $Q$ , a dimensionless quantity from which the free molecule flow can be obtained by

$$G = \frac{1}{4} Q A \bar{v} \Delta p.$$

$G$  is the free molecule flow in pressure volume units per unit time,  $A$  is the cross-sectional area open to flow  $[\pi(r_o^2-r_i^2)]$ ,  $\bar{v}$  is the mean thermal speed of the gas being transported  $[(8kT/\pi m)^{1/2}]$ ,  $k$  is Boltzmann's constant,  $T$  is the absolute temperature,  $m$  is the molecular mass, and  $\Delta p$  is the pressure difference across the ends of the annulus.

Table I gives the transmission probability  $Q$  for some selected values of  $\sigma$  and  $L$ .

These results have been checked in the limits  $\sigma \rightarrow 0$  and  $\sigma \rightarrow 1$  when one expects  $Q$  for the annulus to approach that for a capillary and for the flow between flat plates respectively. The transmission probabilities for these two systems have been given in the previous note,<sup>1</sup> and the annulus results were found to reduce to the capillary and flat plate results in the limiting cases.

The Monte Carlo technique used by Davis<sup>5</sup> for calculating  $Q$  requires relatively large amounts of computer time and this disadvantage increases with increasing  $L$ . Consequently comparison with his results only extends up to an  $L$  of 20, the maximum  $L$  for which he published results. Table II indicates the excellent agreement between the Monte Carlo results and the upper bounds obtained by the variation technique.

For practical use, an empirical equation has been obtained which reproduces the variational results with a maximum error of about 1.5%. This maximum error occurs for values of  $\sigma$  close to unity.

The equation and its range of validity is

$$0 \leq L \leq 100$$

$$Q = \{1 + L[0.5 - A \tan^{-1}(L/B)]\}^{-1},$$

$$0 \leq \sigma \leq 0.9,$$

where

$$A = (0.0741 - 0.014\sigma - 0.037\sigma^2) / (1 - 0.918\sigma + 0.050\sigma^2),$$

$$B = (5.825 - 2.86\sigma - 1.45\sigma^2) / (1 + 0.56\sigma - 1.28\sigma^2).$$

## 2. Analytical approach: the IdaVac code (paper to be submitted as part of Ida Aichinger's PhD)

Analytical methods for vacuum simulations in high energy accelerators for future machines based on LHC performances

Ida Aichinger, Roberto Kersevan, Paolo Chiggiato  
CERN, The European Organization for Nuclear Research, CH - 1211 Geneva, Switzerland  
(Dated: May 2017)

We get the following equation for an isotropic medium with a constant diffusion coefficient  $\mathbf{a}$ :

$$\frac{\partial \mathbf{n}}{\partial t} = \mathbf{a} \left( \frac{\partial^2 \mathbf{n}}{\partial x^2} + \frac{\partial^2 \mathbf{n}}{\partial y^2} + \frac{\partial^2 \mathbf{n}}{\partial z^2} \right),$$

reducing simply to

$$\frac{\partial \mathbf{n}}{\partial t} = \mathbf{a} \frac{\partial^2 \mathbf{n}}{\partial x^2} \quad (5)$$

if diffusion is one-dimensional. This assumption is appro-

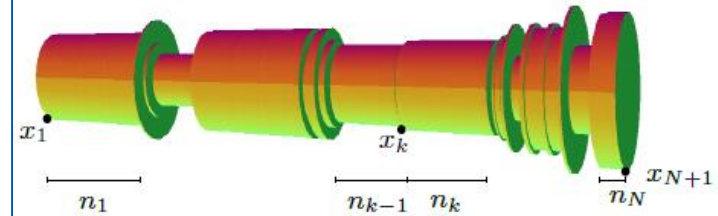


FIG. 1: Segmenting domain in  $N$  parts. Solution  $n_k$  describes density on segment  $k$ .

In order to generate a correct mass balance, continuous flow into and out of the system, e.g. in terms of desorption or pumping, at a rate  $\mathbf{q}$  and  $\mathbf{s}$  per unit volume, must be added to the right side of equation (5)

$$\frac{\partial \mathbf{n}}{\partial t} = \mathbf{a} \frac{\partial^2 \mathbf{n}}{\partial x^2} + \mathbf{q}(x, t) - \mathbf{s}(x, t) \cdot \mathbf{n} \quad (7)$$

## 2. Analytical approach: the IdaVac code (paper to be submitted as part of Ida Aichinger's PhD)

Analytical methods for vacuum simulations in high energy accelerators for future machines based on LHC performances

Ida Aichinger, Roberto Kersevan, Paolo Chiggiato  
*CERN, The European Organization for Nuclear Research, CH - 1211 Geneva, Switzerland*  
 (Dated: May 2017)

$$\eta(\text{H}_2) \sim E_c^{0.74}, \quad \eta(\text{CH}_4) \sim E_c^{0.94},$$

$$\eta(\text{CO}) \sim E_c^{1.01}, \quad \eta(\text{CO}_2) \sim E_c^{1.12}$$

### Photon-induced desorption (PID)

$$\mathbf{H}_{\text{ion}} = \begin{pmatrix} \eta_{\text{H}_2^+ \rightarrow \text{H}_2} & \eta_{\text{CH}_4^+ \rightarrow \text{H}_2} & \eta_{\text{CO}^+ \rightarrow \text{H}_2} & \eta_{\text{CO}_2^+ \rightarrow \text{H}_2} \\ \eta_{\text{H}_2^+ \rightarrow \text{CH}_4} & \eta_{\text{CH}_4^+ \rightarrow \text{CH}_4} & \eta_{\text{CO}^+ \rightarrow \text{CH}_4} & \eta_{\text{CO}_2^+ \rightarrow \text{CH}_4} \\ \eta_{\text{H}_2^+ \rightarrow \text{CO}} & \eta_{\text{CH}_4^+ \rightarrow \text{CO}} & \eta_{\text{CO}^+ \rightarrow \text{CO}} & \eta_{\text{CO}_2^+ \rightarrow \text{CO}} \\ \eta_{\text{H}_2^+ \rightarrow \text{CO}_2} & \eta_{\text{CH}_4^+ \rightarrow \text{CO}_2} & \eta_{\text{CO}^+ \rightarrow \text{CO}_2} & \eta_{\text{CO}_2^+ \rightarrow \text{CO}_2} \end{pmatrix}$$

$$\mathbf{H}_{\text{ion}} \cdot \dot{\mathbf{I}}_{\text{ion}} \cdot \mathbf{n} = \sum_{j=1}^4 \mathbf{H}_{i,j} \cdot \frac{I}{e} \sigma_j \cdot \mathbf{n}_j,$$

**Ion-induced desorption**

+ matrix terms for **electron-induced desorption, thermal outgassing, and eventually permeation and leaks;**

The **complete equation**, with **mass balance**, is the following (with appropriate boundary conditions):

$$\underbrace{\frac{\partial \mathbf{n}}{\partial t}}_{\text{Time variation of particles}} = \underbrace{\mathbf{a} \circ \frac{\partial^2 \mathbf{n}}{\partial x^2}}_{\text{Diffusion through surface}} + \underbrace{\eta_{ph} \cdot \dot{\Gamma}_{ph}}_{\text{Desorption by photons}} + \underbrace{\eta_e \cdot \dot{N}_e}_{\text{by electrons}} + \underbrace{\mathbf{H}_{ion} \cdot \dot{\mathbf{I}}_{ion} \circ \mathbf{n}}_{\substack{\text{Ionization by beam and desorption by ions} \\ \text{Multigasmodel}}} + \underbrace{\mathbf{A} \cdot \mathbf{q}_{th}}_{\text{thermal outgassing}} - \underbrace{\alpha \circ \frac{A \cdot \bar{v}}{4} \circ (\mathbf{n} - \chi_{cryo} \mathbf{n}_e)}_{\text{wall distributed pumping}} - \underbrace{\mathbf{p}_l \circ \mathbf{n}}_{\text{linear pumping}} \quad (18)$$



## 2. Analytical approach: the *IdaVac* code (paper to be submitted as part of Ida Aichinger's PhD, fall 2017)

Analytical methods for vacuum simulations in high energy accelerators for future machines based on LHC performances

Ida Aichinger, Roberto Kersevan, Paolo Chiggiato  
*CERN, The European Organization for Nuclear Research, CH - 1211 Geneva, Switzerland*  
 (Dated: May 2017)

*IdaVac* finds a solution using a Python code optimized for matrix inversion and the solution of a large system of differential equations; Ideal for long geometries (like entire accelerators, the CMS example here below is > 500 m long);  
 Some benchmarking and sample calculations:

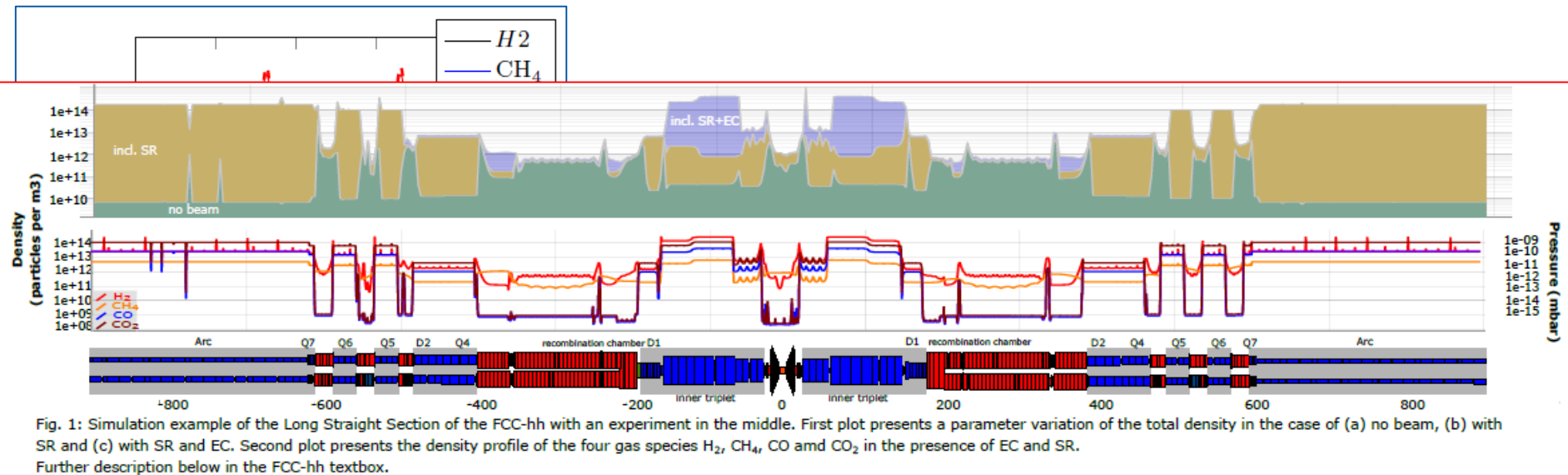


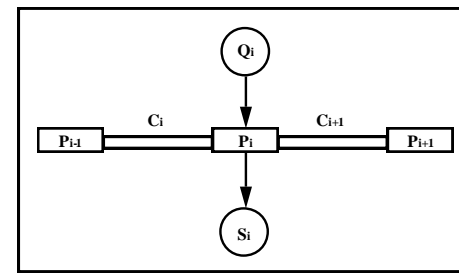
FIG. 3: Exampel 1: Conductance variation in comparison with *IdaVac*(solid line) and *Molflow+*(dashed line) for Geometry 1



### 3. Continuity Principle of Gas Flow (CPoGF);

Slice you accelerator into small elements, and

then apply:  $c_i(P_{i-1} - P_i) + c_{i+1}(P_{i+1} - P_i) + Q_i = S_i P_i$



- You can build your own solver routine using your favorite language and computer.
- You can use a routine like **rkfixed** from **MathCad**.
- You can use a routine like **NDSolve** from **Mathematica**.
- We have solved small problems (N<10 sub-volumes) using **MathCad** on a PC in less than one hour.
- For larger problems, it is worth learning **Mathmatica**.
  - Example: N = 83 sub-volumes with tress separate pumping phases, the computer processing time was 4.5 min on a 266 MHz G3 PowerMac.
  - With **MathCad**, the problem would have taken days due to the overhead needed to **MathCad** more user friendly with a cleaner output.

Ref.: "Vacuum Fundamentals", L. Bertolini, USPAS 2004, College of William and Mary, VA, USA

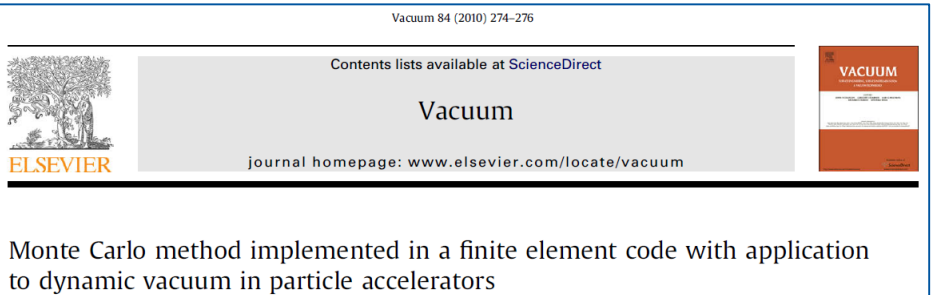
# 4. Finite Elements (commercial code) coupled with TPMC ray-tracing;

(see also slide no.54 , same geometry, with time-dependent Molflow+)

## 2.2. Implementation in a Finite Element (FE) code and algorithm

A Finite Element code has been used for this application for several reasons. Firstly, a complex geometry can be approximated by a mesh. Then, FE codes have their own geometrical pre-processor or have an interface with CAD softwares that allows downloading a geometrical mesh [4]. In our case, the geometry has been created and meshed with CATIA [5]. Then the mesh has been transferred to CASTEM by using a ".dat" format. A procedure called "FEUHV" for tracking particles in UHV conditions has been implemented in the opened-user FE code CASTEM [4]. The surface and volume have to be meshed with triangles and tetrahedrons, respectively. It is required to simplify the analysis of the intersection of the linear trajectory of the particles with the surface. The logic diagram of the routine is given in Fig. 1. Currently, a sticking factor of 1 has been used for the pumping surface; and 0 otherwise.

The module that analyses an eventual intersection of the trajectory and the surface is the most critical in terms of CPU time consumption. To reduce the CPU time, the search for an intersection with the boundary is limited to the elements that are close to the considered particle. They are obtained by using procedures already available in the FE code. In FEUHV, different surface properties can be implemented such as a pumping surface, thermal outgassing or particle induced desorption.



Monte Carlo method implemented in a finite element code with application to dynamic vacuum in particle accelerators

C. Garion\*  
European Organization for Nuclear Research

C. Garion / Vacuum 84 (2010) 274-276

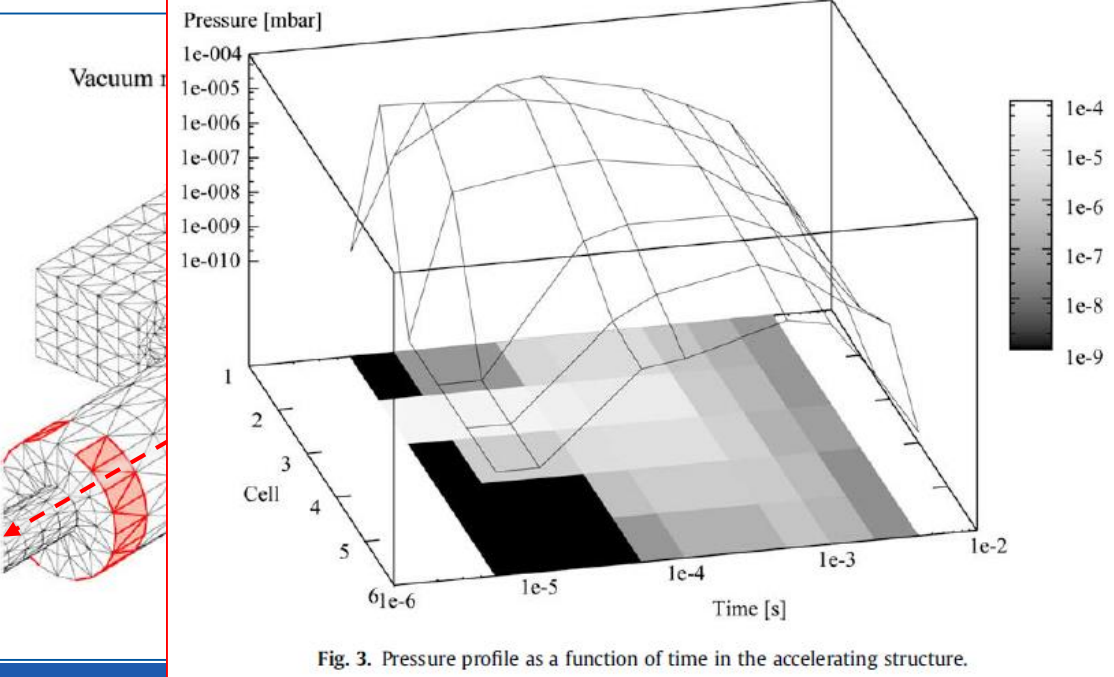
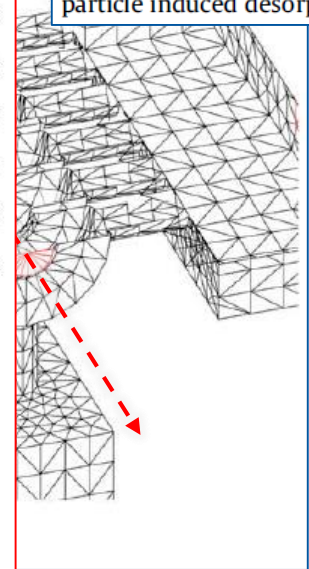


Fig. 3. Pressure profile as a function of time in the accelerating structure.



# 5. Angular Coefficients;

## MOLECULAR FLOW IN COMPLEX VACUUM SYSTEMS

By G.L. Saksaganskii

Translated from the Russian by V.A. Pleshakov

This book provides comprehensive coverage of the basic theory, calculation methods and optimization of high and ultrahigh vacuum systems and equipment. After an explication of molecular kinetic theory as applied to the problems of vacuum technology, the book examines methods (including the Monte Carlo method) of analysing molecular flow in nonequilibrium systems. It goes on to describe the parameters for separate vacuum system components, and ends with a section on molecular flow in structures with absorbing walls. A valuable reference for research scientists and engineers specializing in vacuum and electrophysical apparatus building such as thermonuclear reactors, charged particle accelerators and other high-vacuum devices, this book also serves as a textbook for graduate students who specialize in this field.

### About the author

Dr G.L. Saksaganskii is currently Head of Department at the D.V. Efremov Scientific Research Institute of Electrophysical Apparatus in Leningrad, and leader of the All-Union Section of Apparatus and Instrument-Making of the USSR. He has been chairman of various All-Union conferences and schools on high-vacuum physics and techniques. A prolific contributor to the field's literature, Dr Saksaganskii's main interests are in vacuum system designs for fusion installations, accelerators and accelerating-storage complexes, and in recognition of his contributions to scientific instrument-making he has been awarded the S.I. Vavilov Prize.

### Related titles of interest from Gordon and Breach and Harwood

Particle Accelerators and their Uses, in two parts, by Waldemar Scharf

Recirculating Electron Accelerators, by Roy E. Rand

Theory of Linear Resonance Accelerators, by I.M. Kapchinskiy

The Optics of Charged Particle Beams, by D. Carey

Engineering Aspects of Thermonuclear Fusion Reactors, edited by G. Casini

Particle Accelerators (Journal), Editor in Chief: Denis Keefe

Synchrotron Radiation News: a bi-monthly magazine edited by Pierre Dhez

ISBN: 2-88124-658-3

### GORDON AND BREACH SCIENCE PUBLISHERS

New York · London · Paris · Montreux · Tokyo · Melbourne

## MOLECULAR FLOW IN COMPLEX VACUUM SYSTEMS

G.L. Saksaganskii

## VACUUM TECHNOLOGY

Third, Updated and Enlarged Edition

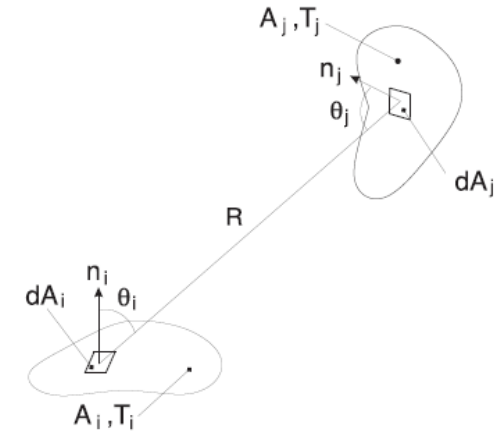
A. ROTH †

Former Deputy Director, and Head of Department of Vacuum Technology, Soreq Nuclear Research Centre, Israel



ELSEVIER

AMSTERDAM · LAUSANNE · NEW YORK · OXFORD · SHANNON · TOKYO



### Contents

PREFACE .....	v
CONTENTS .....	xiii
COMMONLY USED SYMBOLS .....	xix
1. INTRODUCTION .....	1
1.1. The vacuum .....	1
1.1.1. Artificial vacuum .....	1
1.1.2. Natural vacuum .....	5
1.2. Fields of application and importance .....	6
1.2.1. Applications of vacuum techniques .....	6
1.2.2. Importance of vacuum technology .....	10
1.3. Main stages in the history of vacuum techniques .....	11
1.4. Literature sources .....	13
1.4.1. Books .....	13
1.4.2. Journals .....	14
1.4.3. Conference transactions .....	15
1.4.4. Visual and audio-visual aids .....	16
2. RAREFIED GAS THEORY FOR VACUUM TECHNOLOGY .....	17
2.1. Physical states of matter .....	17
2.2. Perfect and real gas laws .....	23
2.2.1. Boyle's law .....	23
2.2.2. Charles' law .....	25
2.2.3. The general gas law .....	26
2.2.4. Molecular density .....	28
2.2.5. Equation of state of real gases .....	30
2.3. Motion of molecules in rarefied gases .....	33
2.3.1. Kinetic energy of molecules .....	33
2.3.2. Molecular velocities .....	34
2.3.3. Molecular incidence rate .....	36
2.4. Pressure and mean free path .....	37
2.4.1. Mean free path .....	37
2.4.2. Pressure units .....	40
2.5. Transport phenomena in viscous state .....	44
2.5.1. Viscosity of a gas .....	44
2.5.2. Diffusion of gases .....	47

xiii



# 5. Angular Coefficients, also called view-factors (VF);

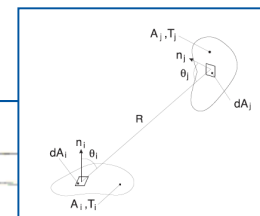


Table 2.2 Equations for calcu	Table 2.2 (continued)	Table 2.2 (continued)	Table 2.2 (continued)	Table 2.2 (continued)	References
Geometric structure	Geometric structure	Geometric structure	Geometric structure	Geometric structure	
					<p>[103]</p> <p>Two coaxial cylinders</p> $\Phi_{21} = \frac{R_1}{R_2} \frac{R_1}{\pi R_2} \left\{ \arccos \frac{B}{A} - \frac{1}{2R_1} \left[ \sqrt{(A+2R_1^2)^2 - 4R_1^2 R_2^2} \right. \right.$ $\left. \left. \times \arccos \frac{R_1 B}{R_2 A} + B \arcsin \frac{R_1}{R_2} - \frac{\pi A}{2} \right] \right\}$ $A = l^2 + R_2^2 - R_1^2; \quad B = l^2 - R_2^2 + R_1^2;$ $\Phi_{22} = 1 - \frac{R_1}{R_2} + \frac{2R_1}{\pi R_2} \arctg \frac{2\sqrt{R_1^2 - R_2^2}}{l} - \frac{l}{2\pi R_2}$ $\times \left\{ \frac{\sqrt{4R_1^2 + l^2}}{l} \arcsin \frac{4(R_1^2 - R_2^2) + (l^2/R_2^2)(R_2^2 - 2R_1^2)}{l^2 + 4(R_1^2 - R_2^2)} \right.$ $\left. - \arcsin \frac{R_2^2 - 2R_1^2}{R_1^2} + \frac{\pi}{2} \left( \frac{\sqrt{4R_1^2 + l^2}}{l} - 1 \right) \right\}$ <p>Inside surface and end-faces of a truncated cone</p> $\Phi_{21} = \frac{\sqrt{(h^2 + R_1^2 + R_2^2)^2 - 4R_1^2 R_2^2} - (h^2 - R_1^2 + R_2^2)}{2(R_1 + R_2)\sqrt{h^2 + (R_1 - R_2)^2}}$ $\Phi_{22} = 1 - \frac{\sqrt{(h^2 + R_1^2 + R_2^2)^2 - 4R_1^2 R_2^2} - h^2}{(R_1 + R_2)\sqrt{h^2 + (R_1 - R_2)^2}}$ <p>Two coaxial cylinders of infinite length</p> $\Phi_{12} = 1; \quad \Phi_{21} = \frac{R_1}{R_2}; \quad \Phi_{22} = 1 - \frac{R_2}{R_1}$ <p>[136]</p>
				<p>Two parallel cylinders of infinite length</p> $\Phi_{12} = \frac{1}{2\pi R} \left[ \sqrt{s^2 - 4R^2} + 2R \arcsin \frac{2R}{s} - s \right]$ <p>A sphere and a disk</p> $\Phi_{12} = \frac{F_{21}}{4\pi R^2}$ <p>A sphere and the inside surface of a cylinder</p> $\Phi_{12} = 1; \quad \Phi_{21} = \left( \frac{R_1}{R_2} \right)^2; \quad \Phi_{22} = 1 - \left( \frac{R_1}{R_2} \right)^2$ <p>Sphere and disk</p> $\Phi_{12} = \frac{1}{2} \left( 1 - \frac{s}{\sqrt{s^2 + R_1^2}} \right)$ <p>Sphere and inside surface of a cylinder</p> $\Phi_{12} = \frac{1}{2} \left[ \frac{s}{\sqrt{s^2 + R_2^2}} - \frac{s-l}{\sqrt{(s-l)^2 + R_1^2}} \right]$ <p>[47]</p>	

## 5. Angular Coefficients, also called view-factors (VF);

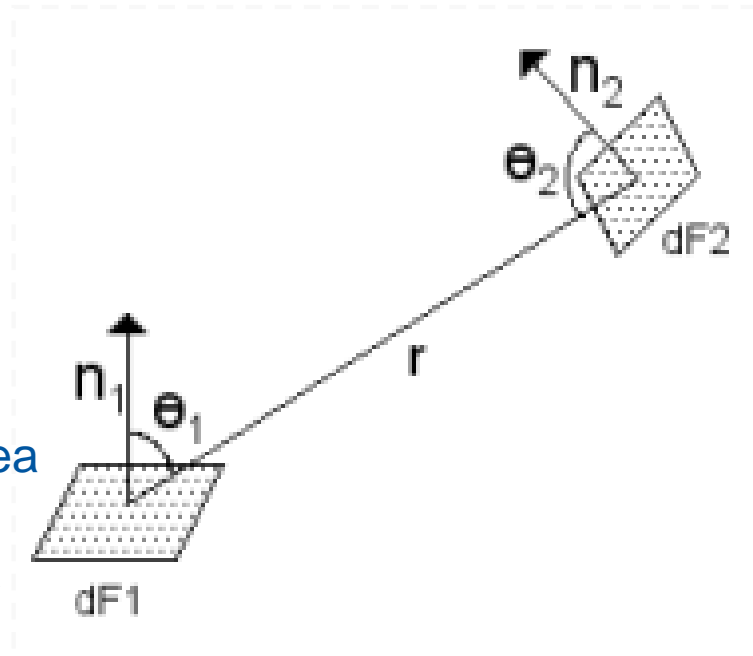
“Standard” formulae, giving coefficients under which each element on a surface sees all the others:

$$d\varphi_{(dF_1 \leftarrow dF_2)} = \frac{\cos \theta_1 \cos \theta_2}{\pi r^2} dF_1 \quad \text{elementary flux}$$

$$P_i = \sum_{j=1}^N \frac{\cos \theta_i \cos \theta_j}{\pi r^2} A_j P_j + E_i \quad P_i = \# \text{ of molecules on } i\text{-th element}$$

$$D_i = \sum_{j=1}^N \frac{\cos \theta_i \cos \theta_j}{\pi r^2} A_j D_j + E_i \quad \begin{array}{l} D_i = P_i \text{ normalized to area} \\ A_i \text{ of element } i; \\ E_i = \text{emitted density/flux} \end{array}$$

$$C_{ij} = \frac{\cos \theta_i \cos \theta_j}{\pi r^2} A_j \quad \text{AC matrix definition}$$



$$D_i = (1 - s_i) \sum_{j=1}^N C_{ij} D_j + E_i \quad \begin{array}{l} \text{final form, matrix equations to solve} \\ s_i = \text{sticking coeff. vector} \end{array}$$

## 5. Angular Coefficients, also called view-factors (VF);

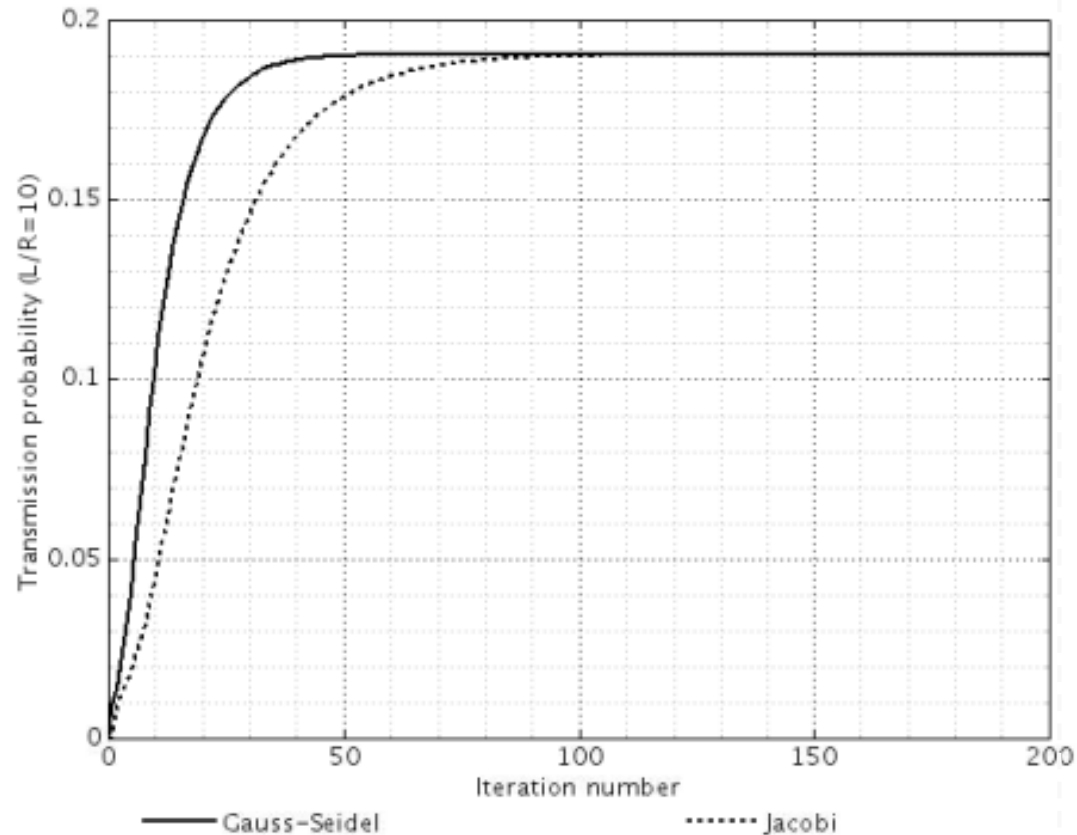
### **Solution methods: iteration**

- Gauss-Seidel (GS)
- Jacobi
- relaxation methods (for GS)

**Gauss-Seidel ~ 2x faster than Jacobi but difficult to parallelize**

### **Convergence speed?**

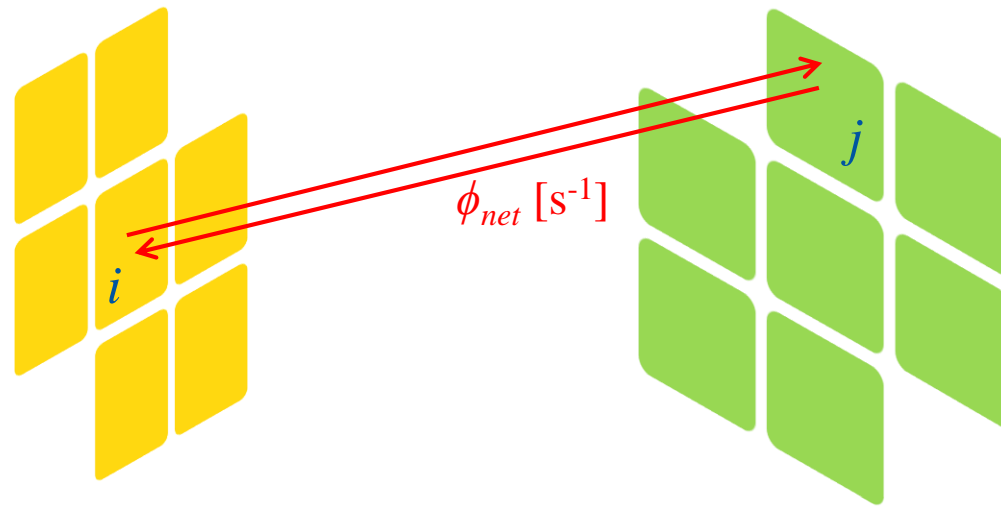
**Calculation of the elements of the AC matrix is  $O(N^2)$  (N being the number of surface elements )**



**Gauss-Seidel and Jacobi convergence speed comparison, L/R=10 circular cross-section tube**

## 5. Angular Coefficients, also called view-factors (VF);

Next 4 slides: "Study, analysis, design and diagnostics of plasma and beam facing components of fusion", E. Sartori, Univ. Padova IT, seminar at CERN, April 2013; See also: Simulation of the gas density distribution in the large vacuum system of a fusion-relevant particle accelerator at different scales - Vacuum 122 (2015) 275-285;



1. pressure distribution  $\mathbf{p}$  at **surfaces**: solving  $\mathbf{p}=\mathbf{M}^{-1} \phi$

a.  $p_i = \Gamma_i (2\pi mk_B T)^{1/2}$

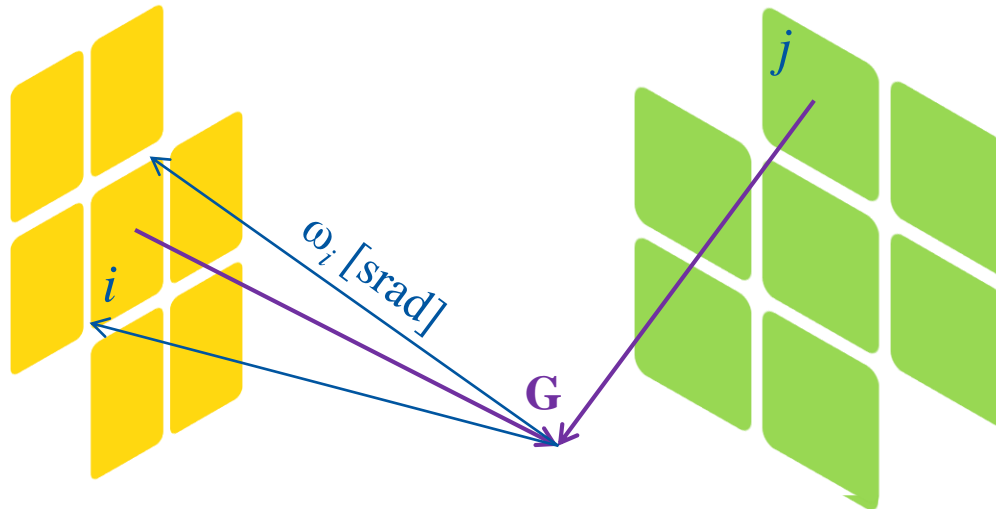
b. reemission cosine law scattering operator

c. very low density: no collisions ( $\lambda L > 0.5$ )

d. view factors  $F_{i \rightarrow j} = F_{j \rightarrow i} \rightarrow$  geometry

e.  $\phi_{net\_i,j} = (\Gamma_i - \Gamma_j) F_{i,j}$

## 5. Angular Coefficients, also called view-factors (VF);



1. pressure distribution  $\mathbf{p}$  at **surfaces**: solving  $\mathbf{p}=\mathbf{M}^{-1} \phi$

2. energy **acomodation** at walls,  $\alpha_E$ :

- different relation between  $\mathbf{p}$  and  $\Gamma$   $\begin{pmatrix} \mathbf{M} & \mathbf{0} \\ \mathbf{0} & \mathbf{M}_T \end{pmatrix} \begin{pmatrix} \mathbf{P} \\ \mathbf{T} \end{pmatrix} = \begin{pmatrix} \phi \\ \phi_T \end{pmatrix}$

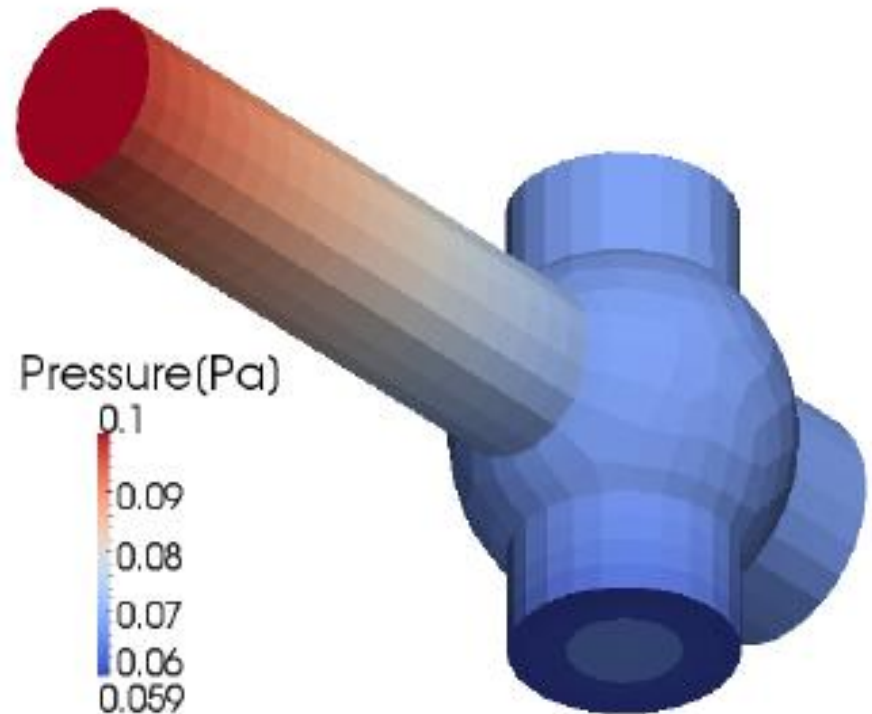
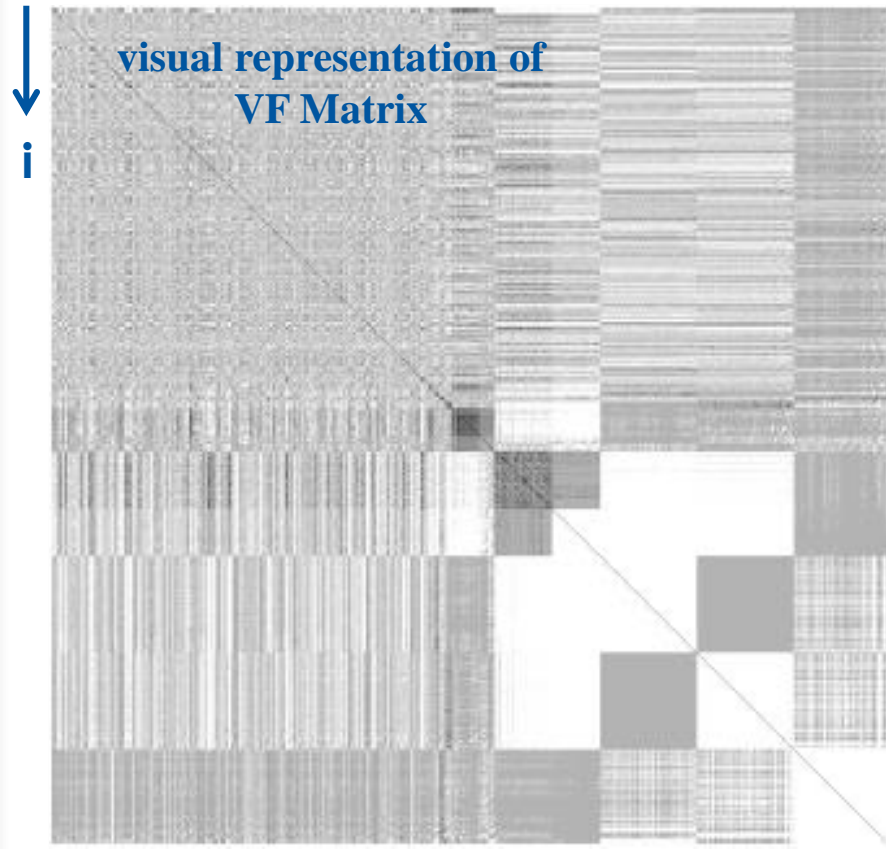
- temperature  $\mathbf{T}$  varies in the domain

( and  $\mathbf{M} = \mathbf{M}(\mathbf{T})$ ,  $\mathbf{M}_T = \mathbf{M}_T(\mathbf{P})$  )

3. extend from surfaces to volume the solution;  $\mathbf{n} = \frac{\sum_i \Gamma_i (2\pi m / (k_B T_{OUT,i}))^{1/2} \omega_i}{\sum_i \omega_i}$

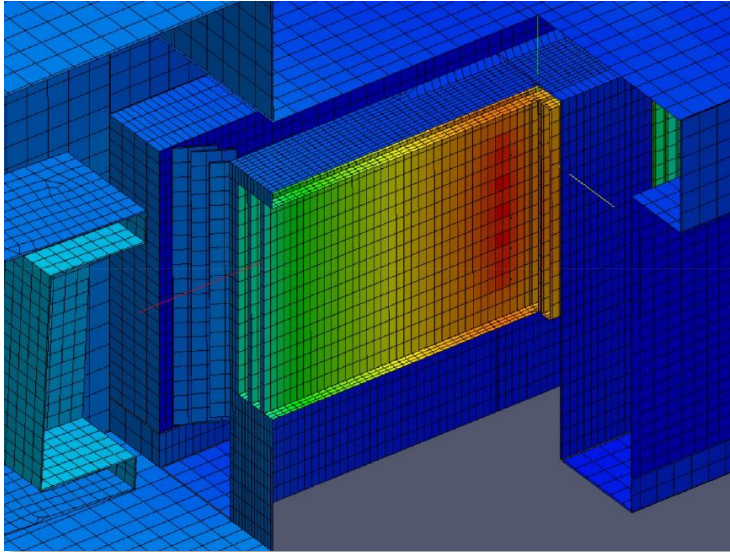
## 5. Angular Coefficients, also called view-factors (VF);

See also: "AVOCADO: A numerical code to calculate gas pressure distribution", Vacuum 90 (2013) 80-88



- Each tiny dot in the VF matrix corresponds to an element; when two elements do not “see” each other, then the corresponding value is zero (white areas in the matrix); Note the symmetry of the matrix: only  $\frac{1}{2}$  of it needs to be evaluated;
- Memory management techniques plus optimized and fast matrix solvers are mandatory;

## 5. Angular Coefficients, also called view-factors (VF);



$$N^3 \rightarrow N^2 \cdot n, \quad n \ll N$$

A diagram illustrating the reduction in complexity. It shows a 2D grid of points with a red outline. A small red octagon is drawn on the grid, representing a localized region. Below the grid, the following calculation is shown:
$$99 \times 4 \rightarrow 1 \times 13 + 13 \times 4$$
$$=$$
$$-84\%$$

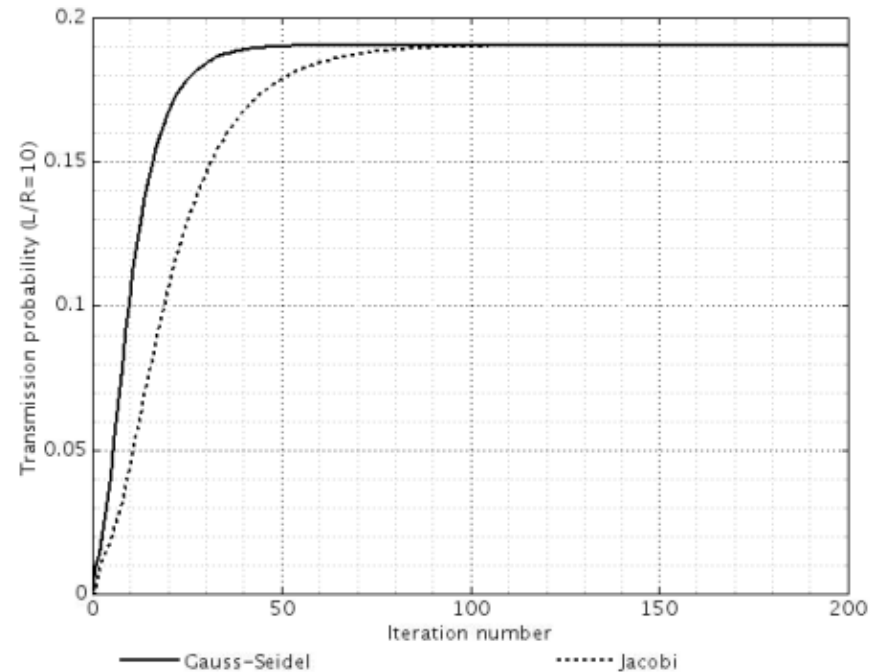
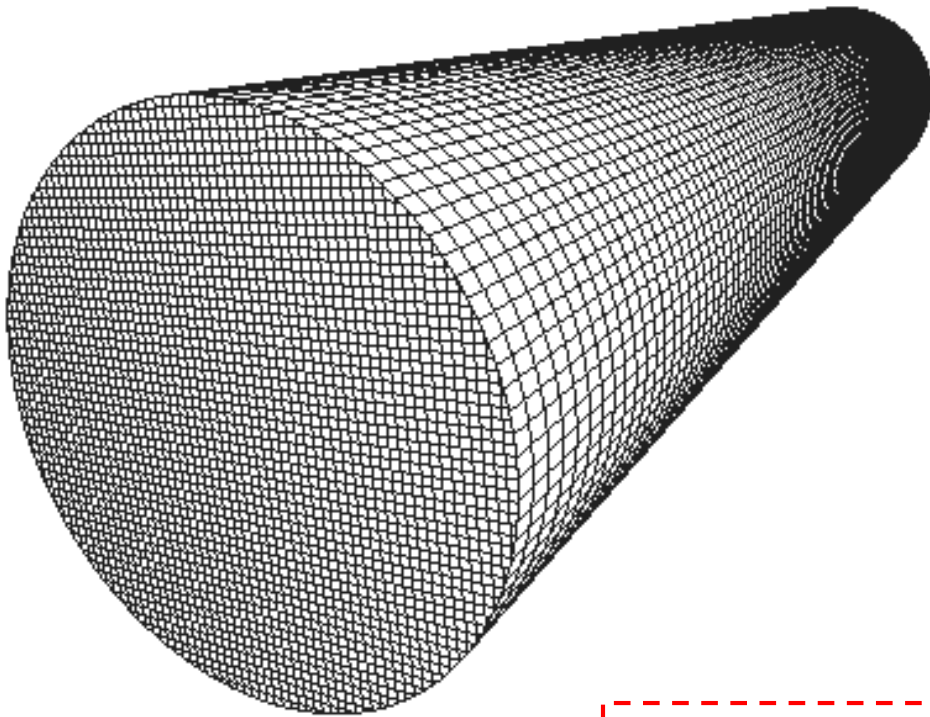
1. ray tracing; hidden surface determination  $N^3$  **complexity**
2. CPU time: **optimization** of algorithms and implementation  
face reconstruction, enclosures, pointer to functions...
3. **parallelization**  
best results with independent processes calculating “slices” of  $M$

**The precise calculation of the VFs requires a ray-tracing technique;**

## 5. Angular Coefficients, also called view-factors (VF);

### Benchmarking with Molflow+ (old version);

Square-grid meshing of the tube used in this example, with  $L/R = 10$ . It has 2827 elements on each end cap facet, and  $100 \times 100$  for the side facets of the tube, generating a 15654<sup>2</sup> matrix (~ 245M elements). Corrections have been made for the elements situated on the edges of the polygons which are partially out-of-bounds of the model.



7'30" to calculate ACs and  
18'30" to run 80 iterations

on 2.4GHz CPU

AC transmission probability calculation for  $L/R=10$ :  
 $W_{Tr}=0.19082662$ , which is outside of the 99.993%  
C.I. indicated above.

10	0.1908990	$\pm 7.70E-05$	0.1909424	0.1909410	0.1909424
----	-----------	----------------	-----------	-----------	-----------

# 5. Angular Coefficients, also called view-factors (VF); **Benchmarking;**

**Texture Scaling**

Texture Range		Current	
Minimum	0.000000	Min:	0.000000
Maximum	0.000020	Max:	0.027224

Auto scale:  Use colormap:  Video Swap: 408KB

Gradient: 0 0.005 0.01 0.015 0.02 0.025

Apply Dismiss

**Process status**

PID	Mem Usage	Mem Peak	CPU	Status
3656	466.05MB	466.12MB	0 %	Waiting: (PIPE10) AC (15568x15568) 81

Restart Process number 1 Change MAX Dismiss

**Simulation**

Mode: Angular Coef Calc AC

#	Density	Des	Abs
1	0.0272239	0.0272239	0.0220581
2	0	0	0.00516537
3	0.0136116	0	0
4	0.0136117	0	0
5	0.0136116	0	0
6	0.0136116	0	0
7	0.0136116	0	0
8	0.0136116	0	0
9	0.0136117	0	0
10	0.0136116	0	0
11	0.0136116	0	0
12	0.0136117	0	0
13	0.0136116	0	0
14	0.0136116	0	0
15	0.0136116	0	0
16	0.0136116	0	0
17	0.0136116	0	0
18	0.0136116	0	0
19	0.0136116	0	0
20	0.0136116	0	0
21	0.0136116	0	0
22	0.0136116	0	0

Color-coded pressure distribution as calculated with Angular Coefficients in Molflow+



## 6. Direct Simulation Monte Carlo (DSMC);

Ref.: “Direct simulation Monte Carlo (DSMC): A numerical method for transition-regime flows—A review”, P.S. Prasanth, J. K. Kakkassery, J. Indian Inst. Sci 2006, **86**, 169-192

- What is it?
- This method takes into account **inter-molecular collisions**, and is therefore useful only in those cases when the study of “**high-pressure**” areas of an accelerator are needed;

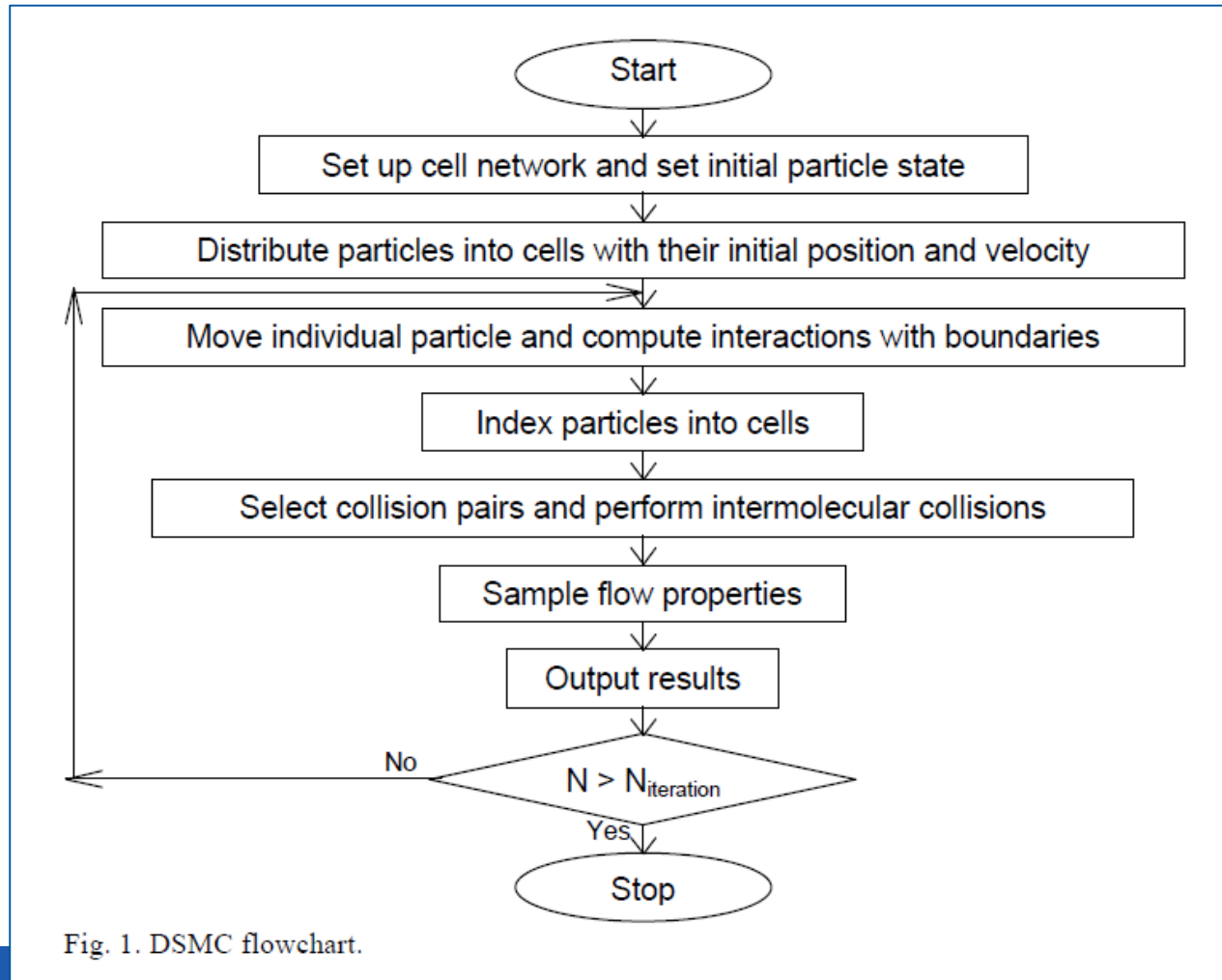


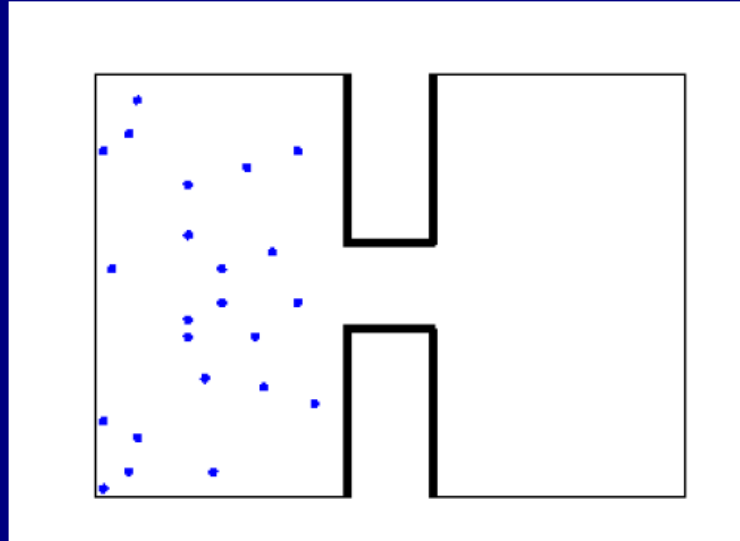
Fig. 1. DSMC flowchart.

## 6. Direct Simulation Monte Carlo (DSMC);

Ref.: “Modeling and calculations of rarefied gas flows – DSMC vs kinetic equation”, F. Sharipov, 51<sup>st</sup> IUVSTA Workshop on Gas Dynamics, Varmdo, Sweden, 9-12 July 2007;  
See also Felix’s web page: <http://fisica.ufpr.br/sharipov/>

- How does it work?

### DSMC, Main ideas

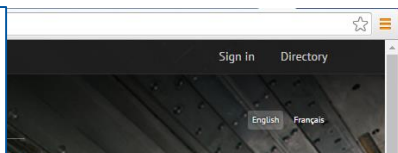
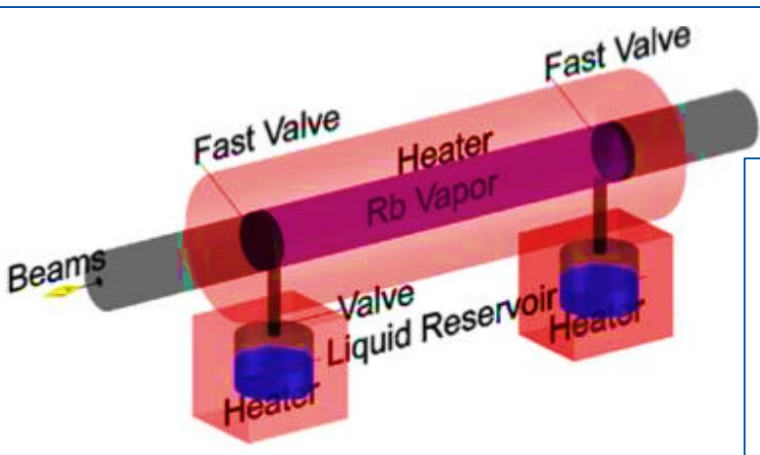


Intermolecular interactions are simulated.  
Macroscopic quantities are calculated.

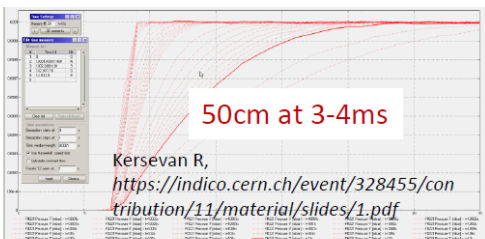
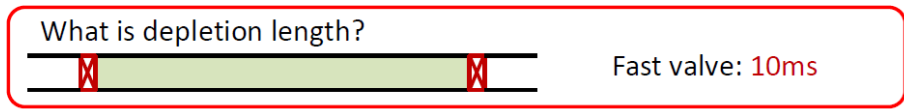
All steps are repeated many times in order to reduce the statistical noise.

## 6. Direct Simulation Monte Carlo (DSMC);

- Some examples can be: **high-pressure areas of proton sources (neutralization), simulation of loss-of-vacuum accidents, neutralization of deuterium ions beams in a neutral beam injectors (tokamaks, like e.g. ITER or JET).** A notable recent example is **the rubidium plasma cell of the AWAKE experiment at CERN:**



### Fast valve, No orifice (iris)

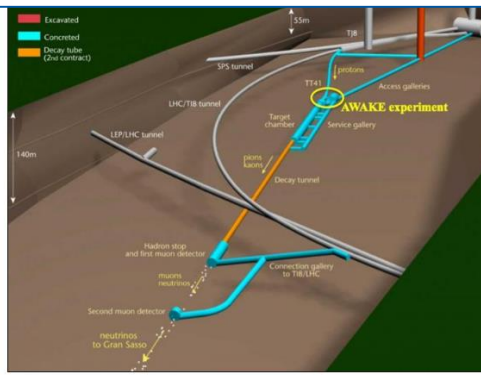


$$f_n(x, t) = \frac{n_0}{2} \left[ 1 + \operatorname{erf} \left( -\frac{x}{t} \sqrt{\frac{m}{2kT}} \right) \right]$$

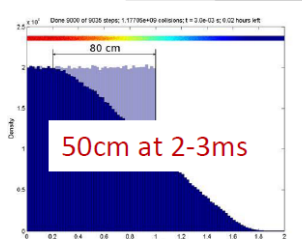
50cm at 1-2ms

$$\frac{n}{n_0} = \left( \frac{2}{\gamma} \right)^{\gamma-1} \left( \frac{2}{\gamma+1} \sqrt{\frac{\gamma}{2}} - \frac{\gamma-1}{\gamma+1} \sqrt{\frac{m}{2kT}} \frac{x}{t} \right)^{2(\gamma-1)}$$

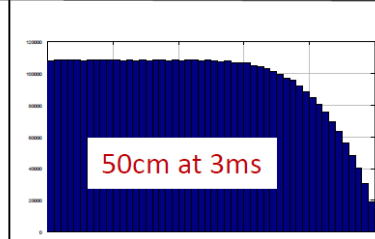
1D Theory (FM+C) + 1D DSMC Petrenko A,  
<https://indico.cern.ch/event/357090/contribution/2/material/slides/2.pdf>



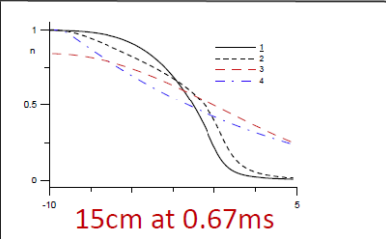
The Proton Driven Plasma Wakefield Acceleration Experiment (AWAKE) is an R&D project based at CERN. It is a proof-of-principle experiment investigating plasma wakefield acceleration by a proton bunch to accelerate charged particles



2D DSMC Petrenko A,  
<https://indico.cern.ch/event/357090/contribution/2/material/slides/2.pdf>



3D DSMC Plyushchev G



Shakhov EM, *Non-stationary rarefied gas flow into vacuum from a circular pipe closed at one end*



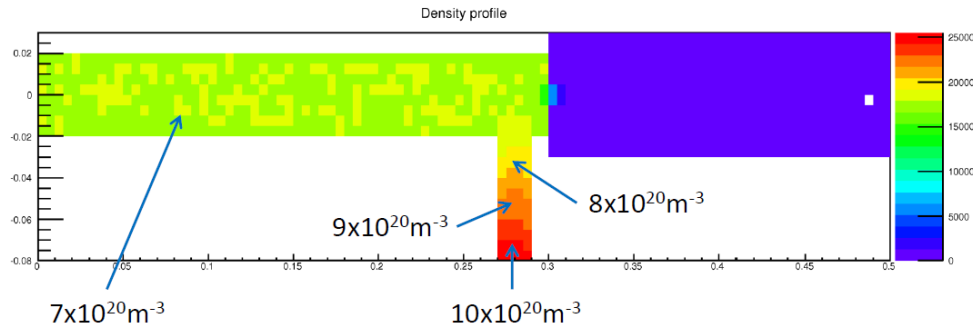
## 6. Direct Simulation Monte Carlo (DSMC);

- The rubidium plasma cell of the AWAKE experiment at CERN (continued):

3D DSMC  
with Source

3D DSMC simulation Double Orifice  
with Source: results

3D DSMC simulation Double Orifice  
with Source (constant density): results

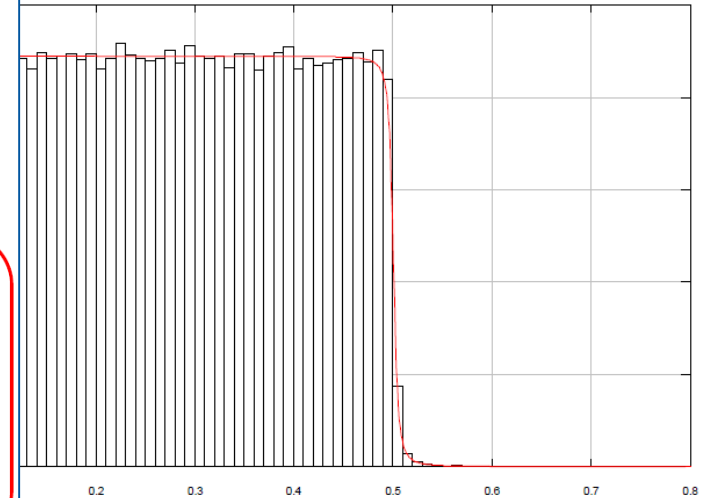


### Conclusions:

- In this case (stationary case) the density near the source is higher than the density in the plasma cell.
- Thus the injection tube (between Rb source and plasma cell) should be very short and should have a large diameter in order to have a smaller density gradient difference.
- The injection tube should be as close as possible to the orifice.

Results are very similar to the simulation with single orifice:

leak rate: 0.52mg/sec  
convergence: 0.5sec



## 6. Direct solutions of the Boltzmann equation;

- Another way of tackling the problem is to find the solution of the Boltzmann equation; There exist a number of methods to solve it, and a short review of some of them can be found in the excellent series of articles on the journal **Vacuum Vol. 109, Pages 1-424 (November 2014)**, « **Advances in Vacuum Gas Dynamics** », Guest Editors: Felix Sharipov and Oleg B. Malyshev;
- It must be said at this point that this kind of solutions are **very rarely applied to solving practical problems of real accelerators' vacuum systems**, or their actual design;
- The DSMC and other methods which include molecular collisions are widely used in the analysis and **design of vacuum pumps**, such as Gaede pumps, **turbomolecular pumps, high-pressure vacuum gauges** (e.g. Pirani), and more...

## 7. Test-Particle Monte Carlo (TPMC);

- The TPMC method is similar to the DSMC, but avoids the cumbersome and sometimes overwhelming complexity of defining density and velocity fields in order to correctly calculate the collision integral in the Boltzmann equation;
- Several vacuum scientists have developed their own code, but in the particle accelerator community the Molflow+ code has become somewhat widespread, and will therefore be used as a template for illustrating how the TPMC method works, without loss of generality;
- The most complete and recent reference for Molflow+ and the companion synchrotron radiation ray-tracing code SYNRAD+ is this:  
Ref. “**Monte Carlo Simulations of Ultra High Vacuum and Synchrotron Radiation for Particle Accelerators**”,  
**M. Ady, PhD thesis EPFL/CERN, May 2016**, <http://cds.cern.ch/record/2157666/files/CERN-THESIS-2016-047.pdf>
- Additional informations, tutorials given in the past, codes and files, and additional documentation can be found here:  
<http://molflow.web.cern.ch/>
- Please visit our web site and give us your feedback.

See also: <https://www.dropbox.com/sh/1vt0x6212x5p5tb/AAD9zFMZ7BUSkww62nUp9wQ-a?dl=0>

## 7. Test-Particle Monte Carlo (TPMC); Flowcharts;

- Ref. “Monte Carlo Simulations of Ultra High Vacuum and Synchrotron Radiation for Particle Accelerators”, M. Ady, PhD thesis EPFL/CERN, May 2016, <http://cds.cern.ch/record/2157666/files/CERN-THESIS-2016-047.pdf>;
- “Monte Carlo method implemented in a finite-element code with application to dynamic vacuum in particle accelerators”, C. Garion, Vacuum 82 (2010) 274-276; see also no.4, slide 18;

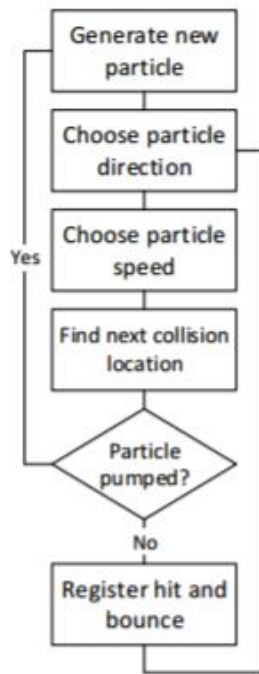


Figure 1.11: Main steps of Molflow's algorithm

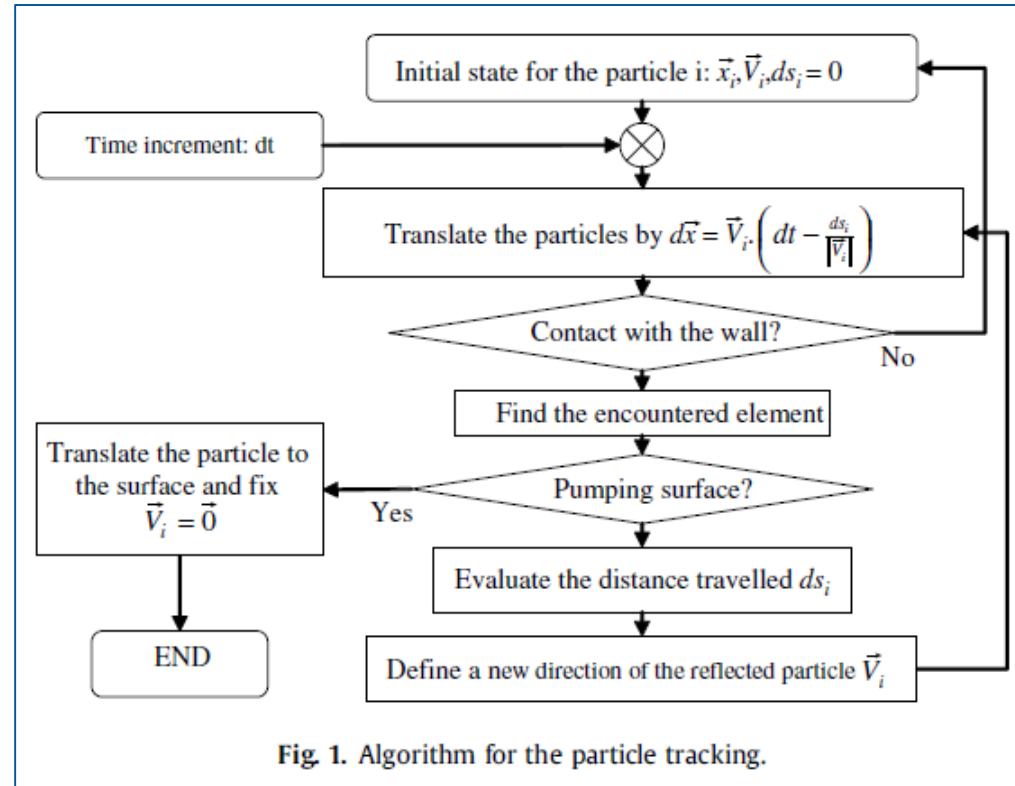


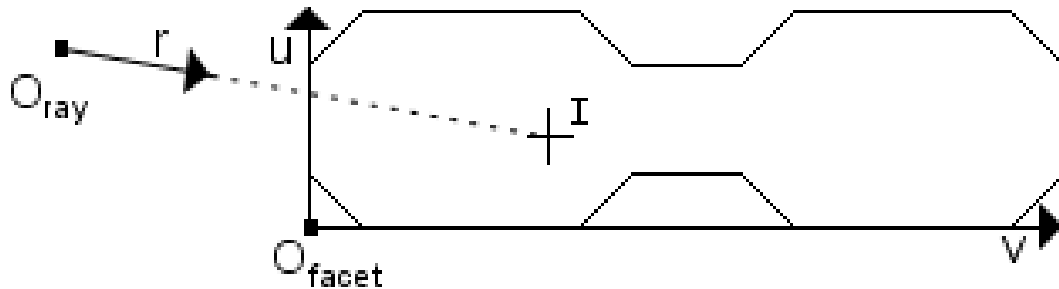
Fig. 1. Algorithm for the particle tracking.

## 7. Test-Particle Monte Carlo (TPMC);

### TPMC: Molflow+ Implementation

#### Ray-plane intersection:

- Use Cramer's rule to find I coordinates.
- $\vec{w} = \vec{u} \wedge \vec{v}$  is **pre-calculated once** for each facet.
- Faster to solve  $I_u$  and  $I_v$  first (best elimination method than solving distance  $I_r$  first).



$$I_u = \frac{(\vec{O}_{fr} \wedge \vec{v}) \cdot \vec{r}}{\vec{w} \cdot \vec{r}} \in [0,1]$$

$$I_v = \frac{(\vec{u} \wedge \vec{O}_{fr}) \cdot \vec{r}}{\vec{w} \cdot \vec{r}} \in [0,1]$$

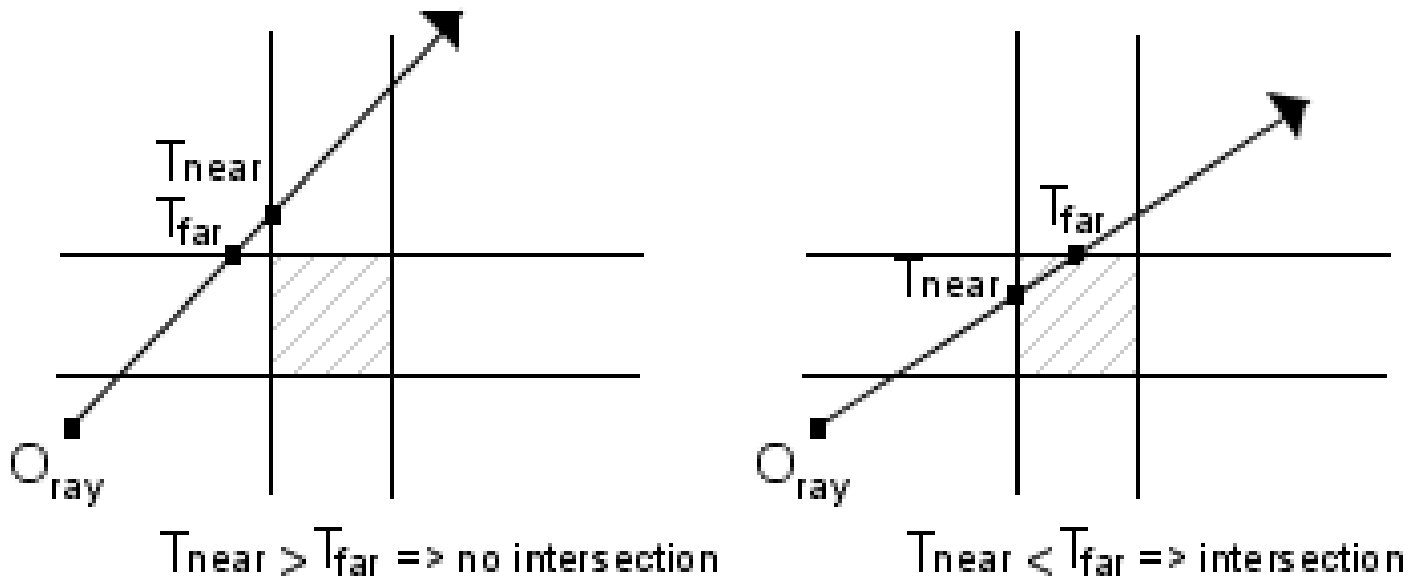
$$I_r = -\frac{\vec{w} \cdot \vec{O}_{fr}}{\vec{w} \cdot \vec{r}} > 0$$

- Jordan curve theorem is used afterwards to check if I falls inside the facet

## 7. Test-Particle Monte Carlo (TPMC);

### AABB Tree optimisation:

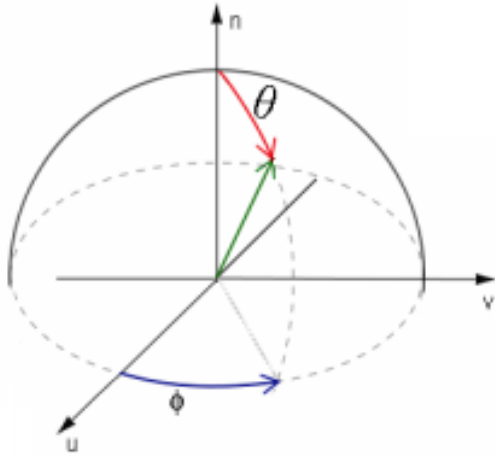
- Use of “**Axis Aligned Bounding Box**” tree structure to speed collision detection
- Box/ray intersection performed using the “**slabs method**”



- Minimum of **8 facets per box** and maximum **tree depth of 5** (using “**best axis**” method for **AABB tree balancing**)
- Result: more than 5 times faster for complex geometries

## 7. Test-Particle Monte Carlo (TPMC);

### Cosine distribution



$$\theta_{gen} = \arccos(\sqrt{1-X})$$

$$\phi_{gen} = 2\pi Y$$

- With  $X$  and  $Y$  uniformly distributed in  $[0,1]$
- Mersenne Twister random number generator: period is  $(2^{19937}-1) \sim 10^{6001}$  (24<sup>th</sup> Mersenne prime number)

**Convergence:** By applying the central limit theorem to the random variable  $X_i$  defined by  $X_i=1$  if the molecule hits the surface (at the  $i$ -th try), 0 otherwise ( $X_i$  follows a Bernoulli distribution), we determine that...

$$\frac{S - Np}{\sqrt{Np(1-p)}}$$

## 7. Test-Particle Monte Carlo (TPMC);

... approaches a standard normal distribution, where  $N$  is the number of generated molecules which have a probability  $p$  to reach the surface and  $S$  the number of successful hits (sum of  $X_i$ ). The confidence interval of a random variable following a standard normal distribution is given by:

$$\Pr(-\alpha < \frac{S - Np}{\sqrt{Np(1-p)}} < \alpha) = \text{erf}\left(\frac{\alpha}{\sqrt{2}}\right)$$

... and can be rewritten as:

$$\Pr\left(-\alpha \frac{1}{\sqrt{N}} \sqrt{p(1-p)} < p - \frac{S}{N} < \alpha \frac{1}{\sqrt{N}} \sqrt{p(1-p)}\right) = \text{erf}\left(\frac{\alpha}{\sqrt{2}}\right)$$

This shows that the convergence speed of  $S/N$  is proportional to  $1/\sqrt{N}$  and means that to increase the accuracy by a factor 10 (to win a decimal), the calculation time has to be multiplied by 100. Useful approximation: From the previous equations, by choosing  $P$  (the probability that  $p$  lies in the interval), we obtain  $\alpha = \sqrt{2} \text{erf}^{-1}(P)$  (see Table 1).

## 7. Test-Particle Monte Carlo (TPMC);

If N is large enough (>10000), the previous eq. can be approximated by:

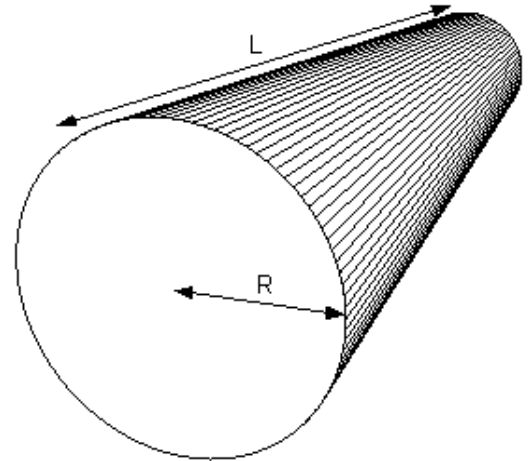
$$\Pr \left( \frac{S}{N} - \alpha \frac{1}{\sqrt{N}} \sqrt{\frac{S}{N} \left( 1 - \frac{S}{N} \right)} < p < \frac{S}{N} + \alpha \frac{1}{\sqrt{N}} \sqrt{\frac{S}{N} \left( 1 - \frac{S}{N} \right)} \right) = P$$

The associated **confidence interval** and **quantile values** are indicated in **Table 1**

<b>P</b>	<b><math>\alpha</math></b>
<b>68.3%</b>	<b>1</b>
<b>95.4%</b>	<b>2</b>
<b>99.7%</b>	<b>3</b>
<b>99.993%</b>	<b>4</b>

## 7. Test-Particle Monte Carlo (TPMC): Benchmarking;

**Table 2** shows the **transmission probability W** of a **cylindrical tube** calculated with the TPMC method (sticking=0). The calculation of this table took **approximately 18 hours on a quad-core 2.4 GHz CPU (total of  $\sim 10^{11}$  hits)**. All calculations have been done using 64-bit double-precision floating points. The values of W are rounded to 7 digits ( $\pm 5E-8$ ).



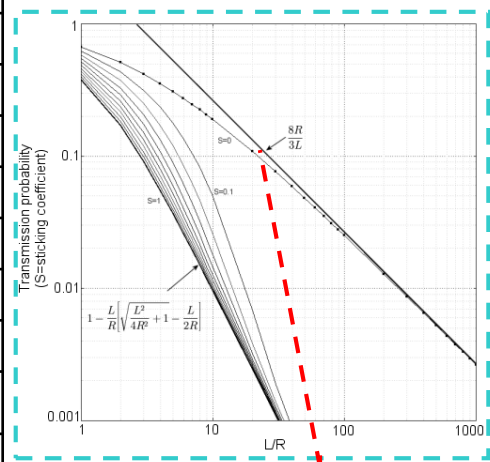
**Note:** The differences between our results and those of [1-3] are due to the statistical error but also to the fact that ***the ray-tracing algorithm which we have implemented considers the tubes' cross-sections as polygons with 100 sides, rather than using an exact analytic expression for their circular cross-section.*** For example, for the L/R=10 case (**0.190899**), the transmission probabilities for  $10^8$  molecules for the cases with polygons with **50** and **25** sides are **0.190807** and **0.190222**, respectively. We made a more accurate test with a tube with **1000** side facets, and we found after  $\sim 10^{10}$  molecules:

$$W_{L/R=10} = \frac{1,866,689,276}{9,776,167,553} = 0.190942848... (\pm 1.5624E-5, 99.993\% \text{ CI})$$

# 7. Test-Particle Monte Carlo (TPMC): Benchmarking;

L/R	$W_{\text{MolFlow+}}$ ( $10^8$ molecules per tube)	Confidence Interval 95%	W[1] Mohan, Tompson, and Loyalka (2007)	W[2] Cole (1977)	W[3] Gómez-Goñi and Lobo (2003)
1	0.6719460	± 9.20E-05	0.6719839	0.6719839	0.6719839
2	0.5141760	± 9.80E-05	0.5142305	0.5142305	0.5142305
3	0.4200210	± 9.67E-05	0.4200554	0.4200553	0.4200554
4	0.3565140	± 9.39E-05	0.3565727	0.3565722	0.3565727
5	0.3104550	± 9.07E-05	0.3105253	0.3105246	0.3105253
6	0.2754060	± 8.76E-05	0.2724388	0.2754382	0.2754388
7	0.2477170	± 8.46E-05	0.2477357	0.2477353	0.2477357
8	0.2252460	± 8.19E-05	0.2252631	0.2252628	0.2252631
9	0.2065980	± 7.94E-05	0.2066414	0.2066407	0.2066414
10	0.1908990	± 7.70E-05	0.1909424	0.1909410	0.1909424
20	0.1092860	± 6.12E-05	0.1093207	0.1093040	0.1093207
30	0.0769090	± 5.22E-05	0.0769378	0.0769120	0.0769378
40	0.0594415	± 4.63E-05	0.0594504	0.0594220	0.0594504
50	0.0484607	± 4.21E-05	0.0484765	0.0484480	0.0484764
60	0.0409377	± 3.88E-05	0.0409393	0.0409130	0.0409393
70	0.0354403	± 3.62E-05	0.0354394	0.0354150	0.0354394
80	0.0312529	± 3.41E-05	0.0312473	0.0312250	0.0312473
90	0.0279465	± 3.23E-05	0.0279452	0.0279250	0.0279452
100	0.0252784	± 3.08E-05	0.0252764	0.0252580	0.0252764
200	0.0129592	± 2.22E-05	0.0129448	--	0.0129448
500	0.0052708	± 1.42E-05	0.0052630	--	0.0052630
1000	0.0026505	± 1.01E-05	0.0026476	0.0026461	0.0026476

**Table 2:**  
Transmission probability calculation for cylindrical tubes with different L/R and Sticking=0  
Compare with Smith and Lewin's paper;



## 7. Test-Particle Monte Carlo (TPMC): Benchmarking;

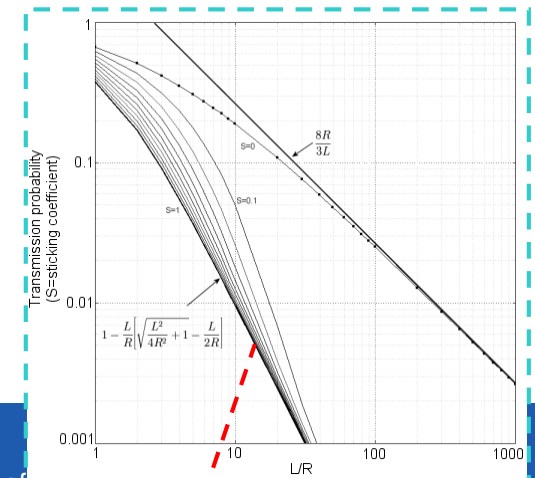
L/R	$W_{\text{moflow+}}$ ( $10^8$ molecules per tube)	95% C.I.	$W_{\text{exact}}$ (rounding 8 digits)
1	0.38191984	± 9.52E-05	0.38196601
2	0.17156285	± 7.39E-05	0.17157288
3	0.09167758	± 5.66E-05	0.09167309
4	0.05573967	± 4.50E-05	0.05572809
5	0.03709115	± 3.70E-05	0.03708798
6	0.02631460	± 3.14E-05	0.02633404
7	0.01960858	± 2.72E-05	0.01961539
8	0.01514748	± 2.39E-05	0.01515500
9	0.01204008	± 2.14E-05	0.01204994
10	0.00979321	± 1.93E-05	0.00980486
20	0.00248444	± 9.76E-06	0.00248758
30	0.00110761	± 6.52E-06	0.00110865
40	0.00062576	± 4.90E-06	0.00062422
50	0.00040022	± 3.92E-06	0.00039968
60	0.00027787	± 3.27E-06	0.00027762
70	0.00020439	± 2.80E-06	0.00020400
80	0.00015629	± 2.45E-06	0.00015620
90	0.00012341	± 2.18E-06	0.00012343
100	0.00010023	± 1.96E-06	0.00009998
200	0.00002477	± 9.76E-07	0.00002500
300	0.00001085	± 6.46E-07	0.00001111
400	0.00000558	± 4.63E-07	0.00000625
500	0.00000374	± 3.79E-07	0.00000400
600	0.00000253	± 3.12E-07	0.00000278
700	0.00000180	± 2.63E-07	0.00000204
800	0.00000143	± 2.34E-07	0.00000156
900	0.00000113	± 2.08E-07	0.00000123
1000	0.00000089	± 1.85E-07	0.00000100

**Table 3: Comparison between TPMC simulations and exact results for tubes with a sticking of 1 (i.e. direct inlet to outlet transmission only).**

**Note:** after  $10^8$  molecules, 27 out of 28 (~96.4%) values in this table lay in the 95% confidence interval. We have used the expression

$$1 - \frac{L}{R} \left[ \sqrt{\frac{L^2}{4R^2} + 1} - \frac{L}{2R} \right]$$

to calculate  $W_{\text{exact}}$ .



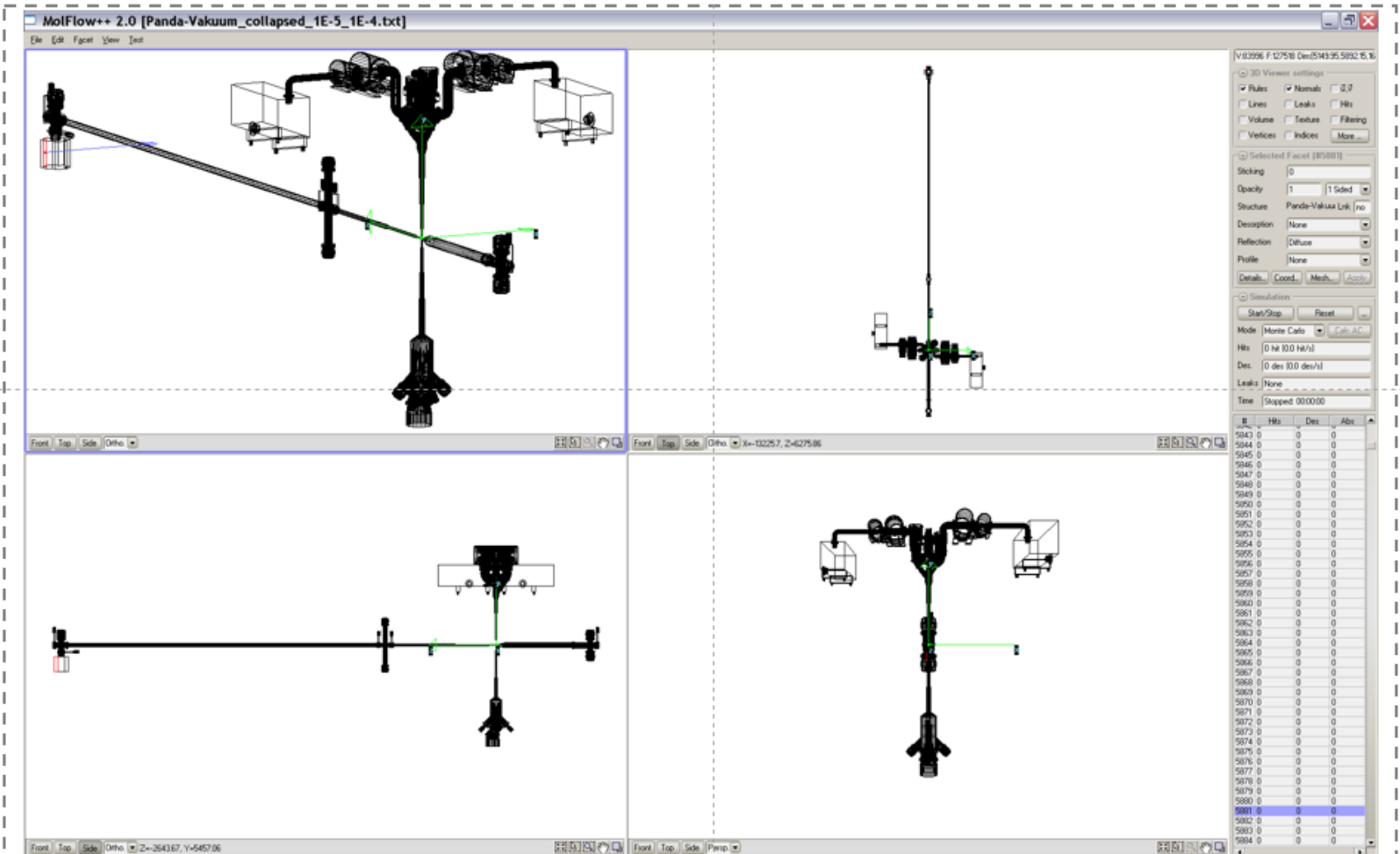
## 7. Test-Particle Monte Carlo (TPMC): Benchmarking;

- Apart from validation, solutions are higher

Another

# PANDA experiment at GSI

Four-pane view of the Molflow+ standard screen. Each pane can show independent views, in "orthographic" or "perspective" mode



**Geometry: 127,518 facets, ~ 84,000 vertices**  
(STL file courtesy of A. Gruber, PANDA Exp., GSI Lab., personal comm.)



# 7. Test-Particle Monte Carlo; Seminal papers:

## Monte Carlo Calculation of Molecular Flow Rates through a Cylindrical Elbow and Pipes of Other Shapes\*

D. H. DAVIS

Lawrence Radiation Laboratory, University of California, Livermore, California

(Received February 23, 1960; and in final form March 4, 1960)

A method is devised for the calculation of molecular flow rates through pipes where the mean free path for intermolecular collisions is large compared to the dimensions of the pipes. Results of the calculation are given for a straight cylindrical pipe, a cylindrical elbow, the annulus between two concentric cylinders, a straight cylindrical pipe with restricted openings, and a straight cylindrical pipe with restricted openings and a plate to block the direct beam between the openings.

### INTRODUCTION

THE problem<sup>1</sup> of this paper is the calculation of molecular flow rates through isolated parts of vacuum systems, for example, the calculation of flow rates from a vacuum tank through a connector to a pump. The problem is one of classical kinetic theory, general analysis of which was developed by H. A. Lorentz<sup>2</sup> and P. Clausing.<sup>3</sup> An excellent account of the historical development of the problem is given by T. D. Lee<sup>4</sup>

The purpose of this paper is to describe a method of calculating flow rates in complicated connectors in vacuum systems which is not beset by the difficulties of complicated integrals in the usual ways. The method is illustrated through the example of the cylindrical elbow. Although only the calculation of the elbow is described in detail, the results for other shapes are given. A calculation for a straight pipe was made for comparison with Clausing's.<sup>3</sup>

The purpose of this paper is to describe a method of calculating flow rates in complicated connectors in vacuum systems which is not beset by the difficulties of complicated integrals in the usual ways. The method is illustrated through the example of the cylindrical elbow. Although only the calculation of the elbow is described in detail, the results for other shapes are given. A calculation for a straight pipe was made for comparison with Clausing's.<sup>3</sup>

The purpose of this paper is to describe a method of calculating flow rates in complicated connectors in vacuum systems which is not beset by the difficulties of complicated integrals in the usual ways. The method is illustrated through the example of the cylindrical elbow. Although only the calculation of the elbow is described in detail, the results for other shapes are given. A calculation for a straight pipe was made for comparison with Clausing's.<sup>3</sup>

The purpose of this paper is to describe a method of calculating flow rates in complicated connectors in vacuum systems which is not beset by the difficulties of complicated integrals in the usual ways. The method is illustrated through the example of the cylindrical elbow. Although only the calculation of the elbow is described in detail, the results for other shapes are given. A calculation for a straight pipe was made for comparison with Clausing's.<sup>3</sup>

The purpose of this paper is to describe a method of calculating flow rates in complicated connectors in vacuum systems which is not beset by the difficulties of complicated integrals in the usual ways. The method is illustrated through the example of the cylindrical elbow. Although only the calculation of the elbow is described in detail, the results for other shapes are given. A calculation for a straight pipe was made for comparison with Clausing's.<sup>3</sup>

The purpose of this paper is to describe a method of calculating flow rates in complicated connectors in vacuum systems which is not beset by the difficulties of complicated integrals in the usual ways. The method is illustrated through the example of the cylindrical elbow. Although only the calculation of the elbow is described in detail, the results for other shapes are given. A calculation for a straight pipe was made for comparison with Clausing's.<sup>3</sup>

flow rate through a pipe with two openings:

$$F_i = K_i P_{i \rightarrow j} - K_j P_{j \rightarrow i} \quad i, j = 1, 2, \quad i \neq j \quad (1)$$

where  $F_i$  is the net number of molecules per unit time that flow through opening  $i$ ,  $K_i$  is the number of molecules that enter the pipe per unit time through opening  $i$ , and  $P_{i \rightarrow j}$  is the probability that a molecule entering opening  $i$  will leave by opening  $j$ . The extension of Eq. (1) to a pipe with several openings is

$$F_i = \sum_{j=1}^M [K_i P_{i \rightarrow j} - K_j P_{j \rightarrow i}] \quad (2)$$

$i, j = 1, 2, \dots, M.$

From assumptions (2) and (3), the probabilities  $P_{i \rightarrow j}$  are independent of the flow in the rest of the system. These probabilities depend only on the distribution of the position and angle at which the molecules enter the pipe at an opening, and the mechanics of a single molecule in the pipe. The effect on the flow rate of such quantities as the pressure and temperature of the gas is contained in the factors  $K_i$ . The geometrical dependence of the flow rate is contained in the factors  $P_{i \rightarrow j}$ .

The purpose of this paper is to illustrate how the factors  $P_{i \rightarrow j}$  can be calculated and to give values for several cases. Before this can be done, however, the distributions of the position and angle at which the molecules enter the pipe at the openings, and the mechanics of molecules in the pipe need to be specified. For their specification additional assumptions are necessary.

The distribution of the position and angle is based on the assumption that the openings are connected to large containers in which the gas is Maxwellian. From this assumption, the probability that a molecule enters an elementary area of an opening is proportional to this area; the probability that a molecule enters in an elementary solid angle is proportional to the cosine of the angle with respect to the normal to the surface (cosine law).

The mechanics of the molecules in the pipe is based

## Monte Carlo Calculation of Molecular Flow Rates through a Cylindrical Elbow and Pipes of Other Shapes

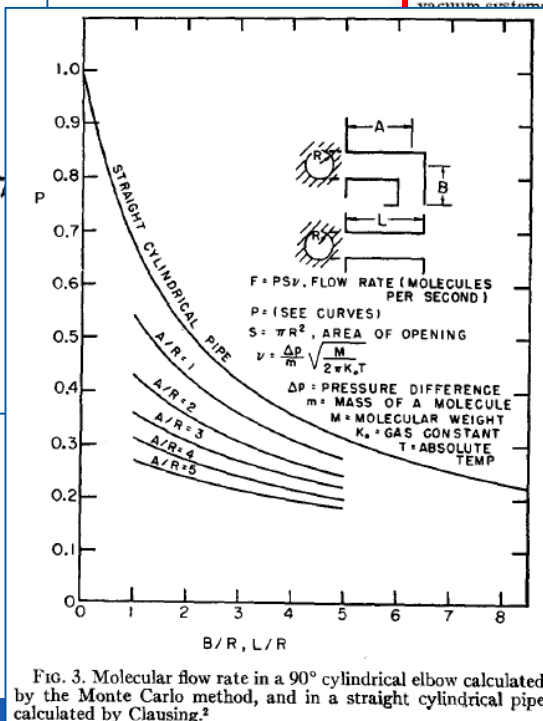
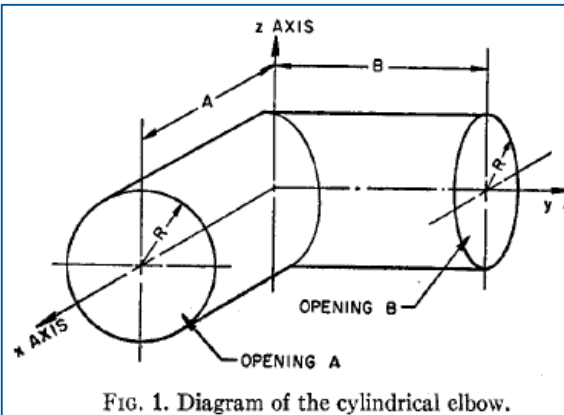
D. H. Davis

Citation: Journal of Applied Physics 31, 1169 (1960); doi: 10.1063/1.1735797

View online: <http://dx.doi.org/10.1063/1.1735797>

View Table of Contents: <http://aip.scitation.org/toc/jap/31/7>

Published by the American Institute of Physics



# 7. Test-Particle Monte Carlo;

## Seminal papers:

### Monte Carlo Calculation of Molecular Flow Rates through a Cylindrical Elbow and Pipes of Other Shapes

D. H. Davis

Citation: *Journal of Applied Physics* 31, 1169 (1960); doi: 10.1063/1.1735797

View online: <http://dx.doi.org/10.1063/1.1735797>

View Table of Contents: <http://aip.scitation.org/toc/jap/31/7>

Published by the American Institute of Physics

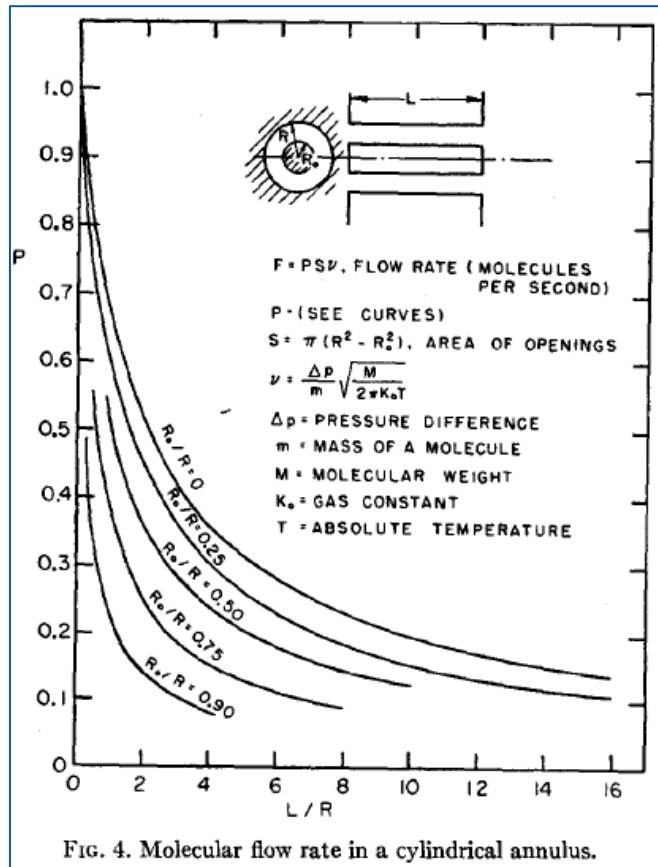


FIG. 4. Molecular flow rate in a cylindrical annulus.

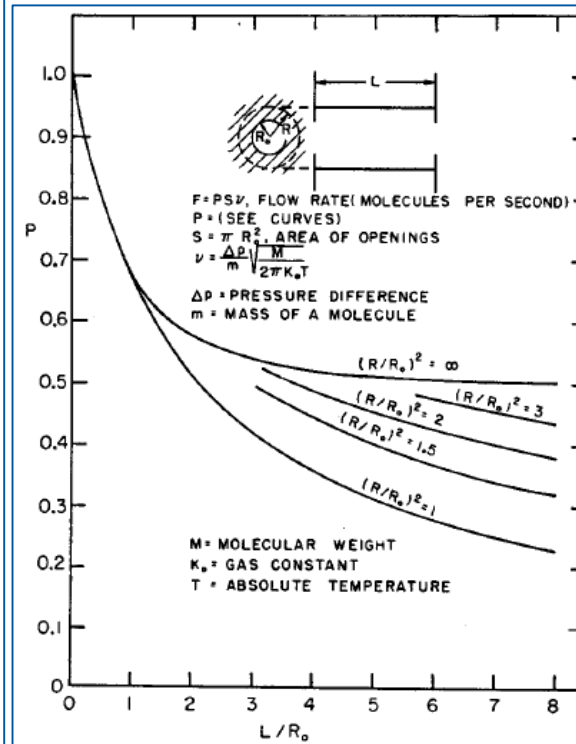


FIG. 5. Molecular flow rate in a cylindrical pipe with restricted openings.

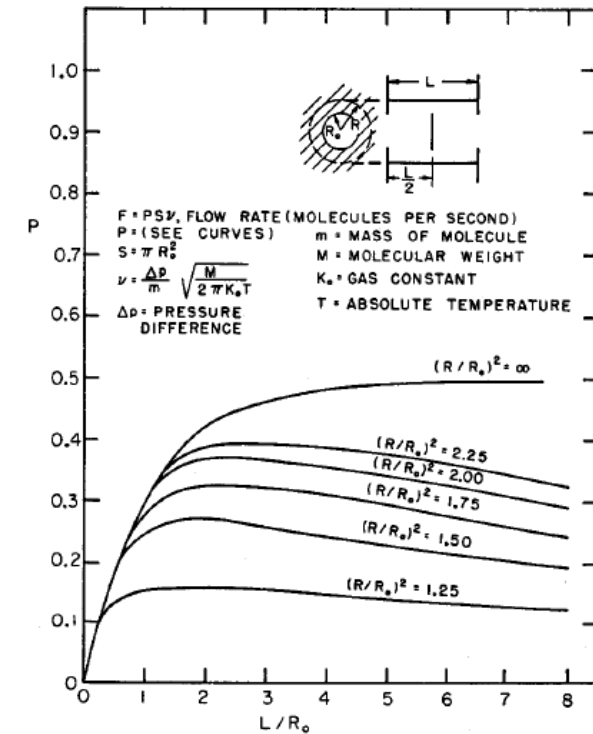


FIG. 6. Molecular flow rate in a cylindrical pipe with restricted openings and a central blocking plate.

Long tubes, elbows, baffles, restricted openings... these are the building blocks necessary to properly design and build the vacuum system of accelerators and their components, such as pumps, tapers, beam-screens, bellows, etc...

## 7. Test-Particle Monte Carlo; Seminal papers:

### Free Molecular Conductance of a Cylindrical Tube with Wall Sorption

Craig G. Smith and Gerhard Lewin

Plasma Physics Laboratory, Princeton University, Princeton, New Jersey  
(Received 26 October 1965)

A Monte Carlo method was used to calculate the probability that a molecule passes through a cylindrical tube with wall sorption. This probability is presented as a function of the ratio of length to radius and the sticking coefficient  $s$  of the wall. For  $s = 0$ , the results confirm those of Clausing for the conductance of a tube of finite length. For  $s \neq 0$ , wall pumping can greatly reduce the flow of gas, even for very small values of  $s$ . The backscattering, total flux retained by the wall, and its distribution along the tube also are presented. Finally, the collimation of the emerging beam is investigated.

The conductances, in the absence of wall sorption, of tubes and a variety of other geometries have been calculated for the free molecular flow regime. Analytic expressions for the simpler geometries were derived by Clausing.<sup>1</sup> Integral equations have been derived and solved numerically for the conductance of tapered tubes and slots by Riehley and Reynolds.<sup>2</sup> More complicated situations have been treated numerically by Davis<sup>3</sup> and Chubb<sup>4</sup> with a Monte Carlo technique, which consists of tracing the random walk of many independent particles and performing the appropriate averages.

Here we employ this technique to investigate the case of a cylindrical tube of finite length with partially adsorbing walls. The latter feature is characterized by a parameter, the sticking coefficient  $s$ , which is here defined as the probability, per individual collision with the wall, that a particle is permanently adsorbed by the wall.<sup>5</sup> We determine the probability that a particle either emerges at the exit aperture, is scattered back through the entrance aperture, or sticks to the wall. In addition, the axial distribution of adsorbed molecules on the wall is calculated, as is the profile of the emerging beam. To obtain actual fluxes, one multiplies the appropriate probability by the flux through the entrance aperture. The conductance of the tube is the flux through the tube per unit pressure difference across it.

This information is desired for a number of problems. If, for instance, it is required to pass a beam of charged particles from a high to a low pressure chamber, then the connection must be optically transparent, and the usual condensation traps may not be employed.

<sup>1</sup> P. Clausing, *Ann. Physik* **7**, 961 (1932).

<sup>2</sup> E. A. Riehley and T. W. Reynolds, *NASA Tech. Note D-2330* (1964).

<sup>3</sup> D. H. Davis, *J. Appl. Phys.* **31**, 1169 (1960).

<sup>4</sup> J. N. Chubb, *Culham Laboratory* (unpublished).

<sup>5</sup> A particle which, in an actual situation, is first adsorbed and then later re-emitted is considered here to have been reflected. Time does not explicitly enter in the Monte Carlo technique, since only the particle trajectories are of interest.

Some pumping action can be obtained by a straight tube with adsorbing walls, and this was the motivation for the present investigation. The results also will be of interest to those concerned with measuring the pumping speed of cryogenic surfaces or other pumps located at the end of a tube and perpendicular to the axis,<sup>6</sup> and to those who must appraise the collimating effect of such a tube in molecular beam devices.

The following assumptions have been made in treating this problem:

- (1) The flow is steady; transient phenomena are excluded.
- (2) Free molecular conditions prevail; there are no collisions between particles.
- (3) The particles enter the tube by molecular effusion from a large chamber. The consequences of this assumption are that the input flux is given by

$$F = \frac{1}{4} N \bar{v} A, \quad (1)$$

where  $N$  and  $\bar{v}$  are the mean density and molecular speed of the particles in the chamber, respectively, and  $A$  is the area of the entrance aperture. And a second consequence is that the particles enter with a velocity directed according to the *cosine law*

$$p \, d\omega = \pi^{-1} \cos \theta \, d\omega = \pi^{-1} \cos \theta \sin \theta \, d\theta \, d\phi, \quad (2)$$

where  $p \, d\omega$  is the probability that a particle enters within the elementary solid angle  $d\omega$  about  $\theta$  and  $\phi$ , the polar and azimuthal angles with respect to the normal to the entrance plane.

(4) For each individual collision of a particle with the tube wall, the probability that the particle is adsorbed by the wall is given by  $s$ , and  $(1 - s)$  is the probability that the particle leaves the wall.

(5) Reflection is diffuse, according to the cosine law, Eq. (2), where the angles are now, with respect to the normal to the tube wall, at the point of impact. The

<sup>6</sup> W. W. Stickney and B. B. Dayton, *Trans. Natl. Ac. Symp. Ser.*, **100** (1964).

The virtue of the Monte Carlo technique is that, with relatively little effort, one may treat extremely complicated situations. This technique has been described in detail elsewhere<sup>3</sup>; here we briefly outline its features. By Assumption (2), particles interact solely with the tube walls, and, therefore, the history of a particle as it bounces down the tube is an event which is statistically independent of the histories of other particles. Thus, one may generate numerically, one by one, a large number of typical particle trajectories, average these paths, and thereby obtain estimates for the probability of various events. Since the trajectories are random in nature, all decisions—such as the starting coordinates in the entrance plane or the direction of reflection, for example—are governed by probability laws. For the actual computation with an electronic

<sup>5</sup> A particle which, in an actual situation, is first adsorbed and then later re-emitted is considered here to have been reflected. Time does not explicitly enter in the Monte Carlo technique, since only the particle trajectories are of interest.

## 7. Test-Particle Monte Carlo; Seminal papers: Smith and Lewin's

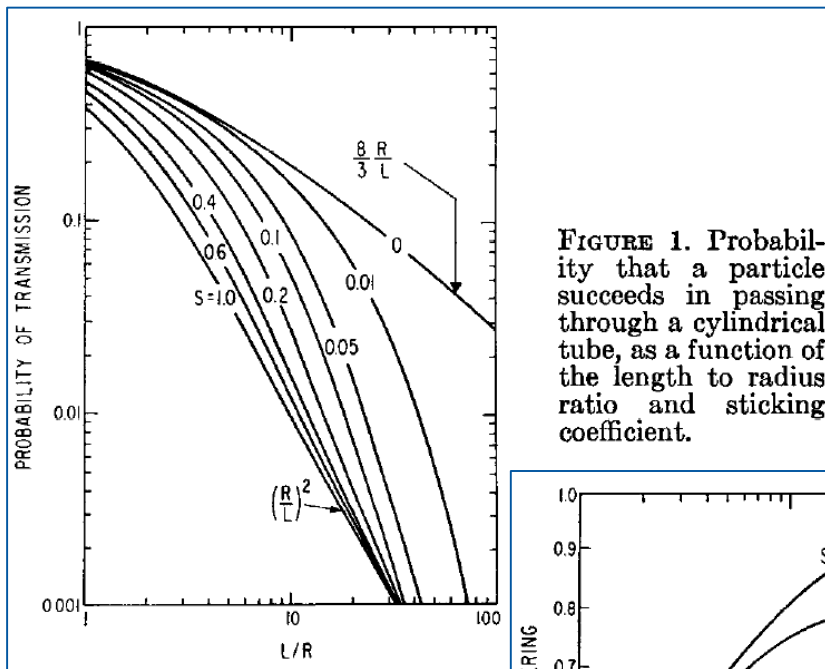


**FIGURE 1.** Probability that a particle succeeds in passing through a cylindrical tube, as a function of the length to radius ratio and sticking coefficient.

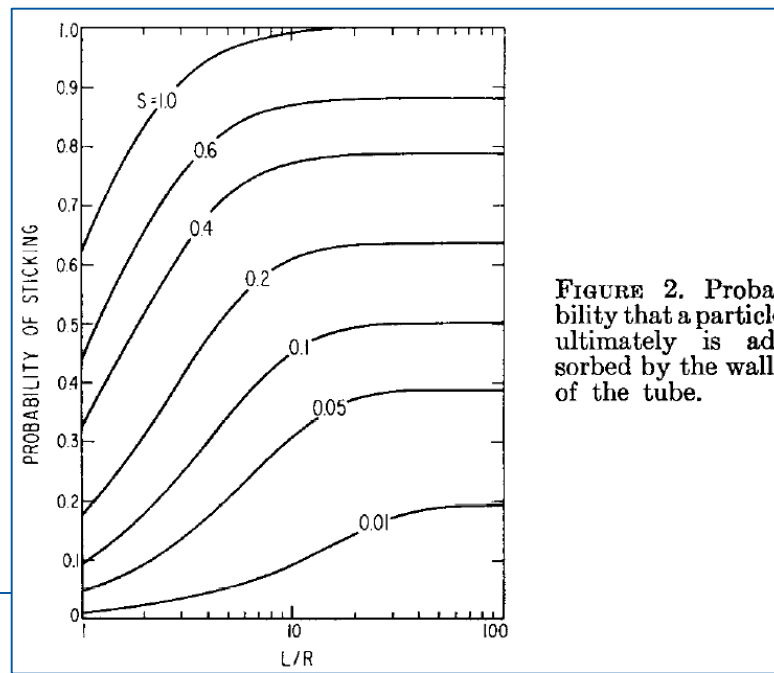


**FIGURE 2.** Probability that a particle ultimately is adsorbed by the walls of the tube.

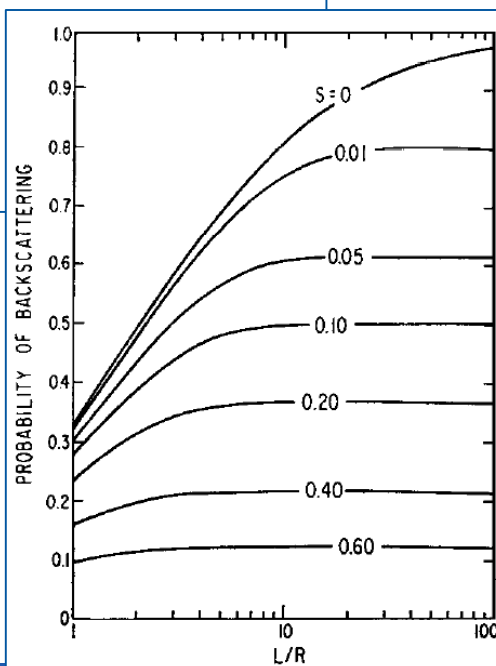
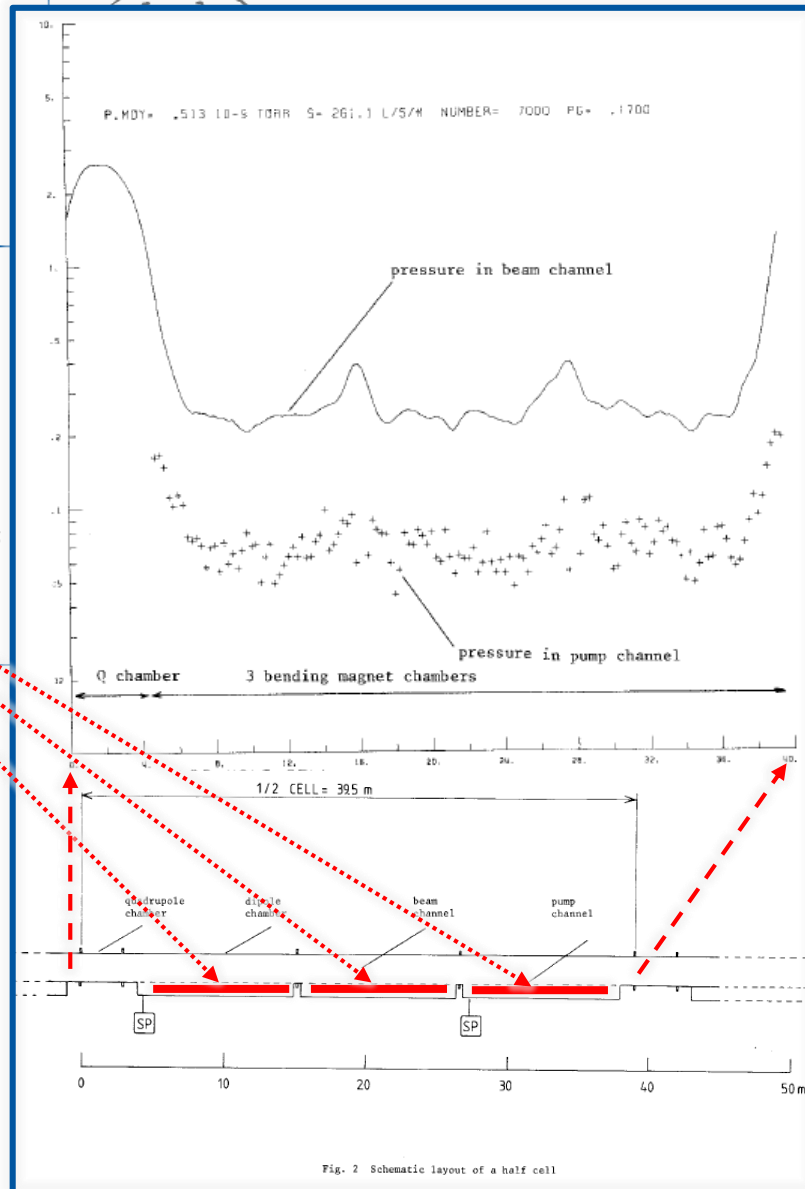
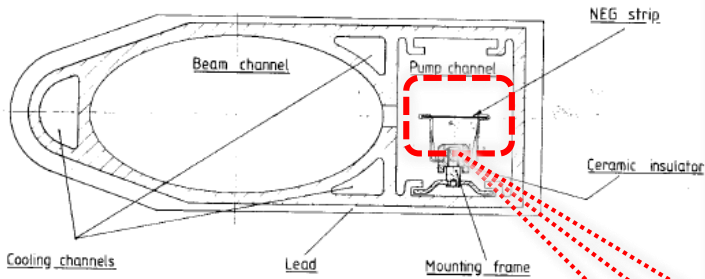


**FIGURE 3.** Probability that a particle is backscattered from the tube.

# 7. Test-Particle Monte Carlo; Seminal papers: LEP pressure profile;

Fig1 - CROSS - SECTION OF THE DIPOLE VACUUM CHAMBER



ARCH

CERN-LEP-VA/86-02

EFFECTIVE PUMPING SPEED

(LEP)

chner

ure distribution in the  
been calculated. The  
orce of degassing and of  
in a half cell of LEP  
connection between the  
se of the average pres-  
average pressure due to  
stronger. The pressure  
ective linear pumping  
in the attached figures

\*present address: Radio Electronics Dept.,  
Sichuan University  
Chengdu, China.

# 7. Test-Particle Monte Carlo; A more recent paper, with time-dependent TPMC

JOURNAL OF  
**Application**  
 Yusuke Suetsugu  
 Citation: J. Vac. Technol. Ser. A  
 View online: <http://dx.doi.org/10.1116/1.3598888>  
 View Table of Contents  
 Published by the American Vacuum Society

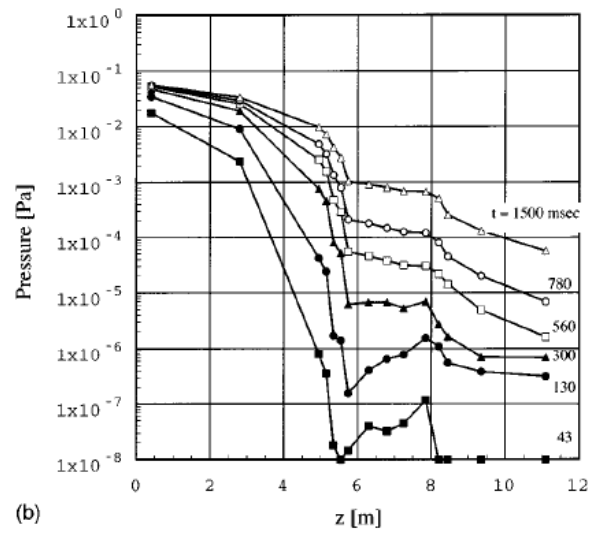
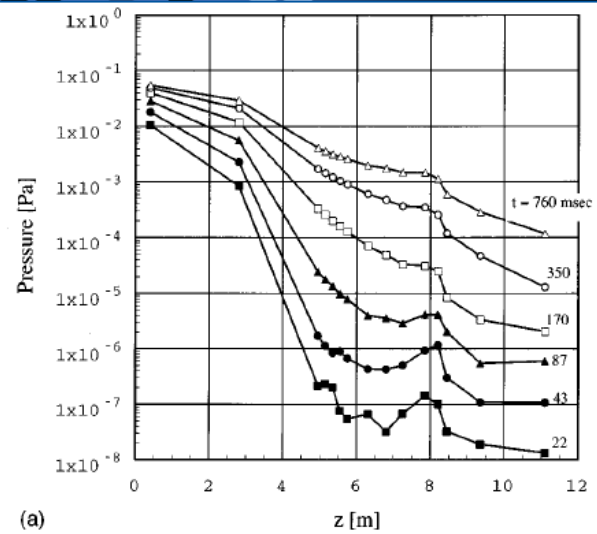


FIG. 3. Pressure profile at some different time along the model beam line in Fig. 2 for cases (a) without and (b) with ADL. The pressures of the ADL sections are plotted at  $z=4.95-5.75$  m. The peaks of pressure due to the intruding gas component can be seen at  $z=7.85$  m ( $R_{11}$ ) for both cases at early stages of gas desorption until the pressure reaches about  $1 \times 10^{-5}$  Pa.

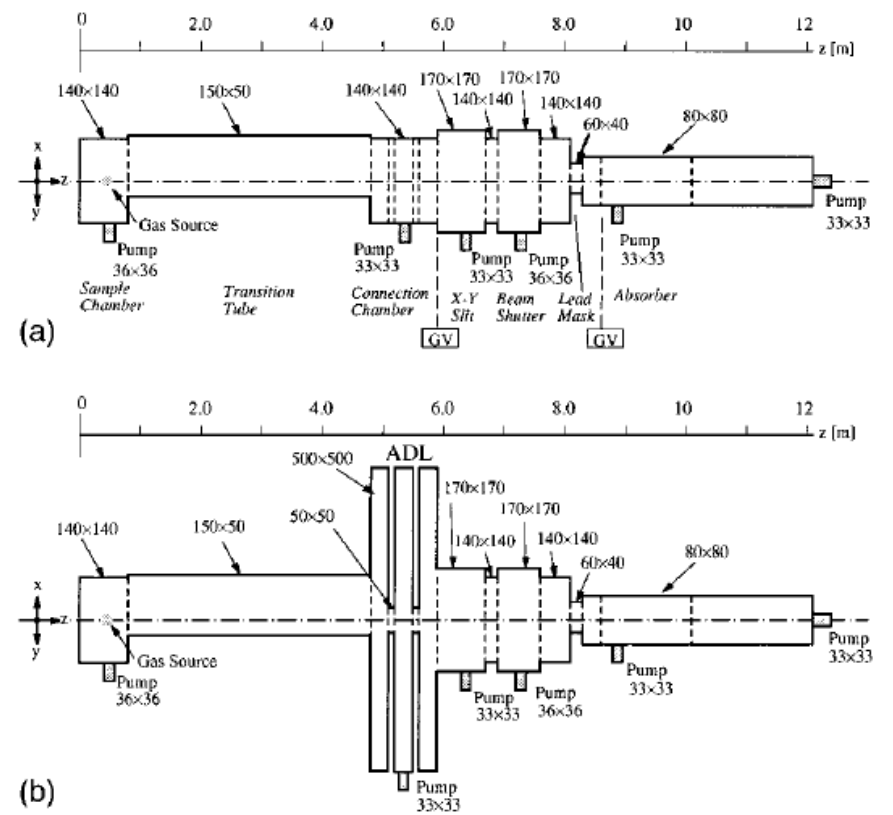
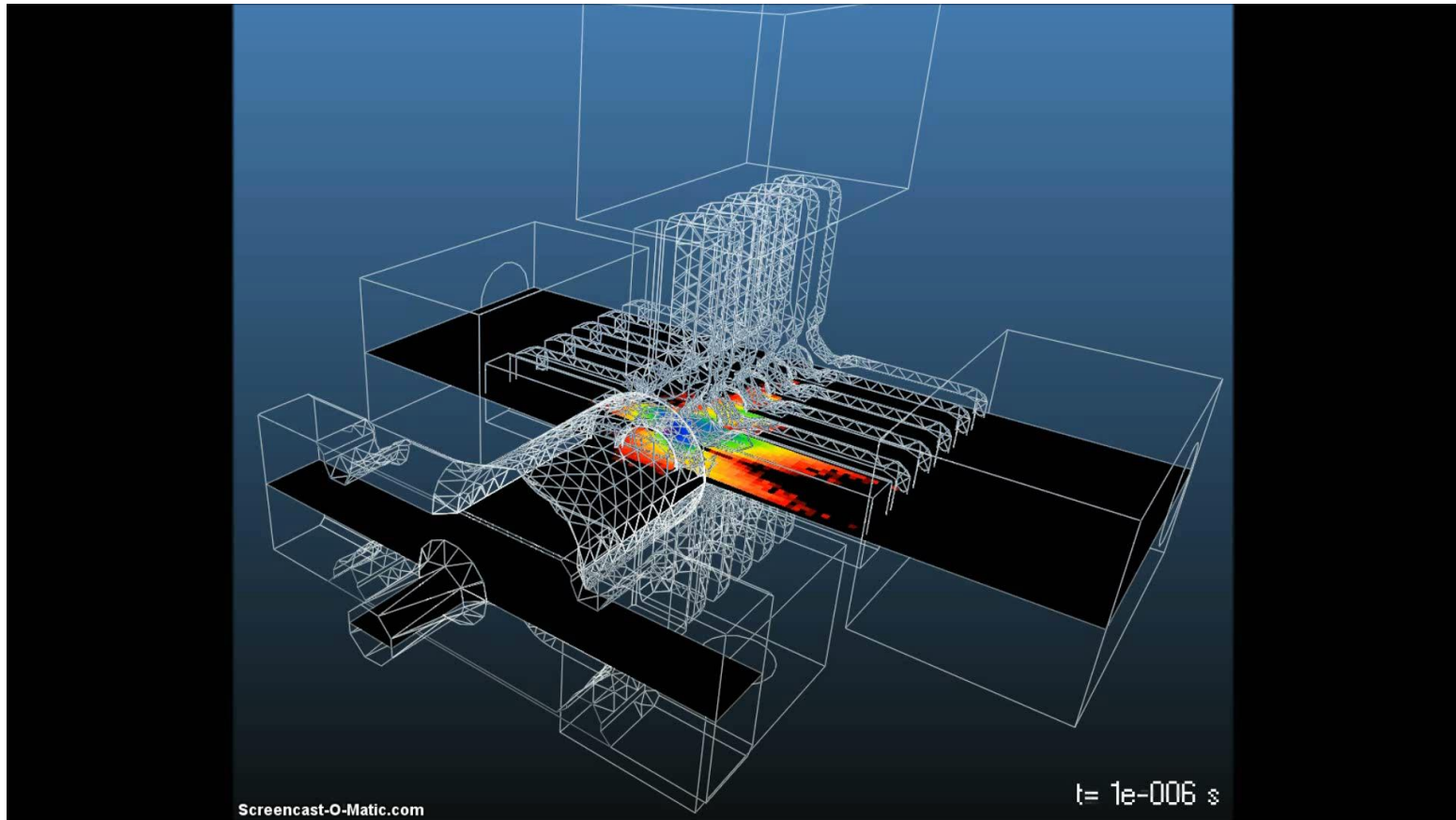


FIG. 2. Model beam lines for calculating the pressure propagation for cases (a) without and (b) with an ADL. The beam lines are divided into 15 regions, which are drawn by broken lines. Regions  $R_3-R_7$  ( $z=4.8-5.9$  m) in (b) correspond to the ADL. A gas source is set in region  $R_1$  (the most left-hand side). The numbers are the cross sections of the chambers and the pump ports in mm. The scale of the  $x$  and  $y$  directions is enlarged.

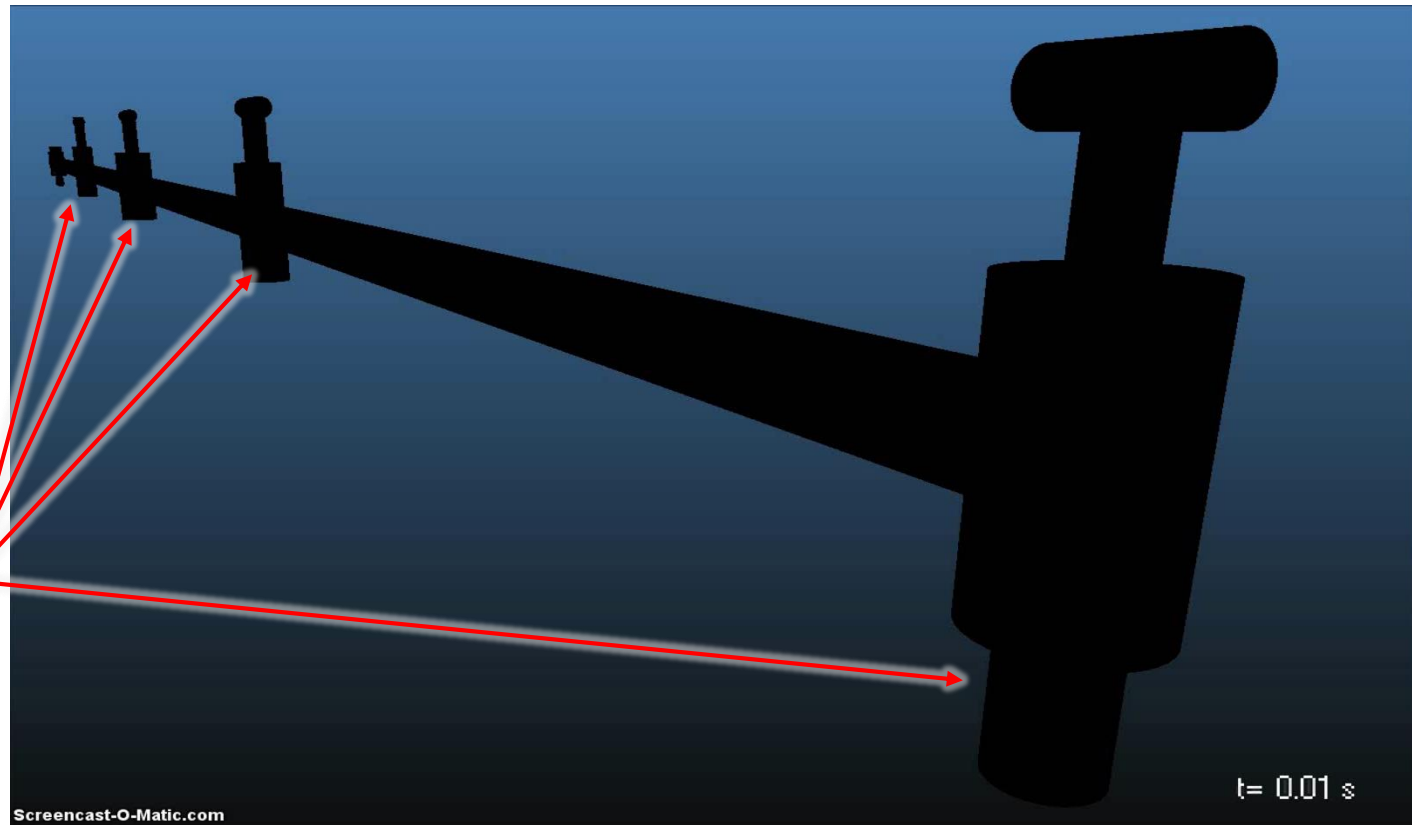


7. Test-Particle Monte Carlo; Another recent paper, with time-dependent TPMC;  
Propagation of the **pressure wave following an RF breakdown** in a cell of the CLIC linear accelerator (see slide 21);



Ref.: M. Ady's PhD thesis, cited above;

7. Test Particle Monte Carlo; Another recent paper, with time-dependent TPMC (Molflow+); Propagation of the **pressure wave following an air-inrush** (breaking a thin aluminum foil or using precision laser-drilled micro-orifices); 4x 7m-long 80 mm ID tubes, with intermediate bellows and pumping stations (pumps off);



Fast Cold-Cathode  
Gauges (with VAT  
modules)

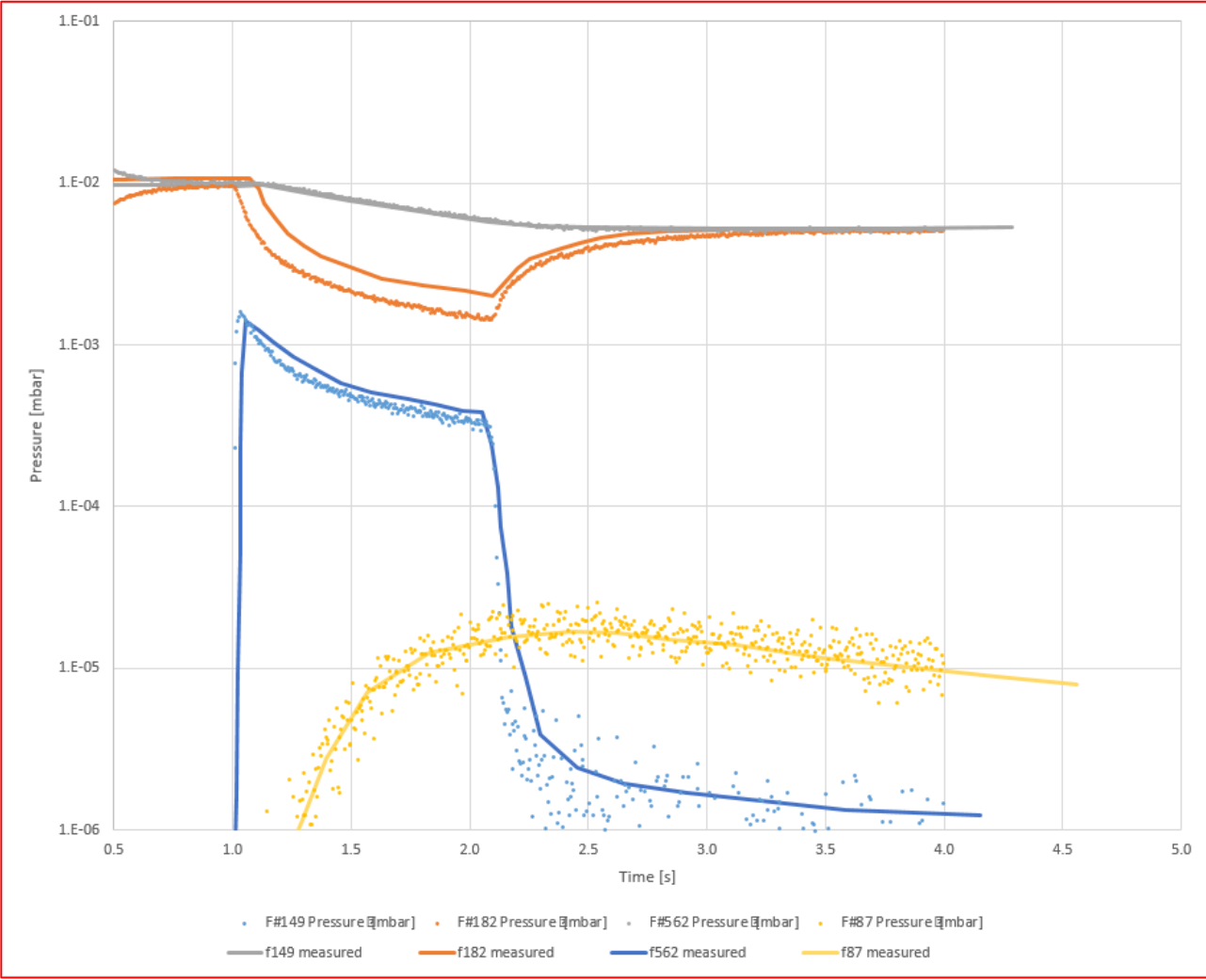
Ref.: M. Ady's PhD thesis, cited above;

# 7. Test-Particle Monte Carlo; Another recent paper, with time-dependent TPMC;

The comparison between the arrival times of the pressure waves at the 4 gauges and the time-dependent simulation is rather accurate **as long as the flow is in molecular regime;**

**Solid lines:** measurements;

**Dots:** Molflow+ simulation;



Ref.: M. Ady’s PhD thesis, cited above; For more examples see also “Gas Dynamics Modelling Efforts at CERN”, R. Kersevan, invited talk Am. Vac. Soc. AVS-61 Conference, Baltimore USA, 2014)



## 7. Test-Particle Monte Carlo; Conductance of other vacuum components:

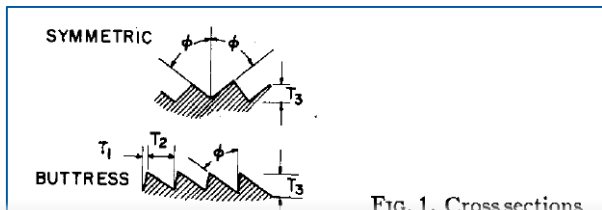


FIG. 1. Cross sections

### CONCLUSIONS

Although the relationship between the structure of surface and the molecular flow conductance as given in this paper is qualitative, the reduction of conductance by surface roughness is clear. Except for the very smoothest surface, surface roughness reduces the conductance below the conductance calculated with the assumption of diffuse reflection from smooth walls. The increase in conductance for the smooth glass surface can, perhaps, be explained by specular reflection.

The corrugated walls introduce a gross surface structure which reduces the conductance by as much as 20%. The measurements and calculations for these cases show that when the gross surface structure is taken into account the conductance is predictable by assuming diffuse reflection from surface elements. The smaller scale surface structure is apparently not so important.

For most applications using engineering surfaces, the reduction in conduction of a few percent is unimportant. However, with careful measurement the effect is easily observable. We propose that the effect of "rougher than rough" surfaces on molecular flow be called the Gaede effect.

## Effect of "Rougher-than-Rough" Surfaces on Molecular Flow through Short Ducts\*

DONALD H. DAVIS, LEONARD L. LEVENSON, AND NORMAN MILLERON†

Lawrence Radiation Laboratory, University of California, Livermore, California 94551

(Received 26 August 1963)

Gaede reported lower molecular flow rates through some tubes than expected if he assumed the walls were 100% diffuse reflecting. He conjectured that back reflection from surface asperities might be responsible. We support Gaede's intuitive guess, having measured flow rates and applied the Monte Carlo calculational method to geometrical models. Our results show that: (1) surface finishes from  $\frac{1}{2}$  to  $64 \mu$  in. ( $0.013$  to  $1.6 \mu$ ) roughness yield flow rates from 5% above to 6% below the diffuse wall prediction; (2) specular reflection can account for the 5% higher value; (3) for cylinders with internal corrugations, fins and threads of groove depth from 0.1 to 15% of the minimum tube radius and included angle between  $30^\circ$  and  $60^\circ$ , conductance is from 15 to 20% lower than conductance assuming diffuse reflection from smooth walls. Experiment and calculation agree within  $\pm 4\%$ .

### INTRODUCTION

THE theory used in the calculation of steady-state flow of rarefied gas through short ducts rests on several assumptions. One of these is that the path taken by a molecule after each encounter at the wall is predicted by applying the cosine law. There are two forms of the cosine law, the diffuse reflection law, in which the reflection direction is independent of the incident direction, and the specular reflection law, in which the angle of reflection is equal to the angle of incidence. For engineering surfaces the diffuse reflection law is much more appropriate. Further comments on these assumptions can be found in the work of Clausing,<sup>1</sup> Lorentz,<sup>2</sup> Loeb,<sup>3</sup> and Davis.<sup>4</sup> The cosine law assumption is consistent with the necessary condition that conductance through a duct be independent of the direction of flow. (If conductance were not independent of flow direction, the second law of thermodynamics would be violated.)

There seems to be nothing wrong with the assumption of diffuse reflection from wall elements; however, measurements of conductance are found to be, in many

cases, lower than the calculated conductance. One of the earliest experimenters to comment on this was Gaede.<sup>5</sup> Gaede suggested that the lower than expected conductance he observed was due to wall asperities. He visualized that this gross wall roughness reflected more molecules back to the entrance of the duct than would a wall which was rough on a molecular scale—thus explaining the reduced conductance. De Marcus<sup>6</sup> theoretically investigated one example of this geometrical effect. De Marcus calculated the conductance of a semi-infinite channel in which the wall has a corrugated or roof-top structure. He found, for example, that the conductance for a channel with a length-to-height ratio of 0.3 and  $45^\circ$  pyramidal corrugations was 96.9% of the conductance of the same channel with smooth but diffuse reflecting walls.

One purpose of this paper is to investigate further the validity of using the assumption of diffuse reflection from surface elements in calculations of conductance through ducts. Agreement between theory and experiment is checked by conductance measurements on cylindrical ducts with corrugated surfaces. Another purpose is to measure the conductance of ducts with engineering surface finishes. The corrugated wall ducts are used because they are amenable to calculation. They also provide an extreme in the reduction of conductance due to surface roughness.

\* Work performed under the auspices of the U. S. Atomic Energy Commission.

† Present address: Centre de Etudes Nucleaires de Saclay, Boite Postale No. 2, Gif-sur-Yvette (Seine-et-Oise) France.

<sup>1</sup> P. Clausing, *Ann. Phys.* 12, 404, 961 (1932).

<sup>2</sup> H. A. Lorentz, *Lectures on Theoretical Physics* (Macmillan and Company Ltd., London, 1927), Vol. 1, Chap. III.

<sup>3</sup> L. B. Loeb, *Kinetic Theory of Gases* (McGraw-Hill Book Company, Inc., New York, 1934), Chap. VII.

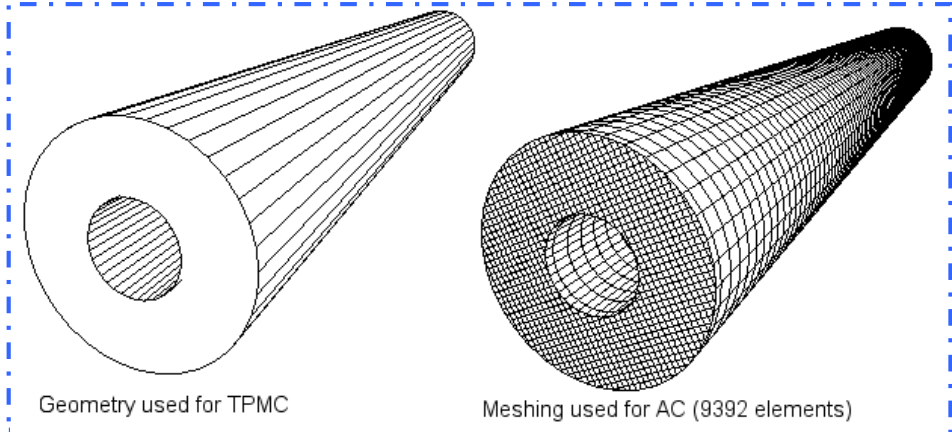
<sup>4</sup> D. H. Davis, *J. Appl. Phys.* 31, 1169 (1960).

<sup>5</sup> W. Gaede, *Ann. Physik* 41, 289 (1913).

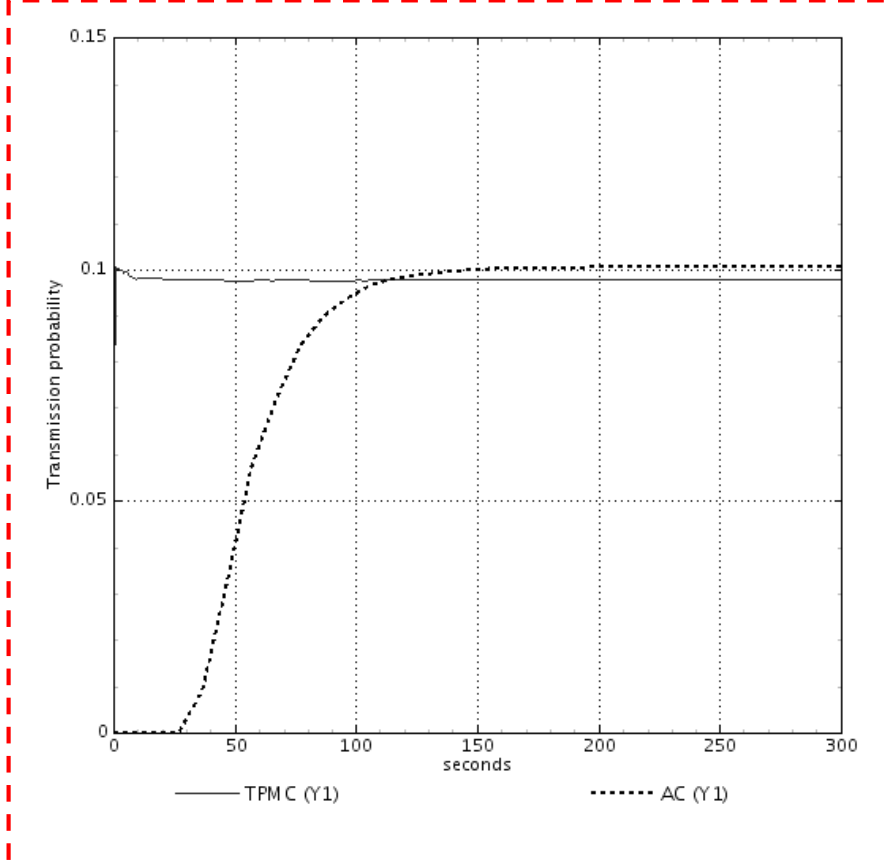
<sup>6</sup> W. C. De Marcus, K-1435, AEC Research and Development Report, Oak Ridge, Tennessee (1959).

7. Test-Particle Monte Carlo vs AC; Benchmarking against each other, same geometry,

Transmission probability W of coaxial tubes [Ref.]:



**Right: Square-grid meshing of the coaxial tubes shown on the left, with  $L/(R1-R2)=25$ ,  $R2/R1=0.4$ .**



Ref.: A. S. Berman, "Free molecular flow in an annulus," J.Appl.Phys. 40, 4991-4992 (1969).

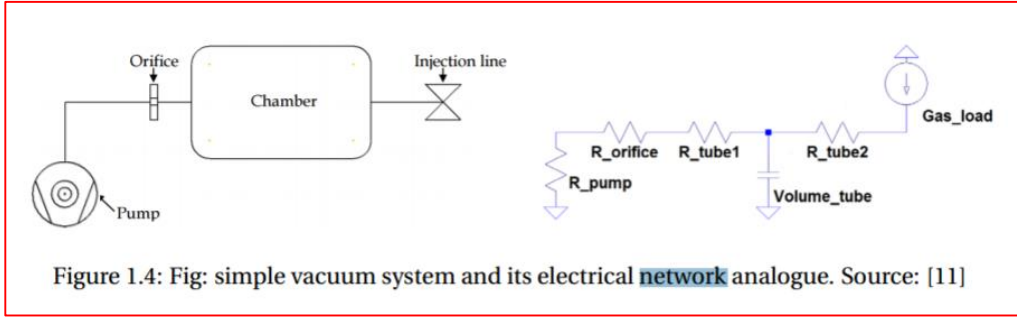
**Result of the calculations: TPMC gives 0.0979 and AC gives 0.1006. Ref. gives a value of 0.09845 for the same geometry).**

### 8. Electric Network Analogy (ENA);

- Based on analogy between  $P=Q/S$  and  $V=IR$ ; analogy between vacuum-related and electrical circuit-related physical quantities;
- Use solver of Kirchhoff networks after assigning proper values to “resistors” (reciprocal of conductance), “current generators” (gas flow), and “losses to ground” (pumping speeds), to finally find the “potential” (pressure);

Table 1.1: Electrical circuit analogy of vacuum systems

Vacuum concept	Electrical analogue
C (conductance)	$Y=1/R$ (admittance)
P (pressure)	U (potential)
dP (pressure difference)	U (voltage)
Q (gas flow)	I (current)
V (volume)	C (capacity)
Pump (with finite pumping speed)	Ground (through resistance)
Gas source	Current generator



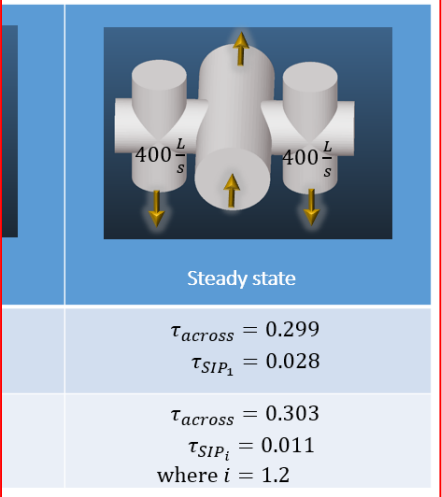
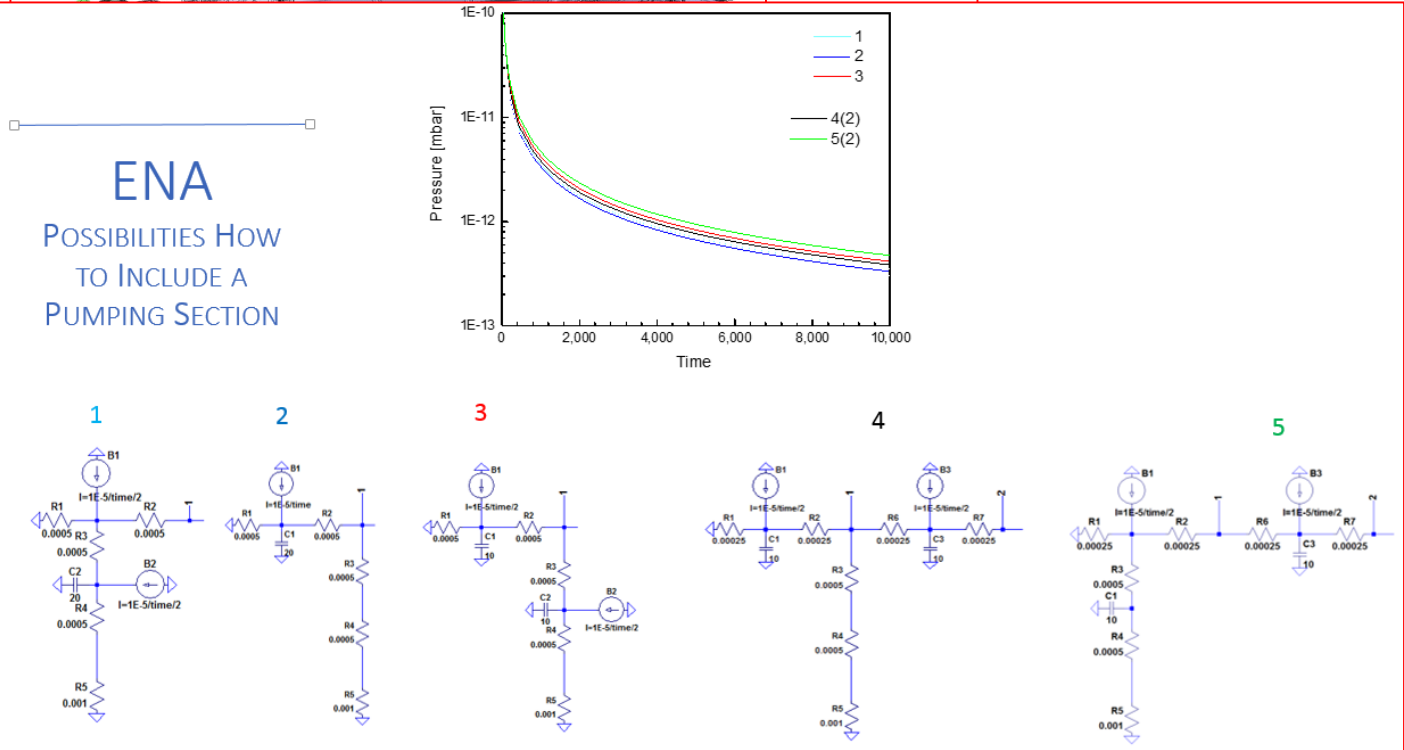
Ref.: M. Ady’s PhD thesis, document cited;

# 8. Electric Network Analogy (ENA); Code used at CERN: LTSpice;

- It is widely used at CERN for everyday's problems, also because it allows to define pressure-dependent pumping speeds and simulate time-dependent pump-downs, which would be impractical to simulate with TPMC or AC;
- The pre-requisite is, though, to pre-calculate either analytically or via TPMC or AC the conductances and effective pumping speeds of the pumps;
- An example: an electrostatic septum for the SPS (source: A. Kukulova, C. Pasquino, CERN)



## TRANSMISSION PROBABILITY IN ACTUAL CONFIGURATION



## Synchrotron radiation, e-cloud, and all the rest;

- Synchrotron radiation, and e-cloud, and other physical effects (impedance instabilities leading to heating and thermal desorption, or ion-induced desorption in large ion storage rings (e.g. GSI) also require sophisticated and dedicated computational tools;
- For lack of time and space, we simply cite **SYNRAD+**, the ray-tracing monte-carlo code companion of Molflow+, which can be used “in series” in order to simulate the vacuum environment of SR light sources;
- The most complete reference is, again, M. Ady’s PhD thesis and bibliography therein;
- Here we use **Jason Carter**’s presentation at the 80<sup>th</sup> IUVSTA workshop in Taiwan, to show the schematics of how SYNRAD+ and Molflow+, used in sequence, can really help design and analyse the vacuum system of any machine were SR is generated;
- This is a very compelling case, since most existing SR light sources are under refurbishing phase or new construction (e.g. ESRF and APS upgrades for the former, and MAX-IV for the latter), but also for hadron machines like the LHC and the future high-energy colliders after it, like the FCC-h;

# Synchrotron radiation, e-cloud, and all the rest;

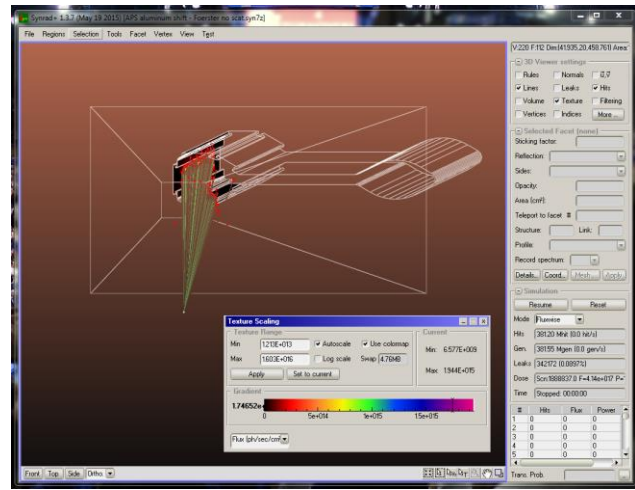
Ref. J. Carter, "APS-Upgrade vacuum system design using SynRad/MolFlow+ with photon scattering", 80<sup>th</sup> IUVSTA Workshop, Taiwan; J. Carter et al., "Benchmarking and calibration of monte carlo vacuum simulations with SYNRAD and Molflow+, proc. IPAC-16

## Use SynRad+ and MolFlow+, sequentially

- Vacuum system analysis freeware created by Roberto Kersevan and Marton Ady of CERN vacuum group;
- MolFlow+
  - 3D Monte Carlo simulations to calculate pressures in the molecular flow regime (HV, UHV)
- SynRad+
  - 3D Monte Carlo simulations of synchrotron radiation distribution
- Coupled simulations
  - Predict dynamic photon stimulated desorption gas loads and pressures
  - Address design requirements for pressures, lifetimes, and conditioning times



MolFlow+ for Windows user interface



SynRad for Windows user interface



• Synchrotron radiation: SYNRAD+;

Schematic of photon stimulated desorption measurement

Note on PSD measurements

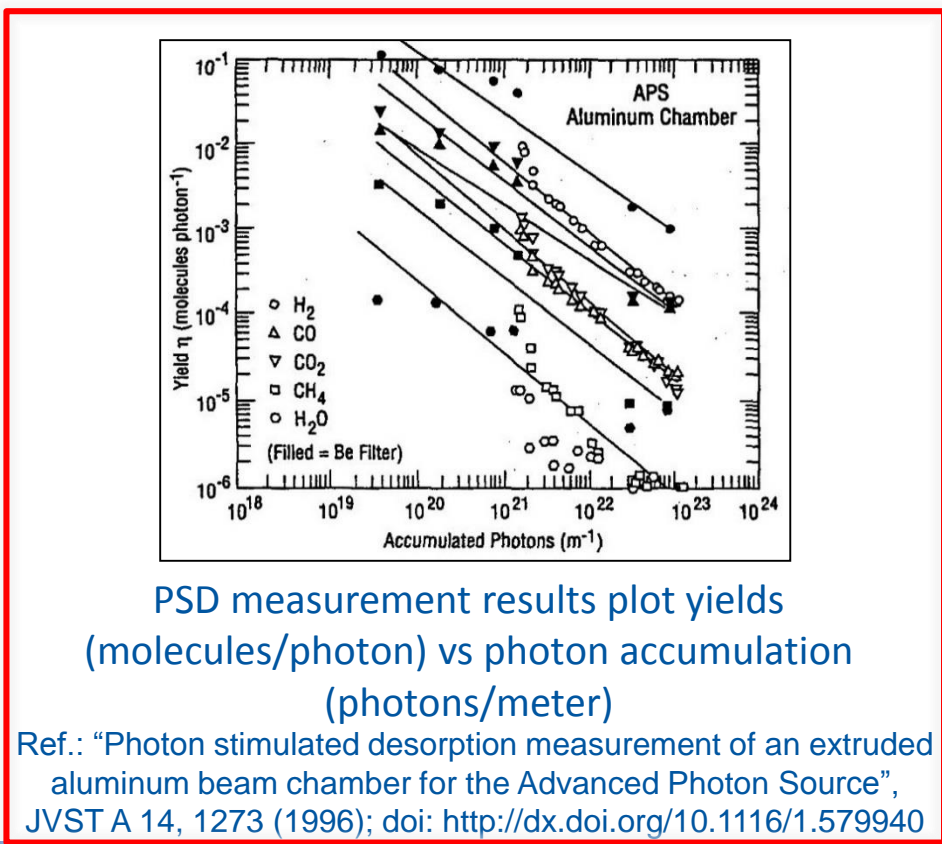
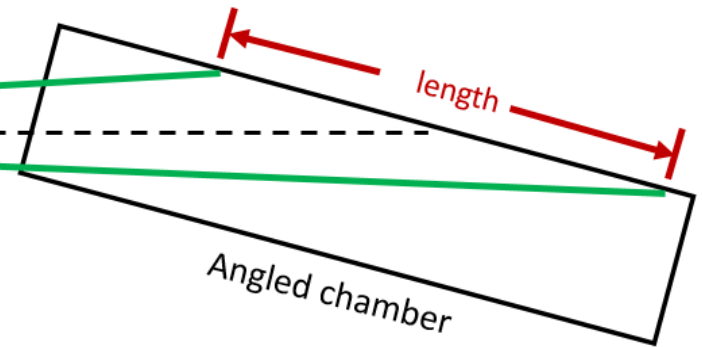
Photon source



Aperture

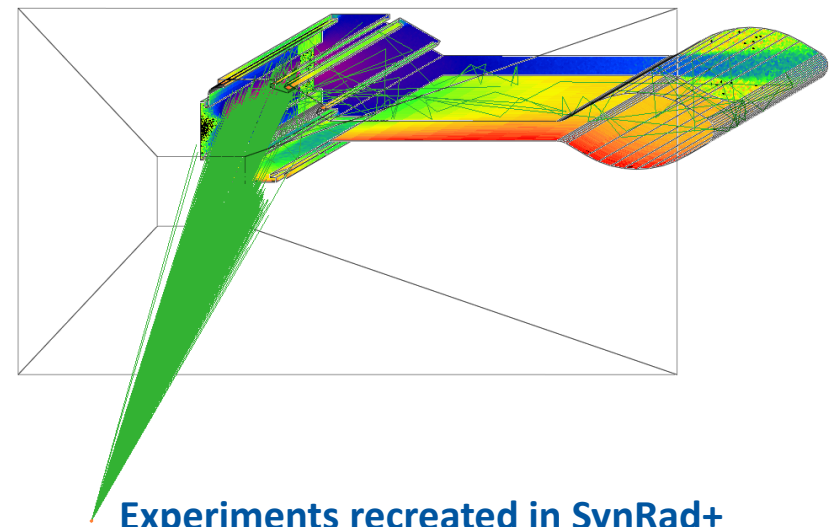


Collimated photon source



PSD measurement results plot yields (molecules/photon) vs photon accumulation (photons/meter)

Ref.: "Photon stimulated desorption measurement of an extruded aluminum beam chamber for the Advanced Photon Source", JVST A 14, 1273 (1996); doi: <http://dx.doi.org/10.1116/1.579940>

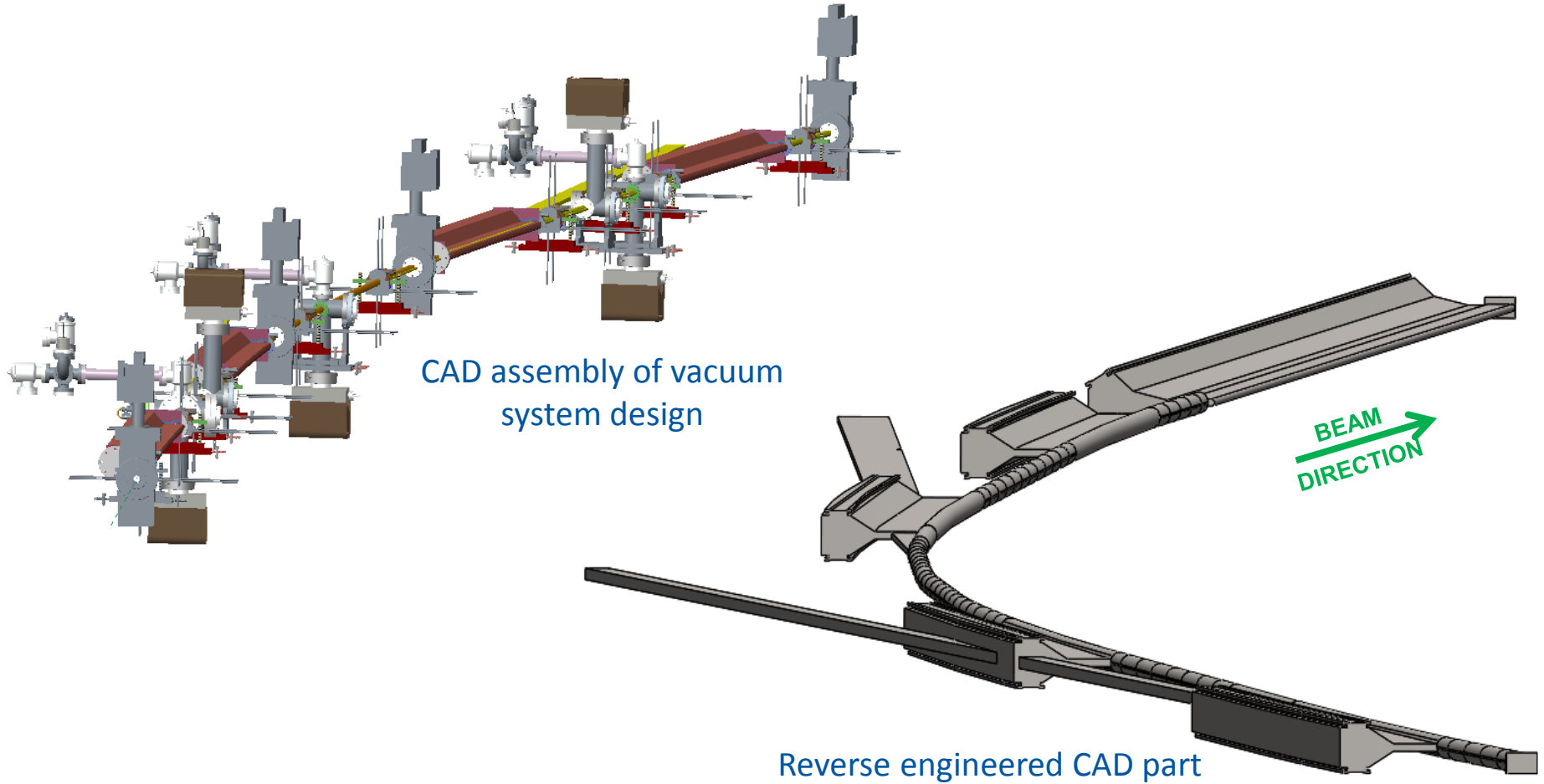


Experiments recreated in SynRad+ and imported into MolFlow+ to determine equivalent mapping of SynRad fluxes (pho/cm2) to MolFlow outgassing (mbar\*L/s)

- Synchrotron radiation;

## Modeling the APS-U vacuum system

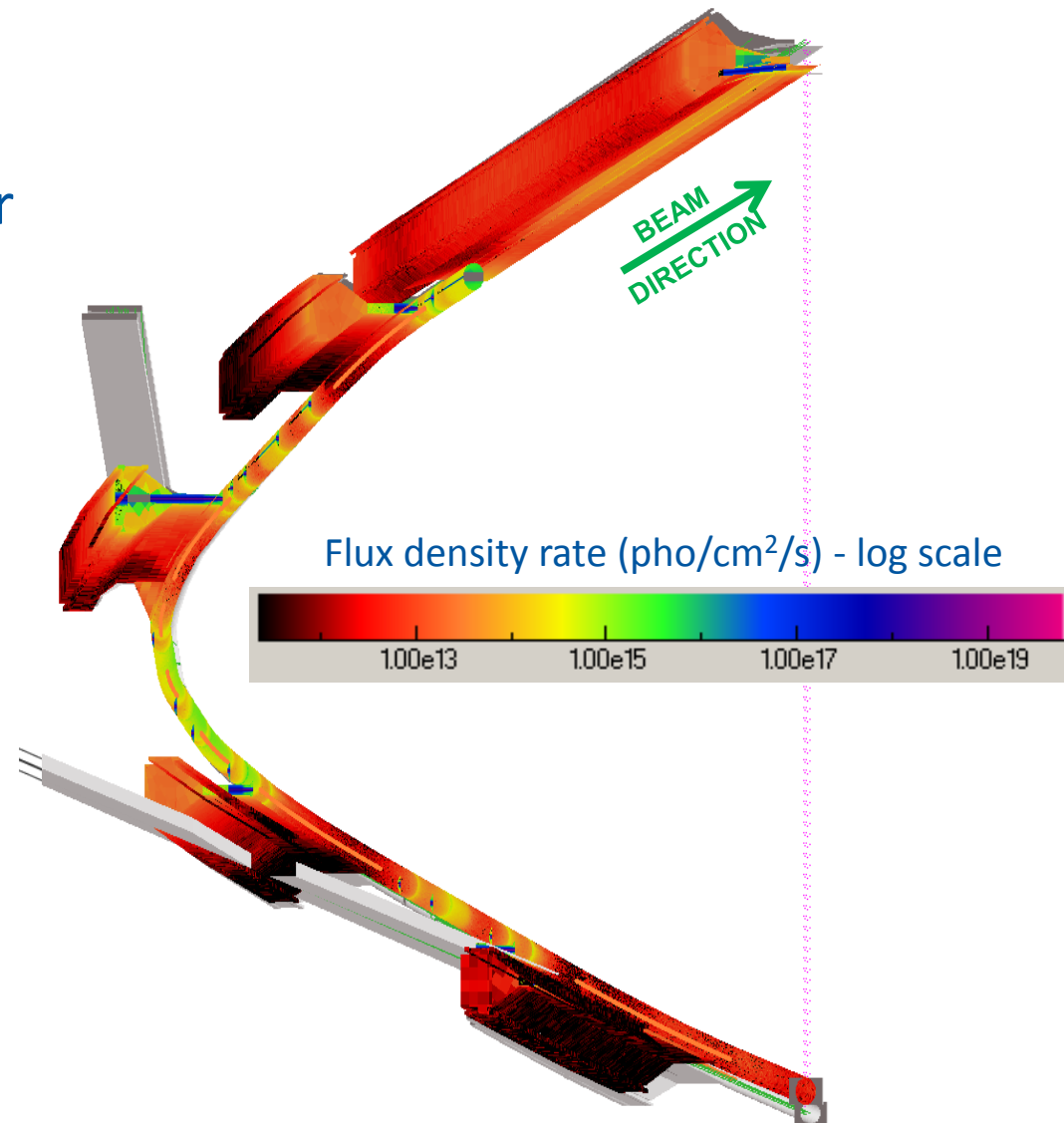
- 3D model built representing interior of vacuum system
  - Captures chamber apertures and conductances
  - Pumping ports simplified for now



- Synchrotron radiation;

## SynRad model of APS-U sector

- Bending magnet elements generate photon flux in model
- Symmetric boundary condition passes downstream photons back to upstream
- Heat load ray trace verified to high accuracy
- Mesh applied to all vacuum surfaces
- Material reflection tables referenced to determine surface scattering

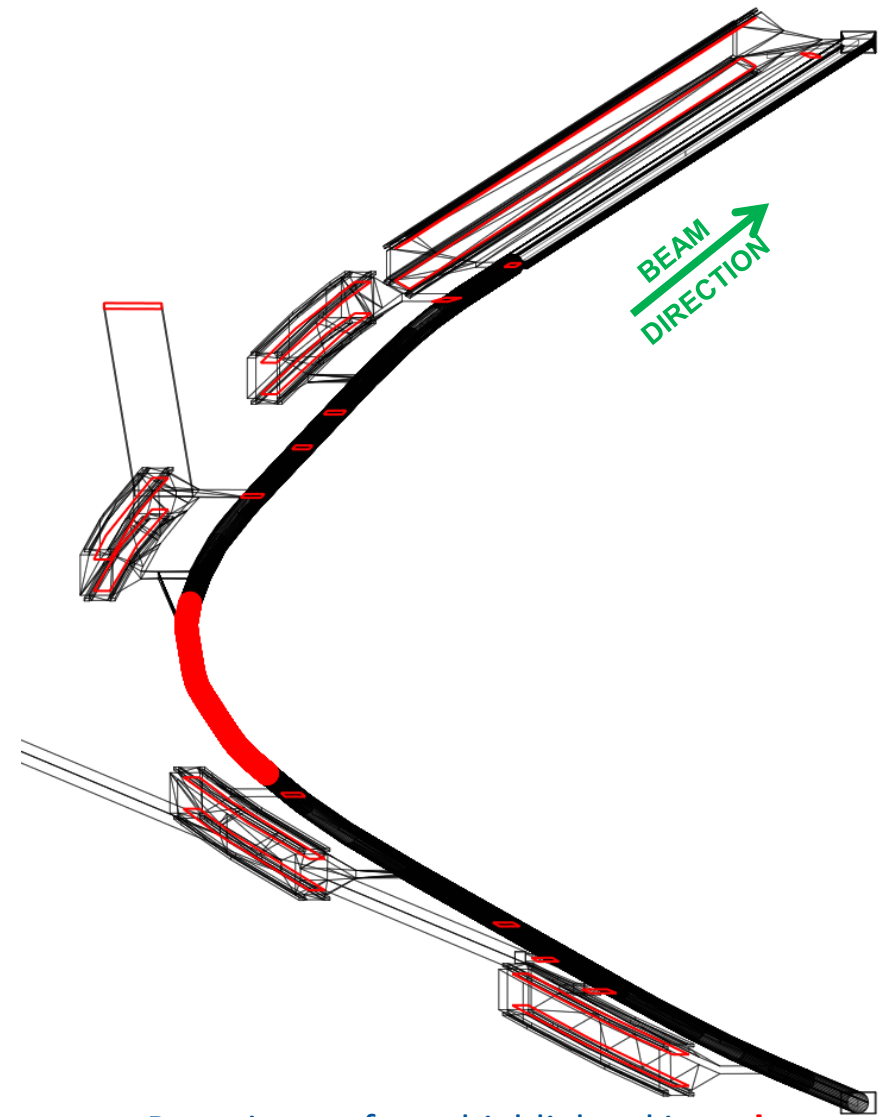


SynRad simulation of synchrotron radiation flux distributions with photon scattering

- Synchrotron radiation;

## MolFlow+ model of APS-U sector

- Define pumping
  - Pumping elements include NEG coating, NEG strips, Ion pumps
  - Unique pumping speeds for various gases
  - Estimate conductance reductions for simplified pumping ports
- Define outgassing
  - Group surfaces by material: aluminum, OFHC, NEG coated surfaces
  - Import PSD yields at a conditioning time point of interest
- Measure pressures along beam path



Pumping surfaces highlighted in **red**  
including NEG coatings, ion pump ports, and NEG  
strip antechambers

## Conclusions:

- Far from being an exhaustive document on all possible ways to calculate vacuum quantities and pressure profiles for accelerators, for lack of time and space, we have tried to show how some codes and algorithms work;
- It has been shown that there is a large number of computational tools which allow the vacuum scientist/engineer to analyse and design the vacuum system of new accelerators, or troubleshoot existing ones;
- The choice of the appropriate method and code depends on the type of accelerator, the level of complexity to which the system has to be modelled and simulated, and other factors, including personal habits like previous knowledge of some code (e.g. ANSYS for FE calculations, LTSpice for electric networks, etc...);
- The interpretation of the results of simulations must take into account the physical basis implemented in the code of choice, and should preferably be benchmarked with another code in case of doubt;
- Modern codes and methods allow a deep inspection of the physics behind the creation of vacuum conditions: I urge every serious student of vacuum science and technology to take the initiative and try to write his/her own code, even a simple one based on some commercial software (e.g. MathCAD), because it is only in doing that that a good understanding of how the vacuum system of an accelerator works and should be designed, avoiding mistakes, and optimizing the available resources (including financial) of the project;

**Good luck to all of you! ☺**